Trends in Analytical Chemistry 130 (2020) 115954

Contents lists available at ScienceDirect

Trends in Analytical Chemistry

journal homepage: www.elsevier.com/locate/trac

Recent advances in chemical multi-way calibration with second-order or higher-order advantages: Multilinear models, algorithms, related issues and applications

Hai-Long Wu*, Tong Wang, Ru-Qin Yu**

State Key Laboratory of Chemo/Biosensing and Chemometrics, College of Chemistry and Chemical Engineering, Hunan University, Changsha 410082, People's Republic of China

ARTICLE INFO

Article history:
Available online 20 June 2020

Keywords:
Multi-way calibration
Multi-way data analysis
Second-order advantage
Higher-order advantages
Quantitative analysis

ABSTRACT

This review discusses the recent advances in both theories and analytical applications of multi-way calibrations based on various high-order analytical data. In the theory part, we focus on some aspects of multi-way calibration, such as multilinear models and their extensions, multi-way calibration algorithms with second-order or higher-order advantages, and other fundamental issues. According to different types of high-order instrument signals, recent applications of second-, third-, and fourth-order calibrations are then discussed, and their contributions to green analytical chemistry are highlighted.

1. Introduction

With the increasing number of available second- and higher-order analytical instruments, the multidimensional experimental data array for each sample can be obtained more and more easily and quickly. It is a challenge for analysts to process and make full use of this kind of data, and is also a major opportunity for the revolution in analytical chemistry. Multi-way calibration is a powerful analytical method based on high-order instrument data for the quantification of analytes of interest in complex systems. The work of multi-way calibration first began in 1978 [1], and in the past two decades, it has made tremendous progress and has become a hotspot of theoretical interest and intensive experimental research [2–23], which benefits from the emergence of more high-order analytical instruments and efficient algorithms, as well as their revolutionary "second-order advantage" [24], that is, one can directly quantify several components of interest even in the presence of uncalibrated components in predicted samples. It realizes the dreams of many analysts in a simple and special way, and a large number of applications in various scientific fields have confirmed its derived benefits: (1) clean-up and pre-separation steps may no longer be needed; (2) in combination with spectroscopic technology, real-time reaction process monitoring of target analytes in complex systems can be achieved; (3) in combination with chromatographic technology, full chromatographic separation of the analytes is not required and the experiment process is much simpler; (4) baseline effects in chromatographic analysis can be easily modeled and removed from the scene; (5) the same calibration set can be applied to multiple scenes with different unknown background interferences; (6) the sensitivity, selectivity and anti-collinearity increase as the number of instrumental modes increases, which can be regard as the "higher-order advantages" [12].

Non-pollution or little pollution during chemical experiment will be the trend of analytical chemistry, while the advantages of the multi-way calibration are highly consistent with the concept of green analytical chemistry. The use of multi-way calibration always makes the analysis process simpler and greener, and "mathematical separation" will completely or partially replace the "physical/chemical separation", which saves time, cost, solvent, manpower and energy. Although some recent reviews have covered multi-way calibration in different fields based on different focuses [15–18,21–23], a more comprehensive review is needed. In this context, this paper systematically reviews models (focus on multilinear models), algorithms with second-order or higher-order advantages, general considerations and recent representative applications for multi-way calibration along the basic logic from theory to practical application, aiming to provide a guide for

* Corresponding author. Fax: +86 731 88821818.
** Corresponding author. Fax: +86 731 88822577.
E-mail addresses: hlwu@hnu.edu.cn (H.-L. Wu), rqyu@hnu.edu.cn (R.-Q. Yu).

https://doi.org/10.1016/j.trac.2020.115954
0165-9936/

analysts. In addition, the contribution of multi-way calibration to green analytical chemistry is highlighted.

2. Terminology and nomenclature

Some confusion and misunderstandings may arise in multi-way analysis area. In this review, we provide the usual terminology and nomenclature. It may help the general reader to understand the remaining of the review.

2.1. Terminology

It is important to first distinguish the "data order" and "data way." The terms "order" and "way" derived from tensor algebra are used to refer to the number of modes of a data array collected from a single sample and the number of ways (modes) of an array for a sample set, respectively. As shown in Fig. 1, the instrument response obtained by a single sample can be zeroth-order (a scalar), first-order (a vector), second-order (a matrix), third-order (a three-modes array) and higher-order tensors. When a group of samples are joined together, the stacked data will yield one-way, two-way, three-way, four-way and *N*-way data arrays, respectively. The procedure performed on zeroth-order tensor data of the reference and predicted samples is known as one-way (univariate) calibration, which requires the signal of the target analyte possessing full selectivity. By analogy, the analysis of first-order tensor, second-order tensor, third-order and higher-order tensor data of the reference and predicted samples is called two-way (first-order) calibration, three-way (second-order) calibration, four-way (third-order) calibration and *N*-way calibration, respectively, which are also collectively called multivariate calibration. In addition, three-way (second-order) calibration and beyond belong to multi-way calibration, which is the focus of this review.

2.2. Nomenclature

Lowercase italics denote scalars; bold lowercase characters represent vectors; bold capitals mean matrices; underlined bold capitals denote three-way or higher-way arrays; the superscript T is the transpose of a matrix; the superscript "+" represents the Moore-Penrose generalized inverse of a matrix; $\|\|_F$ denotes the Frobenius matrix norm; diag(.) means that generating a diagonal matrix by extracting the elements of the vector in parentheses; diagm(.) denotes that generating a column vector by extracting the diagonal elements of matrix in parentheses, which is the inverse process of diag(.). Taking second-order and third-order calibration as an example, related terminologies are listed in Table 1. According to multi-way cyclic symmetry, it is easy to extrapolate the corresponding symbols of the fourth-order or higher-order calibration.

3. Data properties, models and algorithms

3.1. Multi-way data

Multilinear algebra has developed rapidly in the field of analytical chemistry, thanks in part to the fact that modern analytical instruments can easily acquire chemical data that conforms to multilinear structures, which means that instrumental phenomena along various data modes are independent from each other, and also independent on the sample. When performing the second- or higher-order calibration, it requires each sample to be capable to generate second- or higher-order data. Second-order tensor data can be obtained by common second-order analytical instruments such as excitation-emission matrix (EEM) fluorescence (or phosphorescence) spectroscopy, high performance liquid chromatography with photodiode array detection (HPLC-DAD), capillary electrophoresis-DAD (CE-DAD), gel permeation chromatography-DAD (GPC-DAD), LC-fluorescence detection (LC-FLD), LC-mass spectrometry (LC-MS), gas chromatography-MS (GC-MS), CE-MS, LC-nuclear magnetic resonance (LC-NMR), LC-matrix-assisted laser desorption ionization-time of flight-MS (LC-MALDI-TOF-MS), temperature-dependent near-infrared (NIR) spectroscopy as well as by first-order analytical instruments combined with a linear mode such as UV−vis spectrophotometer or fluorometer following the first-order kinetic reaction. Third-order tensor data

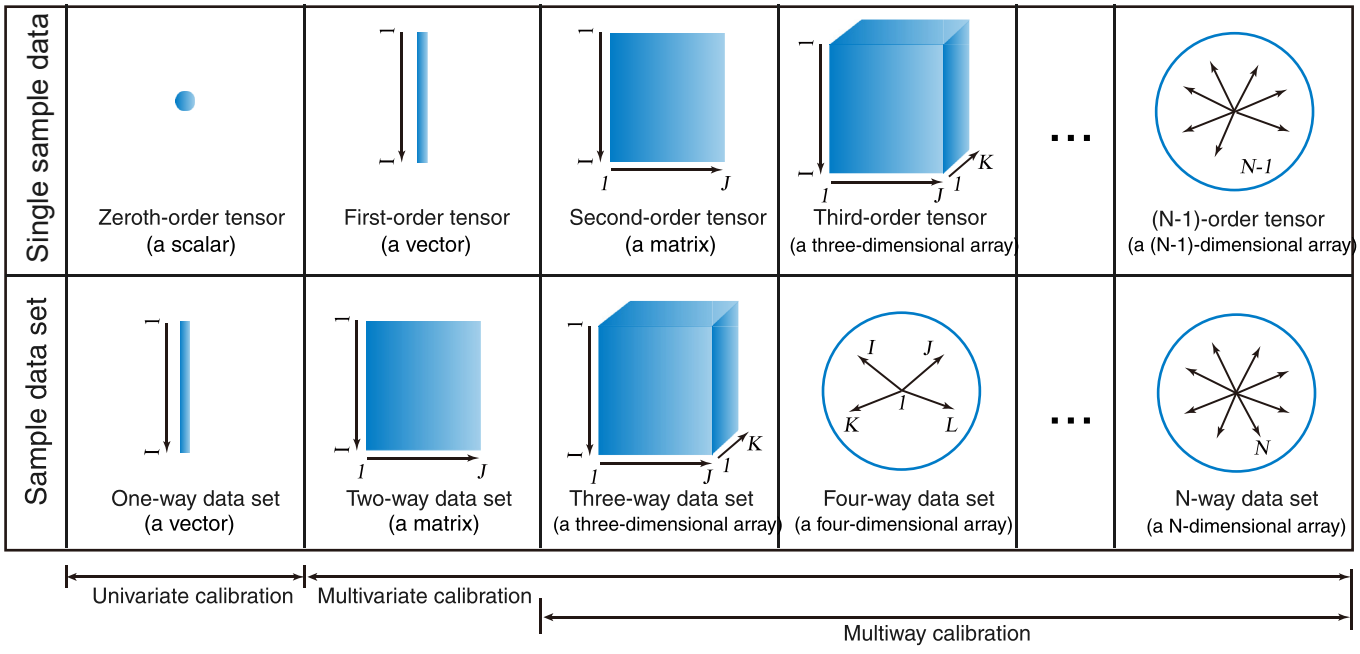

Fig. 1. Relationships and differences between the concepts of "data order" and "data way".

Table 1
Terminology for second- and third- order calibration.

Terminology	Second-order calibration	Terminology	Third-order calibration
$\underline{\mathbf{X}}_{I\times J\times K}$	Three-way data array	$\underline{\mathbf{X}}_{I\times J\times K\times L}$	Four-way data array
$\underline{\mathbf{E}}_{I\times J\times K}$	Three-way residue array	$\underline{\mathbf{E}}_{I\times J\times K\times L}$	Four-way residue array
I, J, K	The size of three modes of $\underline{\mathbf{X}}_{I\times J\times K}$	I, J, K, L	The size of four modes of $\underline{\mathbf{X}}_{I\times J\times K\times L}$
x_{ijk}	The (i, j, k)th element of $\underline{\mathbf{X}}_{I\times J\times K}$	x_{ijkl}	The (i, j, k, l)th element of $\underline{\mathbf{X}}_{I\times J\times K\times L}$
e_{ijk}	The (i, j, k)th element of $\underline{\mathbf{E}}_{I\times J\times K}$	e_{ijkl}	The (i, j, k, l)th element of $\underline{\mathbf{E}}_{I\times J\times K\times L}$
A, **B**, **C**	The three underlying profile matrices of $\underline{\mathbf{X}}_{I\times J\times K}$ with the size of $I\times N$, $J\times N$, $K\times N$, respectively	**A**, **B**, **C**, **D**	The four underlying profile matrices of $\underline{\mathbf{X}}_{I\times J\times K\times L}$ with the size of $I\times N$, $J\times N$, $K\times N$, $L\times N$, respectively
a_{in}, b_{jn}, c_{kn}	The (i, n)th, (j, n)th, and (k, n)th elements of **A**, **B**, **C**, respectively	a_{in}, b_{jn}, c_{kn}, d_{ln}	The (i, n)th, (j, n)th, (k, n)th and (l, n)th elements of **A**, **B**, **C**, **D**, respectively
$\mathbf{a}_{(i)}$, $\mathbf{b}_{(j)}$, $\mathbf{c}_{(k)}$	The ith, jth, kth row vectors of matrices **A**, **B**, **C**, respectively	$\mathbf{a}_{(i)}$, $\mathbf{b}_{(j)}$, $\mathbf{c}_{(k)}$, $\mathbf{d}_{(l)}$	The ith, jth, kth, lth row vectors of matrices **A**, **B**, **C**, **D**, respectively
$\mathbf{X}_{i..}$, $\mathbf{X}_{.j.}$, $\mathbf{X}_{..k}$	The ith horizontal, jth lateral, and kth frontal slices of $\underline{\mathbf{X}}_{I\times J\times K}$, respectively	$\mathbf{X}_{ij..}$, $\mathbf{X}_{.jk.}$, $\mathbf{X}_{..kl}$, $\mathbf{X}_{i..l}$	The slice matrices of $\underline{\mathbf{X}}_{I\times J\times K\times L}$
$\mathbf{X}_{I\times JK}$, $\mathbf{X}_{J\times KI}$, $\mathbf{X}_{K\times IJ}$	The stretched matrices of $\underline{\mathbf{X}}_{I\times J\times K}$	$\mathbf{X}_{I\times JKL}$, $\mathbf{X}_{J\times KLI}$, $\mathbf{X}_{K\times LIJ}$, $\mathbf{X}_{L\times IJK}$	The fully stretched matrices of $\underline{\mathbf{X}}_{I\times J\times K\times L}$
$\mathbf{E}_{i..}$, $\mathbf{E}_{.j.}$, $\mathbf{E}_{..k}$	The ith horizontal, jth lateral, and kth frontal slices of $\underline{\mathbf{E}}_{I\times J\times K}$, respectively	$\mathbf{X}_{..i}^{J\times KL\times I}$, $\mathbf{X}_{.j.}^{K\times LI\times J}$, $\mathbf{X}_{..k}^{L\times IJ\times K}$, $\mathbf{X}_{.l}^{I\times JK\times L}$	The pseudo-fully stretched matrices of $\underline{\mathbf{X}}_{I\times J\times K\times L}$
		$\mathbf{E}_{ij..}$, $\mathbf{E}_{.jk.}$, $\mathbf{E}_{..kl}$, $\mathbf{E}_{i..l}$	The slice matrices of $\underline{\mathbf{E}}_{I\times J\times K\times L}$

can also be directly obtained by third-order hyphenated analysis instruments, such as two-dimensional liquid chromatography with DAD or MS detection (LC^2-DAD or LC^2-MS), LC-EEM, two-dimensional gas chromatography with MS detection (GC^2-MS), etc. Another common method for collecting third-order data is to record EEM of a sample as a function of reaction time [25], pH [26], volume of quencher [27], etc. Some special strategies, such as second-order hyphenated instruments data as a function of reaction time like LC-DAD-kinetic, are also possible. Multiple chromatographic columns can also be connected, such as GC^3-MS, which would be capable to directly obtain fourth-order and higher-order data. Analogously, second- and third-order instruments combined with multiple extra experimental variable modes can also obtain high-order data, such as EEM-kinetic-pH [28], EEM-irradiation time-pH [29], HPLC-DAD-kinetic-pH [30].

As mentioned above, the formation of high-order data based on the excitation-emission fluorescence and hyphenated chromatographic techniques has been investigated in great detail. Data generated by EEMs combined with second- or higher-order calibration can be considered a very green and effective analytical method, because on the one hand, fluorescence data is highly sensitive and easy to acquire, and it is easy to utilize derivatization, fluorescence enhancement, etc. to obtain signals of extremely small amounts of analytes. On the other hand, a EEM data set usually possesses a strict trilinear structure (although the correct expression should be low-rank trilinear, meaning that it can be modeled using a small number of components, ideally equal to the number of chemical components in the system), therefore various types of multi-way calibration algorithms can handle it. “Mathematical separation” completely replaces “physical/chemical separation” in fluorescence analysis, which simplifies pre-processing steps, saves analysis time, allows working with a small volume of (non-toxic or low-toxic) solvents and makes real-time and non-destructive analysis possible.

When multi-way calibration is performed on hyphenated chromatographic data, a powerful analytical strategy of “physical/chemical separation plus mathematical separation” will be formed. The obvious advantage of this strategy is to allow quantitation of analytes of interest in the presence of overlapping chromatographic peaks and unknown interference, which greatly saves analysis time and consumption of organic solvents, simplifies pretreatment steps such as purification and improves the versatility of chromatographic methods. In addition, baseline drifts can be easily modeled and removed, and retention time shifts can also be handled by flexible multi-way calibration algorithms.

3.2. Multilinear models

After getting the multilinear data, analysts need to choose models and algorithms according to data properties and analytical requirements. In this part, we mainly focus on the multilinear models and their different forms of expression, which may help the reader understand the multilinear data structure.

3.2.1. Trilinear model

Many models have been used to analyze three-way data, including the famous Tucker3, CANDECOMP/parallel factor analysis (PARAFAC), bilinear decomposition-based multivariate curve resolution (MCR) model and latent variables-based models. The Tucker3 model was firstly suggested by Tucker in 1966 to process the three-way data in the field of psychometrics [31]. It decomposes a three-way data array $\underline{\mathbf{X}}_{I\times J\times K}$ into three eigenvector matrices and a three-way core array. Generally, these matrices are abstract factors and only have a mathematical significance without a clear physical meaning. In addition, rotation ambiguities will lead to non-unique solutions. Harshman [32], Carroll and Chang [33] then simultaneously proposed the trilinear CANDECOMP/PARAFAC model (or PARAFAC model, or trilinear decomposition model, or trilinear component model, or trilinear model for short in the chemometric literatures), which is a specific form of the Tucker3 model, with the same number of components N in each mode and the $N\times N\times N$ superdiagonal core array with ones in the superdiagonal and zeros elsewhere. In this way, relative unique solutions with a clear physical/chemical meaning can be achieved by the decomposition of PARAFAC model. These outstanding properties brought a major revolution to analytical chemistry, and made the dream of simultaneous qualitative and quantitative analysis of multiple components in the presence of unknown interference to come true, so this important model is detailed in this section. According to this trilinear component model, each element x_{ijk} of three-way data array $\underline{\mathbf{X}}_{I\times J\times K}$ can be described as:

$$x_{ijk}=\sum_{n=1}^{N}a_{in}b_{jn}c_{kn}+e_{ijk},\quad \text{for } i=1,2,\ldots,I;\ j=1,2,\ldots,J;\ k=1,2,\ldots,K \tag{1}$$

where a_{in} and b_{jn} are the (i, n)th and (j, n)th elements of the qualitative profile matrices **A** and **B**, and usually represent the normalized intensities of component n in the instrumental channels i and j, respectively; c_{kn} is the (k, n)th element of the concentration profile matrix **C**, and represents the relative concentration

or score of component n in the kth sample; N denotes the number of detectable components, including the analyte(s) of interest, background and unknown interferences; the remaining symbols have been explained in Table 1. In addition, taking an EEM data set as an example, the graphical representation of trilinear component model is intuitively shown in Fig. 2, where $\underline{\mathbf{I}}$ represents a $N \times N \times N$ three-way superdiagonal core data array in which ones are located on the superdiagonal while zeros are located elsewhere. The inverse procedures to return three-way data array $\underline{\mathbf{X}}_{I\times J\times K}$ is described in Fig. 3, which helps to further understand the graphical representation of the trilinear model.

Moreover, the classical matrix representation of trilinear model has the following forms:

(1) stretched matrices form,

$$\mathbf{X}_{I\times JK} = \mathbf{A}(\mathbf{C}\odot\mathbf{B})^{\mathrm{T}} + \mathbf{E}_{I\times JK} \tag{2}$$

$$\mathbf{X}_{J\times KI} = \mathbf{B}(\mathbf{A}\odot\mathbf{C})^{\mathrm{T}} + \mathbf{E}_{J\times KI} \tag{3}$$

$$\mathbf{X}_{K\times IJ} = \mathbf{C}(\mathbf{B}\odot\mathbf{A})^{\mathrm{T}} + \mathbf{E}_{K\times IJ} \tag{4}$$

where $\odot$ is the Khatri-Rao product.

(2) slice matrices form,

$$\mathbf{X}_{i..} = \mathbf{B}\mathrm{diag}(\mathbf{a}_{(i)})\mathbf{C}^{\mathrm{T}} + \mathbf{E}_{i..}, \quad \text{for } i = 1, 2, \ldots, I, \tag{5}$$

$$\mathbf{X}_{j.} = \mathbf{C}\mathrm{diag}(\mathbf{b}_{(j)})\mathbf{A}^{\mathrm{T}} + \mathbf{E}_{j.}, \quad \text{for } j = 1, 2, \ldots, J, \tag{6}$$

$$\mathbf{X}_{..k} = \mathbf{A}\mathrm{diag}(\mathbf{c}_{(k)})\mathbf{B}^{\mathrm{T}} + \mathbf{E}_{..k}, \quad \text{for } k = 1, 2, \ldots, K, \tag{7}$$

Many second-order calibration algorithms have been developed based on these matrix representations [34–36].

3.2.2. Quadrilinear model

If a single sample can produce $I \times J \times K$ third-order tensor data, one can obtain a $I \times J \times K \times L$ four-way data array $\underline{\mathbf{X}}_{I\times J\times K\times L}$ by stacking data of L samples along the sample mode. The graphical representation of quadrilinear model is shown in Fig. 4 and each element x_{ijkl} of four-way data array $\underline{\mathbf{X}}_{I\times J\times K\times L}$ can be described as:

$$x_{ijkl} = \sum_{n=1}^{N} a_{in}b_{jn}c_{kn}d_{ln} + e_{ijkl}, \ \text{for } i=1,2,\ldots,I; j=1,2,\ldots,J; \\ k=1,2,\ldots,K; \ l=1,2,\ldots,L \tag{8}$$

where a_{in} and b_{jn} are the same as in Eq. (1); c_{kn} describes the profile in the third instrumental mode; d_{ln} represents the relative concentration or score of component n in the lth sample. $\underline{\mathbf{I}}$ represents a $N \times N \times N \times N$ four-way superdiagonal core data array in which ones are located on the superdiagonal while zeros are located elsewhere.

Compared with trilinear model, the matrix representation of quadrilinear model have more variants, such as the fully stretched matrices form [37], the fully slice matrices form [37] and the pseudo-fully stretched matrices form [38]. Their details are in Supplementary material. Based on these different matrix representations, quadrilinear decomposition algorithms with different performances were developed. For example, the objective functions of four-way PARAFAC and alternating quadrilinear decomposition (AQLD) algorithm [39] were designed according to the fully stretched matrices form and the pseudo-fully stretched matrices form of quadrilinear model, respectively. Recently, Xie et al. suggested a novel "slicing" concept to describe the quadrilinear model. Some high-order tensor symbols were creatively defined from the perspective of high-dimensional space. Based on the "slicing" boxes (three-way data arrays) representation of quadrilinear model, slicing alternating quadrilinear decomposition (SAQLD) algorithm with fast convergence speed was developed. The details can be seen in Ref. [40].

3.2.3. Quinquelinear model and extension

In the quinquelinear model, each element x_{ijklm} of five-way data array $\underline{\mathbf{X}}_{I\times J\times K\times L\times \mathrm{M}}$ can be expressed as:

$$x_{ijklm} = \sum_{n=1}^{N} a_{in}b_{jn}c_{kn}d_{ln}f_{mn} + e_{ijklm}, \ \text{for } i=1,2,\ldots,I; \\ j=1,2,\ldots,J; \ k=1,2,\ldots,K; \ l=1,2,\ldots,L \ ; \ m=1,2,\ldots,M \tag{9}$$

By analogy, trilinear, quadrilinear and quinquelinear model can be further extended to the general multilinear model (or called the M-way PARAFAC model). In general multilinear model, the new nomenclature needs to be used to break through the limitations of traditional alphabets, however, their relevant meanings are easily understood by analogy to trilinear, quadrilinear and quinquelinear models. Each element $x_{i_1 i_2 \ldots i_M}$ of M-way data array $\underline{\mathbf{X}}_{I_1\times I_2\times\ldots\times I_M}$ can be described as:

$$x_{i_1 i_2 \ldots i_M} = \sum_{n=1}^{N} a^{(1)}{}_{i_1 n}\, a^{(2)}{}_{i_2 n} \cdots a^{(M)}{}_{i_M n} + e_{i_1 i_2 \ldots i_M} \\ i_1 = 1, 2, \ldots, I_1; \ i_2 = 1, 2, \ldots, I_2; \ i_M = 1, 2, \ldots, I_M \tag{10}$$

where $a^{(1)}{}_{i_1 n}$, $a^{(2)}{}_{i_2 n}$, …, and $a^{(M)}{}_{i_M n}$ are the (i_1,n)th, (i_2,n)th, …, and (i_M, n)th elements of the underlying profile matrices $\mathbf{A}^{(1)}{}_{I_1\times N}$, $\mathbf{A}^{(2)}{}_{I_2\times N}$, …, and $\mathbf{A}^{(M)}{}_{I_M\times N}$, respectively. $e_{i_1 i_2 \ldots i_M}$ is the element of M-way residue array $\underline{\mathbf{E}}_{I_1\times I_2\times\ldots\times I_M}$.

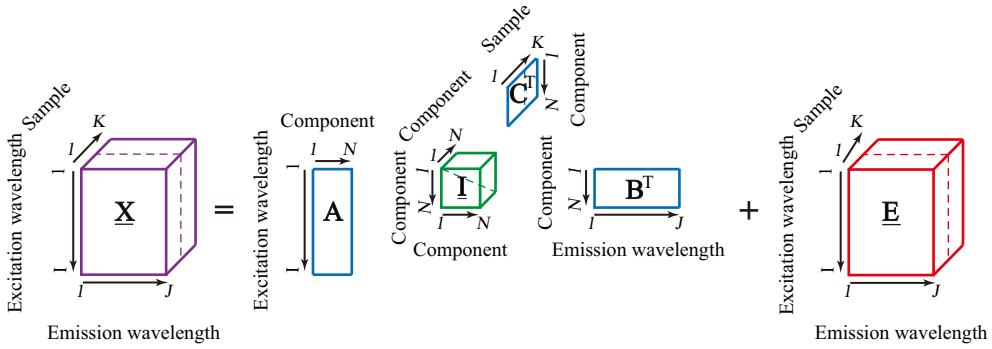

Fig. 2. Graphical representation of the trilinear model for three-way EEM-samples data array.

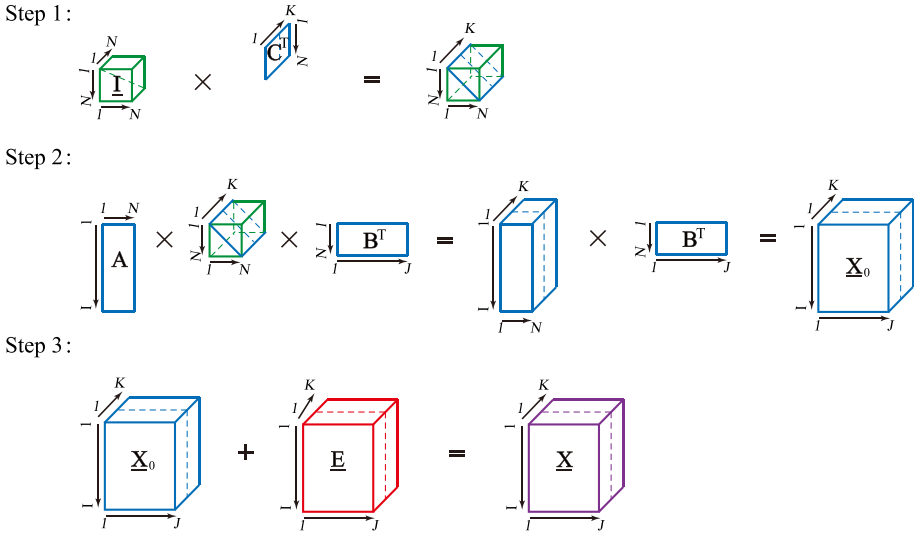

Fig. 3. The inverse procedures to return three-way data array $\underline{\mathbf{X}}_{I\times J\times K}$.

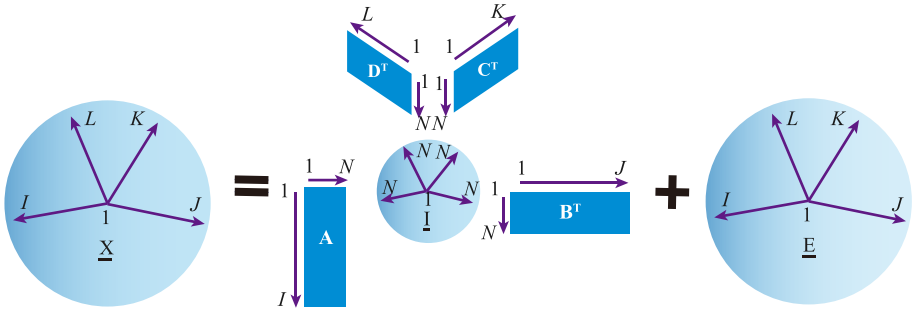

Fig. 4. Graphical representation of the quadrilinear model.

Similarly, two basic matrix representations of multilinear model including the fully stretched matrices form and the pseudo-fully stretched matrices form can be obtained (see Supplementary material for details). Based on these matrix representations, it is easy to develop and derive multilinear decomposition algorithms for higher-order data according to alternating least squares (ALS).

3.3. Some models for non-multilinear data

Bilinear decomposition-based MCR model is the most widely used model for processing non-multilinear data, especially chromatographic data [41], because elution time profiles are seldom constant across samples in chromatographic experiments. This model can extract the related information of the pure analytes through a bilinear model decomposition of data matrix $\mathbf{X}$ into the produce of a concentration or elution profiles matrix and a spectral profiles matrix $\mathbf{S}^{\mathrm{T}}$. For a second-order chromatographic data set consisting of a series of samples, an augmentation step should be implemented to form the column-wise augmented matrix $\mathbf{X}_{aug}$ (usually unfolded the sample matrices along the retention time direction). Similarly, $\mathbf{X}_{aug}$ can be decomposed into an augmented elution profiles matrix $\mathbf{C}_{aug}$ and a spectral profiles matrix $\mathbf{S}^{\mathrm{T}}$. In matrix form this model can be written as

$$\mathbf{X}_{aug} = \mathbf{C}_{aug}\mathbf{S}^{\mathrm{T}} + \mathbf{E}_{aug} \tag{11}$$

where $\mathbf{X}_{aug}$ is a column-wise augmented data matrix with a size of [I (number of retention time points in each sample) $\times$ K (number of samples)] $\times$ J (number of spectral channels); $\mathbf{C}_{aug}$ is the augmented elution profiles matrix with a size of $IK \times N$, which includes the augmented elution profiles of N components; $\mathbf{S}$ is a $J \times N$ spectral matrix consisting of all spectral profiles. $\mathbf{E}_{aug}$ is an augmented residual matrix. Note that $\mathbf{C}_{aug}$ in here is not associated with $\mathbf{C}$ in the multilinear model. After the number of components is determined and the initial values are estimated, advisable constraints such as non-negativity and unimodality can be used to drive the ALS optimization process to obtain the final solutions. The above is the implementation process of the well-known MCR-ALS algorithm. When it is extended to process a four-way data array, the four-way data array should be unfolded into a super-augmented bilinear matrix in advance.

When data modes are mutually dependent or data with highly complex structures deviates slightly from multilinearity, latent variables-based model may be a good choice [42–45]. The related algorithms include unfolded or multi-way partial least-squares with residual multilinearization (U-PLS/RML and N-PLS/RML) [46], which will be introduced later.

Bilinear decomposition-based MCR model and latent variables-based model are flexible and allow modeling multi-way data array even when the multi-way data array is not strictly multilinear. However, every coin has two sides, their flexible structures may cause some shortcomings. For example, the decomposition of bilinear models is usually not unique and requires appropriate initial values and constraints to ensure reasonable results; the decomposition of latent variables-based models does not provide accurate qualitative profiles with clear chemical meaning. Their

details have been introduced in Refs. [41,47,48] and [44–46], respectively, therefore they are not further described herein.

3.4. Characteristics and advantages of multi-way calibration based on multilinear models

3.4.1. Uniqueness property

It is well known that the decomposition of a bilinear matrix is not unique due to the existence of rotational ambiguities. However, when a *M*-way data array conforms to the multilinear model, according to Kruskal's uniqueness condition, the uniqueness of the decomposition is guaranteed when if $(2N + M - 1)$ is less than or equal to the sum of the *k*-ranks of *M* components matrices, where *N* is the component number and *M* is the dimension number of the data array [49–51]. The uniqueness property of multilinear decomposition is a relative uniqueness property rather than an absolute one in the mathematical sense. It means that only column permutations and scaling transformations of the resolved matrices are allowed without altering the residuals of the fit. To express it algebraically, an alternative solution in trilinear decomposition is represented as:

$$\mathbf{A}^* = \mathbf{A} \times \mathbf{D}_a \times \mathbf{P}; \qquad \mathbf{B}^* = \mathbf{B} \times \mathbf{D}_b \times \mathbf{P}; \qquad \mathbf{C}^* = \mathbf{C} \times \mathbf{D}_c \times \mathbf{P} \tag{12}$$

where $\mathbf{D}_a$, $\mathbf{D}_b$, and $\mathbf{D}_c$ are diagonal matrices; $\mathbf{P}$ is a permutation matrix. From the aspect of space, $\mathbf{D}_a$, $\mathbf{D}_b$, and $\mathbf{D}_c$ must satisfy the requisite condition shown in Fig. 5, which denotes that the effect of rescaling brought by the three $\mathbf{D}$ matrices must cancel each other out. In each iterative calculation of the algorithm, two matrices (eg. $\mathbf{A}^*$ and $\mathbf{B}^*$) are usually normalized to minimize the effect of $\mathbf{D}$ matrices.

The multi-way calibration method with the relative uniqueness property is fully capable of solving the problem of quantitative analysis in analytical chemistry. Taking second-order calibration as an example, the column of the analyte of interest in the resolved matrix can be determined by finding a column in qualitative matrices ($\mathbf{A}^*$ and $\mathbf{B}^*$) that has the greatest correlation with the standard profile. The relative concentration information of each analyte is collected in quantitative matrix ($\mathbf{C}^*$), and the quantitative analysis is performed by inserting the relative concentration of each analyte of interest into the corresponding pseudo-univariate calibration curve.

3.4.2. Multi-way cyclic symmetry

Professor Olivieri has the foresight to propose that multi-way data analysis will develop from zero-order calibration, first-order calibration, second-order calibration to higher-order calibration and even *N*-order calibration. Accordingly, he also proposed versatile methods for analytical figures of merit (FOMs) of multi-way calibration [13]. More fortunately, Wu and coworkers discovered the inherent cyclic symmetry of the multilinear decomposition model, which not only normalizes the mathematical symbol of multi-way data analysis but also makes the multilinear decomposition algorithm easier to expand to higher-way, providing an important theoretical basis for the expansion and development of multilinear decomposition algorithms [5]. As depicted in Fig. 6, all physical modes, subscripts, elements, vectors in resolved matrices, stretched matrices and sliced matrices obey the inner law. For example, the stretched matrices form of trilinear model (Eqs. (2)–(4)) can be expressed according to three-way cyclic symmetry, and it can be extended to the stretched matrices form of multilinear model (Supplementary material, Eqs. (S.13)–(S.17)) according to multi-way cyclic symmetry. Therefore, the related multilinear decomposition formulas from second-order calibration to *N*-order calibration can easily obtained just by exchanging the symbols.

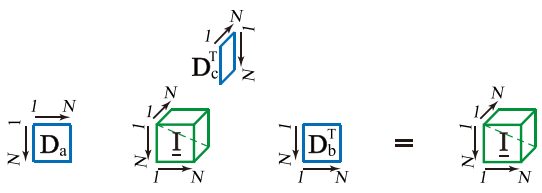

Fig. 5. The requisite condition which $\mathbf{D}_a$, $\mathbf{D}_b$, and $\mathbf{D}_c$ must satisfy in trilinear decomposition.

3.4.3. Second-order and higher-order advantages

In 1978, Ho and coworkers determined perylene in mixtures with anthracene by processing EEM fluorescence data, calibrating only with single-component perylene solutions, which achieved the second-order advantage for the first time, although the feature was not given such name at the time [1]. In 1994, Booksh and Kowalski defined a concept in the context of second-order calibration, that is, the "second-order advantage": the ability to quantify target analytes in the presence of unknown interferents [24]. The concept is still in use today. In addition, when implementing third-order calibration and higher-order calibration, more additional advantages might be obtained. The known "third-order advantages" not only maintain the second-order advantage but also have some additional benefits: (1) higher sensitivity and selectivity as well as improvement of other FOMs; (2) better resolution for the data with high collinearity effects, which is the direct consequence of Kruskal's condition, and one can introduce the fourth mode to relieve the serious collinearity; (3) decomposing the third-order data array for a single sample [5,11,12]. However, the breakthrough brought by the discovery of the third-order advantage is not as big as the discovery of second-order advantage, and the complete third-order advantage and the higher-order advantage are still unknown and need further exploration.

3.5. Multi-way calibration algorithms

3.5.1. Second-order calibration

Second-order calibration algorithms with second-order advantage can be classified into three groups including non-iterative algorithms, iterative algorithms and residual bilinearization-based algorithms. Classical non-iterative algorithms are rank annihilation factor analysis (RAFA) [52], generalized rank annihilation method (GRAM) [53], and direct trilinear decomposition (DTLD) [54]. The RAFA method as a landmark work was first proposed by Ho et al. The principle of RAFA is to make clever use of the relationship between the number of components which produce the response signal and the rank of the matrix. When the calibration sample signal containing only a target component is eliminated, the rank of the signal matrix of the prediction sample containing the unknown interference is reduced by 1, and the concentration of the target component in the prediction sample can be calculated by using the obtained multiple relationship. Although the calculation of RAFA is rather complicated and can only be used to quantify an analyte in a sample at a time, this method can quantify target analyte in the presence of unknown interference, that is to say, the second-order advantage is obtained, which has attracted great attention. In 1986, RAFA was improved by Kowalski and coworkers and was renamed GRAM, which can obtain the concentration of several analytes in a single sample at a time. Based on this, Kowalski and coworkers developed DTLD in 1994, which can efficiently and simultaneously analyze data from multiple samples. Both GRAM and DTLD

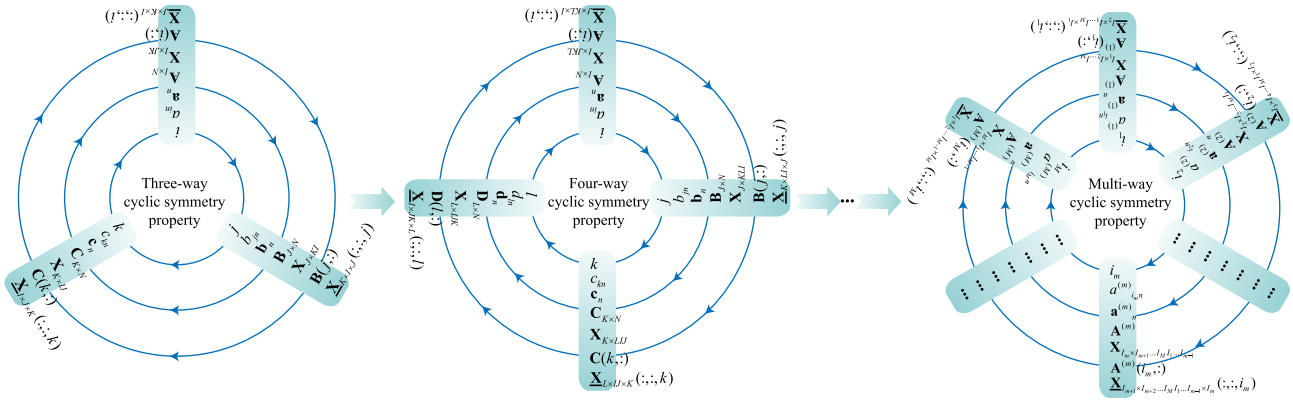

Fig. 6. Visualization of the cyclic symmetry property from trilinear model to multilinear model.

estimate the intrinsic profiles of each component in each sample by solving an eigenvector/eigenvalue problem. This type of algorithm is insensitive to the estimated number of components. However, DTLD requires the construction of two pseudo-samples, which unavoidably brings the loss of sample information. Moreover, DTLD can occasionally yield imaginary solutions and exhibit inflated variance, especially when the data array does not strictly conform to the trilinear model or when signal-to-noise ratio (SNR) is low. Therefore, they are generally applicable to a three-way data array with a good trilinear structure and high SNR, while possessing difficulty in accurately estimating the number of components.

The second group is iterative algorithms, which achieve the relatively unique decomposition of models by using ALS method. This kind of algorithm has a good resistance to model deviation and instrument noise. Nowadays, they have become the most widely used second-order calibration algorithms. The popular iterative second-order calibration algorithms including parallel factor analysis (PARAFAC) [32,34], alternating trilinear decomposition (ATLD) [35] and related derived algorithms [36,55], as well as multivariate curve resolution-alternating least squares (MCR-ALS) [41]. PARAFAC originated in the field of psychometrics and was later applied in the field of analytical chemistry. Through the strict minimization of residual sum of squares, PARAFAC can provide a good fit to three-way trilinear data array. However, PARAFAC algorithm also has some shortcomings, such as sensitivity to the number of components, initial values and data collinearity, slow convergence and easily dropping into the “swamp” of calculation. To overcome the weakness of the classical PARAFAC algorithm and other non-iterative algorithms, our group has done a lot of systematic and in-depth research works and developed a series of efficient algorithms. The earliest one is the alternating trilinear decomposition (ATLD) algorithm [35]. Its iterative calculation is based on the small size slice matrices, therefore the running memory is reduced and the calculation efficiency is greatly improved. The convergence rate of ATLD is still the fastest among all iteration algorithms reported so far. In addition, ATLD is insensitive to the overestimated component number and initial values. These features make the ATLD algorithm very advantageous when dealing with large-scale data, especially chromatography-based second-order data. A weakness of ATLD can be considered to require response data with a high SNR, therefore, a series of new algorithms were proposed later. The self-weight ATLD (SWATLD) [36] and the alternating penalty trilinear decomposition (APTLD) [55] optimize the objective function from different angles, which retains the advantages of fast convergence and insensitivity to the overestimated component number, and shows satisfactory performance when handling the data with higher noise and collinear levels. Yu et al. systematically compared the performance of PARAFAC, ATLD and SWATLD algorithms in the iterative optimization process [56], and proposed the algorithm combination methodology (ACM) [57]. The random initial values firstly are optimized by ATLD, and then the results of ATLD are optimized by SWATLD. Finally, PARAFAC is used to optimize the results of SWATLD, so that the advantages of each algorithm are utilized in a complementary way. Besides, our group have also developed many alternative algorithms with some enhanced features, such as coupled vectors resolution (COVER) [58], alternating COVER (ACOVER) [59], alternating coupled matrices resolution (ACOMAR) [60], alternating slice-wise diagonalization (ASD) [61], constrained PARAFAC (CPARAFAC) [62], pseudo-ALS (PALS) [63], penalty diagonalization error (PDE) [64], alternating fitting residue (AFR) [65], alternating normalization weighted error (ANWE) [66], alternating asymmetric trilinear decomposition (AATLD) [67], self-weighted alternating normalized residue fitting (SWANRF) [68], alternating coupled two unequal functions (ACTUF) [69], constrained alternating trilinear decomposition (CATLD) [70] and alternating residual trilinearization (ART) [71]. All of the above algorithms can decompose common trilinear model well and show certain advantage in specific situations. In 1995, Tauler et al. proposed the multivariate curve resolution-alternating least squares (MCR-ALS) for solving the problem that some three-way data arrays easily deviated from the trilinear structure [41]. The three-way data array is first unfolded into an augmented matrix with bilinear structure along the nonlinear mode (eg. a retention time mode with time shifts), and then MCR-ALS based on the bilinear model is employed to decompose the bilinear augmented matrix data, therefore it can well handle the non-trilinear chromatography data such as HPLC-DAD, GC-MS and LC-MS. However, MCR-ALS is sensitive to the pre-estimated component number. In addition, good initial values and sensible constraints (such as nonnegativity, unimodality, closure, etc.) are required to guarantee a unique solution due to the rotational ambiguities. Therefore, many related publications have discussed and developed effective initialization and constraint methods to obtain a reasonable decomposition of MCR-ALS [48,72]. Recently, Wang et al. proposed the alternating trilinear decomposition-assisted multivariate curve resolution (ATLD-MCR), which is implemented by using the pre-decomposition results of ATLD as the initial values and MCR strategy for each sample slice matrix [73]. Compared with the classical MCR-ALS, it shows stronger performance in some specific complex situations such as the presence of embedded overlap. PARAFAC2 as a variant of PARAFAC is also able to model non-trilinear chromatographic data with retention time profiles changes [74,75]. However, PARAFAC2 may need to consider more restricted conditions during use and is less flexible than MCR-ALS [76].

The third group is residual bilinearization-based algorithms, including the bilinear least-squares with residual bilinearization (BLLS/RBL) [77], unfolded and multiway PLS with RBL (U-PLS/RBL and N-PLS/RBL) [45], artificial neural network with RBL (ANN/RBL) and unfolded principal component analysis with RBL (U-PCA/RBL) [78]. U-PLS/RBL and N-PLS/RBL are the most popular algorithms and have a lot of applications. Notice that they are two-block algorithms and preserve the second-order advantage only by combining with RBL [44], which models the residues of U-PLS or N-PLS for the test sample as a sum of bilinear contributions from the unexpected components. U-PLS/RBL and N-PLS/RBL are flexible and may model three-way data arrays with trilinearity deviations in some cases [7], because they work under the latent variable philosophy. However, the increased flexibility comes at the price of some disadvantages, the most obvious one being that they do not provide accurate qualitative chemical profiles information for each pure component. As one can see, each algorithm has been shining in its own best-fit application fields. In actual analysis, it is recommendable to select one or more suitable algorithms based on the characteristics of the data and requirements for analysis.

It is worth mentioning that some classic methods, such as unfolded principal component analysis (U-PCA) and unfolded partial least squares (U-PLS) [42], can also process second-order data by rearranging them into vectors and then apply first-order calibration algorithms. Another classic method is multiway partial least squares (N-PLS) [43], which is a genuine multiway method. They were first used to analyze chemical second-order data before the above methods were developed, however, they do not possess the second-order advantage unless combining with RBL [44]. Recently, multi-level simultaneous component analysis (MSCA) [79–82] and mutual factor analysis (MFA) [83] were proposed to process second-order temperature-dependent NIR spectra. Both are based on the principle of PCA, and need to unfold three-way data array into a data matrix before use. Although they have some potentials in temperature-dependent NIR data analysis, they do not show a clear second-order advantage in quantitative analysis. Therefore, these methods need to construct a sufficiently representative calibration set of samples, which should include all the variability expected in unknown samples, just like first-order calibration.

3.5.2. Third-order calibration

Most of third-order calibration algorithms are direct extensions of the corresponding popular second-order calibration algorithms, and are summarized in Table 2. Four-way PARAFAC [34], AQLD [39] and APQLD [84] were developed by extending three-way PARAFAC, ATLD and APTLD to four-way case. AWRCQLD [38], FSWANRF [85], RSWAQLD [86], AFWRQLD [87] and CAQLD [70] have been applied to process excitation-emission matrix fluorescence-based four-way data array. They use tactfully designed objective functions so they possess a fast convergence speed being able to be applied to lower SNR data. SAQLD was proposed based on the “slicing” boxes representation of quadrilinear model, and it can be regard as a generalization of ATLD to four-way scenario [40]. Among iterative quadrilinear algorithms, usually the number of iterations required for SAQLD to reach the convergence threshold is quite small, however, its performance is not very good when dealing with the low SNR data. The recent FACM inherited the idea of initial values optimization of ACM, and its core iterative process was further optimized and simplified. AQLD and four-way PARAFAC were skillfully implemented in different stages of FACM, and the excellent performances of both have been integrated. In addition, the performances of some popular iterative quadrilinear algorithms were compared by numerical simulations and actual data sets [88]. All of the above algorithms work well for quadrilinear data, but they need to be used with caution when dealing with non-quadrilinear data. Four-way data arrays can be unfolded into a bilinear super-augmented matrix along linear breaking modes, and then the bilinear super-augmented matrix can be decomposed by MCR-ALS to achieve the purpose of processing non-quadrilinear data. APARAFAC seems to use a similar principle to deal with the non-quadrilinear data [89]. It involves decomposition of a three-way data array which is formed by unfolding a four-way data array along the linear breaking mode (usually the elution time mode). U-PLS and N-PLS coupled with RTL, which is the natural extension of RBL to three data modes, can also deal with quadrilinear deviations in some cases [90,91]. TLLS/RTL [90] and U-PCA/RTL [92] are also the extensions of the corresponding BLLS/RBL and U-PCA/RBL, respectively.

3.5.3. Fourth-order calibration and higher-order calibration

There are relatively few researches on fourth-order calibration and higher-order calibration, because the acquisition of the corresponding data is still difficult. The published fourth-order calibration and higher-order calibration algorithms are also collected in Table 2. PARAFAC can be applied to any number of ways. Five-way PARAFAC and *M*-way PARAFAC that can be used to process quinquelinear and multilinear data are easily developed based on multiway cyclic symmetry. Based on similar philosophies, AQQLD, AFWRQQLD, AMLD and CAMLD can be obtained. AQQLD was first developed by Qing et al. for the processing of fourth-order data, which were obtained by recording the HPLC-DAD data of a sample set as function of the reaction time and pH. It also has the advantage of fast convergence rate and being insensitive to the excessive component number [30]. Then AFWRQQLD as a variant of AQQLD was used for the analysis of imidacloprid in environmental waters to deal with the five-way data, which were obtained by recording EEM at different UV irradiation times for different volumes of sample [87]. CAMLD as an extension of CAQLD to *M*-way data array was proposed by Kang and coworkers, the related iterative formulas were also introduced [70]. U-PLS coupled with RQL, which can be regarded as an extension of RBL and RTL to four data modes, has been proposed by Maggio et al. to deal with a five-way excitation-emission-kinetic-pH-sample data array [28]. Furthermore, U-PLS and N-PLS combined with RML can be used for *M*-way data array [46].

Theoretically, all iterative fourth-order calibration algorithms can be extended to the corresponding higher-order calibration algorithms based on multi-way cyclic symmetry principle. For two classical examples, the objective functions of *M*-way PARAFAC can be achieved according to the fully stretched matrices form of multilinear model, while the objective functions of AMLD can be obtained according to the pseudo-fully stretched matrices form of multilinear model. The detailed objective functions and corresponding solutions of *M*-way PARAFAC and AMLD are collected in Supplementary material.

3.5.4. Softwares and toolboxes for multi-way calibration

There are some authoritative and freely available softwares for multi-way calibration. Most of them have graphical user interfaces allowing the execution of algorithms in an easy-to-use graphical environment, which greatly promotes the application of multi-way calibration methods in various fields. Table 3 summarizes a variety of free softwares and toolboxes based on MATLAB that can be employed for multivariate curve resolution and multi-way calibration.

Table 2
Algorithms for third- and higher-order calibration.

Type	Algorithm	Abbreviation	Required data property	Reference
Third-order calibration	(1) Four-way PARAFAC	Four-way PARAFAC	Quadrilinear	[34]
	(2) Alternating quadrilinear decomposition	AQLD	Quadrilinear	[39]
	(3) Alternating penalty quadrilinear decomposition	APQLD	Quadrilinear	[84]
	(4) Alternating weighted residual constraint quadrilinear decomposition	AWRCQLD	Quadrilinear	[38]
	(5) Four-way self-weighted alternating normalized residue fitting algorithm	FSWANRF	Quadrilinear	[85]
	(6) Regularized self-weighted alternating quadrilinear decomposition	RSWAQLD	Quadrilinear	[86]
	(7) Alternating fitting weighted residue quadrilinear decomposition	AFWRQLD	Quadrilinear	[87]
	(8) Alternating weighted quadrilinear decomposition	AWQLD	Quadrilinear	[93]
	(9) Slicing alternating quadrilinear decomposition	SAQLD	Quadrilinear	[40]
	(10) Constrained alternating quadrilinear decomposition	CAQLD	Quadrilinear	[70]
	(11) Four-way algorithm combination method	FACM	Quadrilinear	[88]
	(12) Multivariate curve resolution coupled to alternating least Squares	MCR-ALS	Quadrilinear and non-quadrilinear	[41]
	(13) Augmented parallel factor analysis	APARAFAC	Quadrilinear and non-quadrilinear	[89]
	(14) Unfolded partial least-squares/residual trilinearization	U-PLS/RTL	Quadrilinear and non-quadrilinear	[90]
	(15) Multiway partial least-squares/residual trilinearization	N-PLS/RTL	Quadrilinear and non-quadrilinear	[91]
	(16) Trilinear least-squares/residual trilinearization	TLLS/RTL	Quadrilinear	[90]
	(17) Unfolded principal component analysis/residual trilinearization	U-PCA/RTL	Quadrilinear and non-quadrilinear	[92]
Fourth-order calibration	(1) Five-way PARAFAC	Five-way PARAFAC	Quinquelinear	[34]
	(2) Alternating quinquelinear decomposition	AQQLD	Quinquelinear	[30]
	(3) Alternating fitting weighted residue quinquelinear decomposition	AFWRQQLD	Quinquelinear	[87]
	(4) Unfolded partial-least squares/residual quadrilinearization	U-PLS/RQL	Quinquelinear and non-quinquelinear	[28]
N-way calibration	(1) *M*-way PARAFAC	*M*-way PARAFAC	Multilinear	[34]
	(2) Alternating multilinear decomposition	AMLD	Multilinear	This review
	(3) Constrained alternating multilinear decomposition	CAMLD	Multilinear	[70]
	(4) U-PLS coupled to residual multilinearization	U-PLS/RML	Multilinear and non-multilinear	[46]
	(5) N-PLS coupled to residual multilinearization	N-PLS/RML	Multilinear and non-multilinear	[46]

Table 3
Free software and toolbox for multivariate curve resolution and multi-way calibration.

Name	Algorithm	Available at	Reference
N-way Toolbox	PARAFAC, PARAFAC2, GRAM, DTLD, U-PLS, N-PLS	http://www.models.life.ku.dk/nwaytoolbox	[94]
MCR-ALS GUI	MCR-ALS	http://www.mcrals.info/	[48,72]
MCRC Software	MCR-ALS	http://sharif.edu/~h.parastar/MCRC%20Software.rar	[95]
GUIPRO GUI	MCR-ALS	http://personal.ecu.edu/gemperlinep	[96]
MVC2 GUI	PARAFAC, ATLD, APTLD, SWATLD, BLLS/RBL, U-PLS/RBL, N-PLS/RBL	http://www.iquir-conicet.gov.ar/descargas/mvc2.rar	[97]
MVC3 GUI	Four-way PARAFAC, APQLD, AWRCQLD, TLLS/RTL, U-PCA/RTL, U- PLS/RTL, N-PLS/RTL, MCR-ALS, APARAFAC, PARAFAC2	http://www.iquir-conicet.gov.ar/descargas/mvc3.rar	[98,99]

4. Some fundamental issues

4.1. Data preprocessing

4.1.1. Dealing with the scattering in excitation-emission matrix fluorescence

The EEM spectra often includes light scattering effects, such as first- and second-order Rayleigh and Raman scatterings (Fig. 7(a)), which destroys the multilinear structure of data array, so that multi-way calibration algorithms cannot be used directly. Therefore, data preprocessing is usually necessary before performing EEM fluorescence data analysis. Low-intensity Raman scattering can be removed by subtracting the background signal using a blank sample, however, this method cannot eliminate the effects of Rayleigh scattering. The easiest ways to avoid Rayleigh scattering is to choose an appropriate region of spectra (the black box in Fig. 7(b)). Obviously, this method will result in loss of valid data and may not be suitable for simultaneous analysis of multiple target analytes. To overcome the above shortcomings, many other methods have been proposed to handle Rayleigh scattering for the trilinear modeling, such as inserting missing values or zero values [100,101], application of nonnegativity and unimodality constraints [102,103], weighting methods [104–106], interpolation methods [107,108], modeling Rayleigh scattering by a separate component with the shifting method [109], two-direction resection PARAFAC (TDR-PARAFAC) [110]. These methods directly or indirectly process scattering effects to ensure successful implementation of trilinear decomposition. It is worth mentioning that an interpolation method proposed by Bahram and coworkers is the most frequently cited method [108]. It handles scattering using interpolation in the scattering region in such a way that the interfering signal is, at best, removed. It has the advantage of being fast and does not require additional input other than selecting the scattering region. In fact, this method can be seen as a direct pretreatment, where interpolation values are inserted into the data set. Then multiway calibration algorithms can be implemented.

Recently, Chiappini et al. developed a freely available chemometric MATLAB toolbox 'EEM_corr' with graphical user-friendly interface to deal with scattering from EEM fluorescence data [111]. It was designed for users who would need a simple and fast data pre-processing tool or did not have professional chemometrics and programming experience. Three methodologies including blank subtraction, interpolation method and Gaussian fit-based method were used in the software. Moreover, there are automatic and semi-automatic/manual modes available for the user to select and use while the correction is performed. The GUI codes written in MATLAB environment have been released and can be freely available at https://fbcb.web1.unl.edu.ar/laboratorios/ladaq/download/.

4.1.2. Dealing with time shifts in chromatographic analysis

Retention time shifts in chromatographic data severely affect the implementation of multi-way calibration. Taking second-order calibration as an example, many second-order calibration algorithms require that each chemical component has the same profiles (including the retention time and spectral modes) in all samples, that is, the data should conform to trilinear structure. However, the presence of time shifts may destroy the trilinear or multilinear structure, resulting in erroneous decomposition results. Therefore, many strategies have been developed to solve the problem of retention time shifts when performing second-order or higher-order calibration. The mainstream strategies are based on two basic philosophies. The first one is that using peak alignment methods to remove the effects of time shifts, and then implementing multi-way calibration algorithms. Peak alignment methods can be implemented by two ways: (1) making the utmost of data structure, such as iterative target transformation factor analysis (ITTFA) [112], rank alignment (RA) [113–115], parallel factor analysis alignment and abstract subspace difference (ASSD) method [116]; (2) seeking maximum correlation between chromatograms, such as multi-wavelength correlation optimized warping (COW) [117,118], the interval correlation optimised shifting algorithm (icoshift) [119,120] and the ChromAlign method [121]. The second strategy is to process the chromatographic data with flexible algorithms capable to process non-trilinear or non-multilinear data, which seems to be more direct and faster than the first strategy. For example, MCR-ALS and PARAFAC2 are usually used for handling the second-order chromatographic data with time shifts. In this regard, residual bilinearization-based algorithms

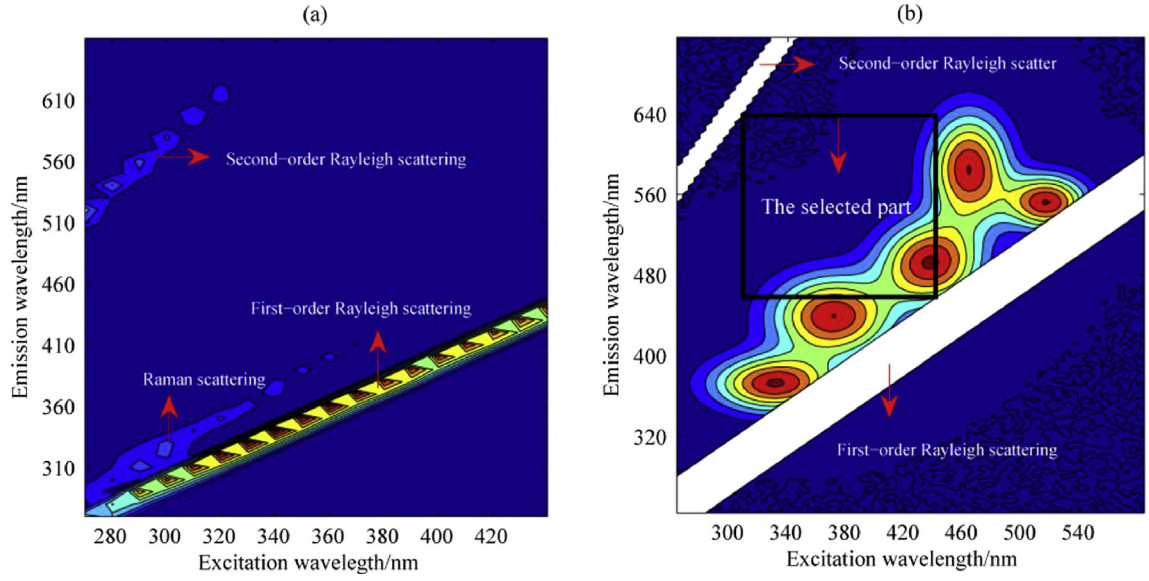

Fig. 7. (a) The EEM spectra of a water sample, where Rayleigh and Raman scatterings are highlighted. (b) A simulated EEM spectra where Rayleigh scatterings are substituted by missing data. Adapted from Ref. [110].

such as U-PLS/RBL and N-PLS/RBL have also been found to be useful. Yin and coworkers found that ATLD algorithm can tolerate slight time shifts when processing HPLC-DAD data and the results obtained by ATLD and MCR-ALS have no significant difference [122]. This property has also been reflected in other articles, which may be because ATLD can explore the trilinear structure of data and use the linear structure to fit the nonlinear structure. However, ATLD is powerless for the data with large time shifts. Recently, Wang and coworkers proposed a novel ATLD-MCR to directly handle second-order chromatographic data with time shifts [73]. ATLD is used to provide very good initial values quickly and efficiently, and the MCR strategy is used in turn for each sample slice matrix.

4.1.3. Dealing with baseline/background drift

Baseline drift often occurs in chromatography and even spectroscopy. It may come from the instability of instrument, gradient elution in chromatography, the changes of fragmentor in LC-MS, the changes in background noise and so on, which produce invalid qualitative or quantitative information and affect the accuracy of the results. Amigo and coworkers have reviewed the mathematical models used in solving chromatographic data issues including baseline/background drift [123]. In general, three approaches are used for baseline/background correction: (1) Subtract a blank background (2) Use curve-fitting methods to fit a curve (eg, a polynomial). or surface, and then subtract this curve or surface from the overall signal. (3) Model and remove the baseline as part of an overall (factor) model. The first approach is the simplest one, but it can only be used when the background drift is constant (eg, background drift resulting from a fixed gradient elution between samples when the instrument is very stable). The second approach is widely available in commercial software, however it is not always the best from a data-quality point of view. The third approach is often recommended and it is easy to use in combination with multi-way calibration methods, because the background drift usually has bilinear or even trilinear structure in higher-order instrumental data. Our research group has also conducted a series of studies on this aspect. In 2007, a chromatographic background drift correction strategy was proposed by Zhang and coworkers for LC-LC-DAD data [124]. The basic idea includes modeling the background drift as one component or factor when performing ATLD algorithm, and then extracting the baseline drift component and subtracting it from the raw data. Therefore, the background drift signal is explicitly modeled and removed from raw data and not included into the calibration. Similarly, the strategy can also be used based on other second-order calibration algorithms, such as PARAFAC and MCR-ALS. In addition, this strategy is also used for the removal of background drift in LC-MS [125] and EEM fluorescence and phosphorescence spectra [126]. What's more, it is also an effective way to make full use of the background information of zero-component region and then remove the background drift in the model. In 2013, Yu and coworkers proposed orthogonal spectral space projection (OSSP) for background drift correction of second-order chromatographic data [127]. The spectra of chromatographic background were estimated by using ATLD to decompose the zero-component region of the three-way data array $\underline{\mathbf{X}}$. Other methods such as the objective subtraction of solvent spectrum with iterative use of PARAFAC and PARAFAC2 (OSSS-IU-PARAFAC and OSSS-IU-PARAFAC2) [128], the method based on PCA and SIMPLISMA [129], are also reported to be used for background drift correction of high-order data in some cases.

4.1.4. Data partition in chromatographic analysis

When there are a lot of analytes of interest to be analyzed or the retention time is long, data partition as a useful preprocessing method is often used before performing second-order calibration on chromatographic data. In this case, firstly, the raw three-way data array should be divided into some sub-arrays along the retention time mode, where each sub-array contains the information of several analytes of interest rather than the information of all anayltes of interest in the raw three-way data array. Then, the second-order calibration algorithm is used to process these sub-arrays with smaller sizes in turn. Two obvious advantages are brought by data partition. On the one hand, it removes the invalid information in the data, and the running speed of the second-order calibration algorithm is greatly improved. On the other hand, it can avoid the influence of data collinearity and nonlinear factors to a certain extent. There are several important factors need to be considered when using data partition strategy in order to make the algorithm work better. (1) The large zero-component regions need to be avoided; (2) a sub-array should not be too large in order to save computing memory; (3) the number of target analytes in one sub-array is generally under ten to avoid potential collinearity resulted from analytes with similar spectra or their linear combination, and two analytes with very similar spectra are best not placed in the same sub-array; (4) the chromatographic peak of target analytes should not be divided by two sub-arrays. Similarly, data partition strategy is also suitable for the pretreatment of higher-order chromatographic data.

4.2. Estimation of the chemical rank

Estimating the chemical rank (the number of factors or components) of the trilinear model is always an important step before decomposing a three-way data array. Although some algorithms (such as ATLD and SWATLD) are insensitive to the overestimated chemical rank, they still require that the selected chemical rank is not less than the underlying one. In general, if wrong chemical rank is selected to fit the model, the fitting error and result deviation will arise and even the two factor degeneracy (2FD) [130] will occur.

To guarantee the successful implementation of the algorithm with acceptable resolution and calibration results, a large number of methods have been developed for estimating the chemical rank of three-way data array. They can be mainly classified into two classes. The first class includes trilinear model-based methods, such as split-half analysis [34], Wu's maximum rank method [35], ADD-ONE-UP [131], core consistency diagnostic (CORCONDIA) [132], self-weighted alternating trilinear decomposition and Monte Carlo simulation (SWATLD-MCS) [133] and angle distribution of loading subspaces (ADLS) [134].

The basic idea of split-half analysis is to divide the three-way data array into two halves and then implement trilinear decomposition on both halves. If a correct number of components is chosen, the same result (same loadings in the undivided modes) on both data sets will be obtained due to the decomposition uniqueness of the trilinear model. However, it requires some splitting skill for different data and a poor splitting scheme may bring the wrong result.

Wu et al. proposed a simple maximum rank method to roughly estimate the chemical rank for ATLD and ATLD's variants, which can be mathematically expressed as:

$$\mathrm{rank}(\underline{\mathbf{X}}) = \max\{\mathrm{rank}(\mathbf{X}_{I\times JK}), \mathrm{rank}(\mathbf{X}_{J\times KI}), \mathrm{rank}(\mathbf{X}_{K\times IJ})\} \quad (13)$$

If the size of the unfolded matrix is too large, it can also be calculated as follows:

$$\mathrm{rank}(\underline{\mathbf{X}}) = \max\left\{\mathrm{rank}\left(\mathbf{X}_{I\times JK}\mathbf{X}_{I\times JK}^{T}\right), \mathrm{rank}\left(\mathbf{X}_{J\times KI}\mathbf{X}_{J\times KI}^{T}\right), \mathrm{rank}\left(\mathbf{X}_{K\times IJ}\mathbf{X}_{K\times IJ}^{T}\right)\right\} \tag{14}$$

or

$$\mathrm{rank}(\underline{\mathbf{X}}) = \max\left\{\mathrm{rank}\left(\sum_{i=1}^{I}\mathbf{X}_{i..}\right), \mathrm{rank}\left(\sum_{j=1}^{J}\mathbf{X}_{.j.}\right), \mathrm{rank}\left(\sum_{k=1}^{K}\mathbf{X}_{..k}\right)\right\} \tag{15}$$

where rank (.) in curly brackets denotes that calculating the rank of a matrix based on a singular value decomposition (SVD) with a default tolerance.

ADD-ONE-UP, proposed by Chen et al., in 2001, fits reconstructed three-way data arrays in turn by using PARAFAC as the number of components gradually increase, and then determines the chemical rank by examining the related residual sum of squares (SSR). The eigenvalues of factor analysis and the residuals of trilinear decomposition are fully used. It has a strong ability to cope with heteroscedastic noise, heavy collinearity and varying backgrounds. However, it is time-consuming due to the need of running PARAFAC for many times, and sometimes it may suffer from 2FDs and obtain inaccurate results.

CORCONDIA is one of the most popular methods, which determine the chemical rank by comparing the superdiagonal array $\underline{\mathbf{T}}$ in PARAFAC model and the least squares-fitted $\underline{\mathbf{G}}$ in Tucker3 model with a gradually increasing number of components. The similarity between $\underline{\mathbf{T}}$ and $\underline{\mathbf{G}}$ can be defined as:

$$\text{core consistency} = 100\left(1 - \frac{\sum_{d=1}^{N}\sum_{e=1}^{N}\sum_{f=1}^{N}\left(g_{def} - t_{def}\right)^2}{N}\right) \tag{16}$$

where g_{def} is the element of $\underline{\mathbf{G}}$; t_{def} is the element of $\underline{\mathbf{T}}$; N is the number of components in the model, which can be regarded as the sum of squares of the elements of $\underline{\mathbf{T}}$. A core consistency close to 100% means that it is an appropriate model. Generally, a core consistency above 90% can be considered as “very trilinear”, whereas a value close to 50% means a problematic model with both trilinear and nontrilinear variation. A value close to zero or even negative implies an invalid model. Once the most suitable chemical rank is exceeded, the core consistency value will decrease sharply, therefore the most suitable chemical rank can be determined. Although CORCONDIA is a useful method, it still suffers from the disadvantage of slow calculation speed.

SWATLD-MCS estimates the chemical rank by comparing the values of sorted mean relative-concentration (SMRC), which are obtained from SWATLD by decomposing one pseudo three-way data array created by Monte Carlo simulation. The method shows a lower computational burden than ADD-ONE-UP and CORCONDIA, because it requires SWATLD to be run only once. In addition, this new methodology can be extended to (1) other second-order calibration algorithms with the property of insensitive to excessive factors and (2) the estimation of the chemical rank of high-dimensional data array when higher-order calibration algorithms combined with MCS are used. For example, AWQLD-MCS as a novel extension of SWATLD-MCS was developed to estimate the chemical rank of four-way data array [135].

ADLS combines the bootstrap resampling and split-half method with some new strategies. The four steps for ADLS are as follows. Firstly, bootstrap resampling is used to get a bootstrap set with 40 resamples; secondly, the global loading and the subloading are obtained by using a three-way analysis algorithm such as PARAFAC or SWATLD; thirdly, the similarity of globalmodel and submodel is measured by the angle of the global loadings and bootstrap subloadings; fourthly, the box plot is used to show the variation of the subspace angle. The range of the angle is 0°−90°, and the angle close to 0° means a fitted model. The largest number of components corresponding to a small range of angles (no more than 45°) is selected as chemical rank.

The second class includes non-model methods including imbedded error (IE) [136], factor indication function (IND) [137], orthogonal projection approach (OPA) [138], multi-way cross-validation [139], the Ratio between Eigenvalues in Smoothed PCA and their counterparts in Ordinary PCA (RESO) [140], principal norm vector (PNV) [141] and so on. In 2004, Wasim and Brereton compared about 20 methods for estimating the number of components in chromatographic systems and analyzed the advantages and disadvantages of these methods [142]. In addition, more and more techniques based on subspace projection have been used to estimate the chemical rank, including two-mode subspace comparison (TMSC) [143], pseudo-sample extraction and the projection technique (PPT) [144], linear transform method incorporating Monte Carlo simulation (LTMC) [145], subspace projection of pseudo high-way array (SPPH) [146], region-based on moving windows subspace projection technique (RMWSPT) [147], vector subspace projection with Monte Carlo simulation (VSPMCS) [148], Fourier transform coupled with robust statistical analysis (DFT-RSA) [149]. This type of method based on subspace projection usually has a fast calculation speed and can overcome a certain degree of data collinearity and noise. However, when there are non-trilinear factors (such as non-trilinear background and scattering) in the system, their accuracy may be affected.

Although all of the above methods can be used for rank estimation of high-dimensional data array, they are difficult to ensure correctness in all practical situations. Therefore, in actual analysis, two or more methods are recommended to confirm the analysis results.

4.3. Experimental design

Designing calibration set and test set is an important part in multi-way calibration method. The calibration set is often prepared by just mixing a series of standard solutions of target analytes, and it does not need to contain all the responsive components presented in a future test sample, which is the embodiment of the second-order advantage. A calibration set often contain more than five calibration samples and their concentration levels are recommended to be designed by uniform design, which is suitable for the concentration of each analyte with multiple levels and is good at avoiding data collinearity. For example, if one wants to design seven concentration levels for four target analytes, an $U_7(7^4)$ uniform design [150,151] for this seven-level, four-factor concentration design needs to be adopted, which means only seven experiments (i.e., seven calibration samples) are required.

A test set usually contains real samples of the system studied and spiked prediction samples. Real samples may contain target analytes and unknown interferents with overlapping signals, however, these unknown interferents do not affect the accurate quantitative analysis of target analytes in multi-way calibration. Spiking is the most common and simple method to evaluate the accuracy of a method. In spiked prediction samples, appropriate amounts of all target analytes are spiked with the system studied.

They are used to validate whether a multi-way calibration method can accurately predict the concentrations of all the analytes of interest in the system studied, even in the presence of interferents. Multilinear decomposition will be implemented in the high-dimensional data array formed by joining calibration and test sample data. It is worth mentioning that as long as the number of components is selected correctly, one can determine the concentration of each target analyte in different real samples with varying backgrounds by only one modeling.

The solvent blanks are samples containing only solvent. Before implementing multilinear decomposition, they can be used to subtract the response of the blank solvent from the response of each sample in order to eliminate or reduce the effects of some factors such as the background value of the solvent, Raman scattering in fluorescence analysis and background drift due to gradient elution in chromatographic analysis. Multi-way calibration methods based on the multilinear models can use an additional component to model the background drift signal, so in some applications of multi-way calibration, the solvent blanks are not necessary.

4.4. Figures of merit

Analytical figures of merit (FOMs) such as sensitivity (SEN), selectivity (SEL), the limit of detection (LOD) and the limit of quantitation (LOQ) are important numerical parameters used to evaluate the quantitative performance of multi-way calibration methods. Professor Olivieri published a review named “Analytical Figures of Merit: From Univariate to Multiway Calibration” in 2014 in Chemical Reviews [13], which summarized sensitivity expressions from univariate to multi-way calibration based on net analyte signal (NAS) concept and uncertainty propagation, respectively, and then the remaining figures of merit are discussed, with emphasis on their peculiarities regarding the multi-way calibration field. The FOMs calculation formula for the multi-way calibration method based on a specific algorithm could be found in the above review.

4.5. General procedure of multi-way calibration

The procedure of the multi-way calibration method is more complicated than that of the zero-order and first-order calibration methods, because more factors should be considered throughout the process, such as the choice of models and algorithms, as well as the above details (Sections 4.1–4.4). The general procedures of multi-way calibration methods can be summarized in the following steps: (1) Obtain high-order data for each sample according to a reasonable experimental design. (2) Perform pre-processing on the data. It can eliminate the effects of non-multilinear factors, such as scattering in fluorescence analysis, time shifts and baseline drifts in chromatographic analysis, and can make the structure of the data conform to the common decomposition model. (3) Select models and algorithms based on data properties. This step is very important because mismatched models can affect computational efficiency and even lead to erroneous results. For a strict multilinear data array, the multilinear decomposition model is the first priority due to its efficient and unique decomposition. Once the model is established, we can determine the corresponding algorithm according to data characteristics. However, the presence of breaking modes may occur in actual analysis, such as time shifts in the chromatogram, in which case algorithms based on the flexible model, such as MCR-ALS based on the MCR bilinear decomposition model, are more appropriate. Of course, data preprocessing in step 2 can also make the data conform to a certain model in advance. (4) Select the appropriate number of components and perform data analysis by using multi-way calibration algorithm. (5) Quantification of each analyte. For the results of general multilinear decomposition algorithms, first identify the column position of analyte in the resolved matrix according to correlation coefficient, and then implement pseudo-univariate calibration for analyte quantitation, that is, the concentrations of each target analyte in prediction samples are predicted by the regression equation obtained in a univariate regression of the resolved relative concentration against the real concentration based on the calibration set. (6) Calculate the figures of merit and generate a report. For example, basic flow chart of the second-order calibration method based on the trilinear model is shown in Fig. 8.

More intuitively, taking the analysis of the three-way HPLC-DAD data array by using second-order calibration method based on the ATLD algorithm as an example, the general procedure is shown in Fig. 9.

5. Applications

Based on the different dimensions of multi-way data array, this paper mainly focuses on the recent applications of the three-, four-, and five-way calibration methods for quantitative analysis of target analytes in complex systems from 2015 to 2020.

5.1. Examples of three-way calibration

EEM fluorescence data, as the most common second-order data, can be easily obtained from a fluorescence spectrophotometer. Broad excitation and emission spectra are important characteristics of molecular fluorescence, therefore signal overlap is very common in fluorescence analysis, which seriously affects the qualitative and quantitative analysis of analytes of interest in complex systems. The second-order calibration method with “second-order advantage” is naturally combined with EEM fluorescence to form a low-cost, fast and green quantitative analysis strategy. The sensitivity of EEM fluorescence is relatively high and the generated three-way EEM data array generally conforms to the trilinear decomposition model. Therefore, almost all second-order calibration algorithms are capable of quantitative analysis of EEM data. Multilinear decomposition model-based second-order calibration algorithms are the most commonly used and preferred algorithms for analyzing this type of data, because they have the characteristics of

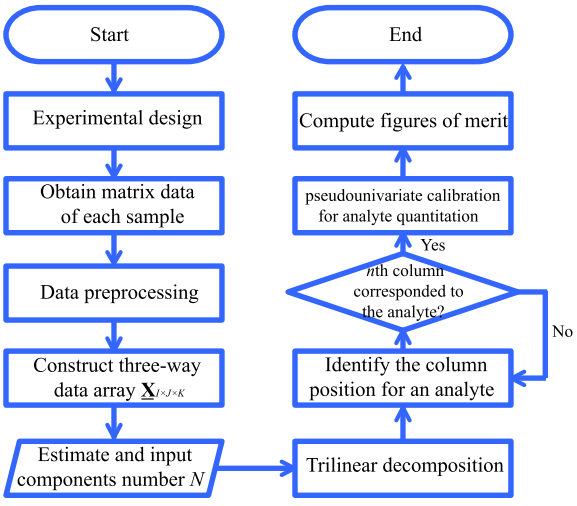

Fig. 8. Basic flow chart of the second-order calibration method based on the trilinear model.

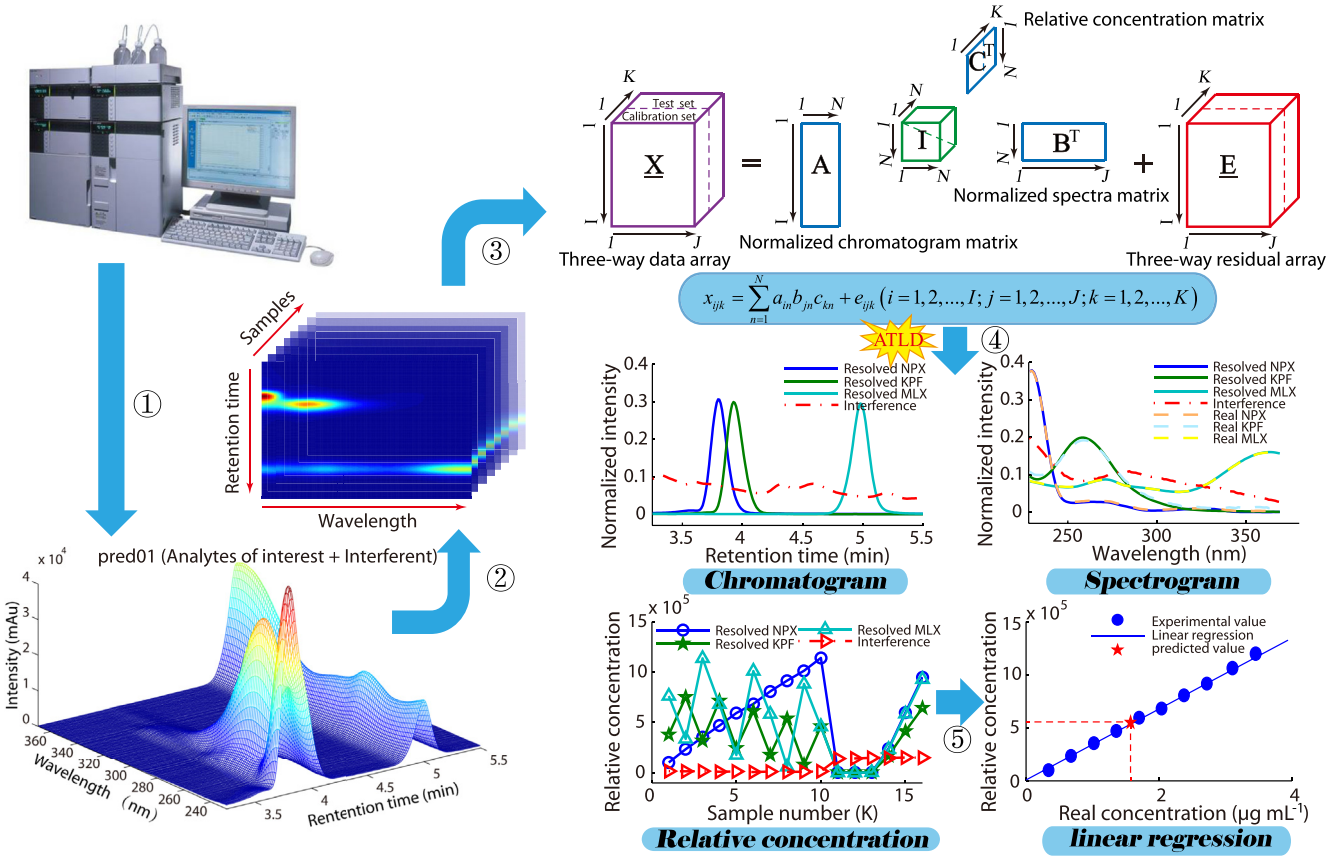

Fig. 9. Main experimental steps of HPLC-DAD assisted with second-order calibration method based on ATLD algorithm. (1) Collecting matrix data of each sample; (2) stacking the data matrix to form a three-way data array; (3) building the trilinear component model for second-order calibration; (4) decomposing the proposed model by ATLD algorithm; (5) univariate linear regression to obtain the actual concentration of each target analyte in prediction samples. Adapted from Ref. [219].

unique decomposition and providing clear qualitative profiles. In a few cases, the EEM data set deviated from trilinearity due to inner filter effects, a report confirmed U-PLS/RBL was more effective [152]. Table 4 summarizes the selected recent examples of second-order/three-way calibration based on trilinear decomposition models, and applications involving EEM data are listed as the first category. Other models and multiple models are also used for EEM data analysis, and the related recent examples are listed in Table 5. In general, the prerequisite for using fluorescence analysis is that the analytes have endogenous fluorescent signals or that chemically derived products of analytes have strong fluorescent signals. Moreover, one can optimize the pH and use sensitizers such as cyclodextrin and sodium dodecyl sulfate (SDS) to increase analytical sensitivity. Complex sample preprocessing and prior separation can often be avoided when using EEM fluorescence coupled with second-order calibration method.

Moreover, UV—vis spectrophotometer or fluorometer combined with a linear mode such as the first-order kinetic reaction or pH can also obtain the second-order data. Second-order calibration methods based on PARAFAC, SWATLD and APTLD algorithms, respectively, have been used for resolving the three-way absorbance spectra-pH data for simultaneous determination of the two colorants tartrazin and sunset yellow illegally added in saffron. To eliminate the rank deficiency, a three-way variation array was obtained by subtracting the first pH spectrum from each spectrum at each pH. Compared with the reported method using HPLC, the separation step and time-consuming analysis can be avoided [153]. Because this type of data often exhibits strong collinearity or deviation from trilinearity in dependence of instrument modes, bilinear-based MCR models and latent variables-based models may perform better. The simultaneous determination of malachite green and crystal violet in water was implemented by absorbance-pH data coupled with N-PLS/RBL. N-PLS/RBL can handle the rank deficiency problem [154]. Kinetic-spectroflourimetric data coupled with MCR-ALS as a non-separative method was proposed for the determination of lysine (lys), leucine (leu) and phenylalanine (phe) enantiomers in their racemic mixture using chiral reagents [155]. Other examples are listed in Table 5. Although the acquisition of this type of second-order data is relatively simple, and the second-order advantage can also be achieved, it has not yet attracted enough attention.

Second-order calibration method also has a large number of applications in chromatography combined with various detectors (such as HPLC-DAD, HPLC-FLD, GPC-DAD, LC-MS, GC-MS, etc.). The structure and properties of these second-order data are very similar. One instrument mode is chromatographic retention time and the other instrument mode is multi-channel spectra or mass spectra. Therefore, the three-way data array obtained by this way may often deviate from trilinearity due to the chromatographic retention time shifts, and the solutions have been given in Section 4.1.2. As shown in Table 4, based on trilinear decomposition model, ATLD algorithm is widely used to process second-order chromatographic data, mainly due to the excellent properties of the ALTD algorithm, such as the fastest convergence and tolerance for slight time shifts. As shown in Table 5, based on other models, MCR-ALS is a popular choice, because it can be applied by augmentation in the time direction in the presence of time profile changes [41]. By this way, non-trilinear data array is

Table 4
Selected recent examples of second-order/three-way calibration based on trilinear decomposition models.

Analytes	Matrix	Algorithm	Challenge	Comment	Reference
EEM data					
Diuretics: amiloride and triamterene	Plasma and urine	ANWE	Overlapped peaks and unknown interferences	Little prior purification and no prior separation	[184]
Phytochemicals: magnolol and honokiol	Herb and plasma	PARAFAC and SWATLD	Overlapped peaks and unknown interferences	Avoid preconcentration and with only simple disposal process	[185]
Antihypertensives: valsartan and amlodipine besylate	Plasma	PARAFAC and ATLD	Analytes have weak fluorescent property; overlapped peaks and uncalibrated interferences	Sodium dodecyl sulfate was used for fluorescence enhancement; a rapid and reliable method	[186]
Anticarcinogen: CPT-11 lactone and CPT-11 carboxylate	PBS buffer and plasma	ANWE	Real-time quantitative analysis; overlapped signals among analytes and interferents	Three-way EEM-kinetic fluorescence data in test set; a simple and fast way for real-time quantitative analysis	[187]
Decongestant: naphazoline; Vitamin: pyridoxine	Eye drops	ATLD	Overlapped peaks and unknown interferences	No pretreatment	[188]
Antidiabetic and antihypertensive drugs: repaglinide and irbesartan	Plasma	ATLD	Analytes are weakly fluorescent drugs; overlapped peaks and unknown interferences	Sodium dodecyl sulfate was used for fluorescence enhancement; a rapid and simple method	[189]
Nephrotoxic aristolochic acids: AA-I and AL-I	Chinese herbal medicines	APTLD and SWATLD	AA-I is non-fluorescent; overlapped signals among analyte and interferents	A chemical derivatization that converted the non-fluorescent AA-I to high-fluorescent AL-I; no prior separation and clear-up process	[190]
The metabolic coenzymes reduced: NADH and FAD	Plasma	CATLD and SWATLD	The quantitative kinetic analysis of analytes in human plasma; overlapped peaks and unknown interferences	Not only the quantitative analysis but also the real-time kinetic analysis	[191]
Aflatoxins: B_1 and G_1	Foodstuffs: maize, flour, honey and edible oil	SWANRF	Analytes with weak fluorescent; overlapped peaks and unknown interferences	Fluorescence detection enhanced through photochemical derivatization; high sensitivity and low LOD (few ppb); LC-MS/MS method as a comparison	[192]
PAHs: DB[*a*,*l*]P, DB[*a*,*h*]-P, DB[*a*,*i*]P, DB-[*a*,*e*]P, N [2,3-*a*]P	Coal-Tar	PARAFAC	Serious multi-peak overlap and unknown interferences	EEMs were recorded at 4.2 K to provide sufficient spectral narrowing; direct determination without chromatographic separation	[193]
Leucomalachite green, leucocrystal violet, malachite green and crystal violet	Fish and shrimp	PARAFAC and ATLD	CV and MG are non-fluorescent; overlapped peaks and unknown interferences	CV and MG were reduced to fluorescent LMG and LCV by reacting with sodium borohydride; dispersive liquid−liquid microextraction was adopted; HPLC-FLD method for confirmation	[194]
Optical brighteners: CBS-X and CXT	Laundry powders, agriculture soils and wastewater	PARAFAC, SWATLD and APTLD	Overlapped peaks and unknown interferences	No separation or preconcentration; comparison of trilinear second-order calibration algorithms	[195]
Phytochemicals: umbelliferone and scopoletin	Traditional Chinese medicine	ATLD	Overlapped peaks and unknown interferences	A fast, simple and economical method; HPLC-DAD method for confirmation	[196]
Arbutin and hydroquinone	Cosmetic products	ATLD	Serious multi-peak overlap and unknown interferences	Low LOD; HPLC-DAD method for confirmation	[197]
Flavan-3-ols catabolites: 3-hydroxyphenylacetic acid, 4-hydroxyphenylacetic acid and syringic acid	Urine	PARAFAC	Overlapped peaks and unknown interferences	A fast and cheap method to screen polyphenol intake and biomarkers	[198]

(*continued on next page*)

Table 4 (*continued*)

Analytes	Matrix	Algorithm	Challenge	Comment	Reference
Bisphenol A	Food simulant	PARAFAC	Experimental design for studying migration of Bisphenol A; overlapped fluorescence signals.	Migration test of Bisphenol A from polycarbonate cups was carried out	[199]
Warfarin and aspirin	Human plasma and urine	ATLD	Overlapped peaks and unknown interferences	Simple pretreatment and no prior separation	[200]
PAHs: naphthalene, fluorene, phenanthrene, anthracene, fluoranthene and pyrene	Oil-field wastewater	PARAFAC	Serious multi-peak overlap and unknown interferences	Neither time-consuming sample pretreatments nor toxic organic reagents; GC–MS method for confirmation	[201]
Dyes: Rhodamine B, rhodamine 6G and rhodamine 123	Chilli	ATLD	Overlapped peaks and unknown interferences	Dyes may be illegally added into food commodities to reinforce the natural color; HPLC-FLD method for confirmation	[202]
Food colorants: cochineal and erythrosine	Cherries in syrup	PARAFAC	The presence of quenching effect; high overlapping signals	The fluorescence signal of erythrosine depends on the amount of cochineal which acts as a quencher; HPLC-DAD method for confirmation	[203]
Agrochemicals: carbendazim and chlorothalonil	Peanut oil	ATLD and APTLD	Overlapped peaks and unknown interferences	Low LOD, low cost, rapidity, eco-friendly and with simple preparation	[204]
Agrochemicals: thiabendazole, indole-3-acetic acid and 1-naphthylacetic acid	Soil and sewage	SWANRF	The signal instability and variation in responses recorded on different instruments; overlapped peaks and unknown interferences	Piecewise direct standardization was applied to correct and compensate the instability and variation of the signals; HPLC-FLD method for confirmation	[205]
Phytochemicals: scopoletin and scopolin	Traditional Chinese medicine	PARAFAC	Overlapped peaks and unknown interferences	Time-resolved fluorescence for qualitative analysis; HPLC-FLD method for confirmation	[206]
Bisphenol A and diphenyl carbonate	Polycarbonate plastics	ATLD	High overlapping signals	Simple sample pretreatment and low cost	[207]
Pirimiphos-methyl	Maize	PARAFAC	Matrix effect and unknown interferences	Piecewise direct standardization (PDS) for overcoming the matrix effect; surfactant micelles for fluorescence enhancement	[208]
Fluoroquinolones: ofloxacin, lomefloxacin and ciprofloxacin	Milk powder, milk and beef	ANWE	Overlapped peaks and unknown interferences	Simple sample pretreatment and low cost	[209]
Absorbance spectra–pH data					
Synthetic colorants: tartrazin and sunset yellow	Adulterated saffron	PARAFAC, SWATLD and APTLD	Overlapping profiles between analytes and unknown interferences; rank deficiency of original data array	Non separative method; a three-way variation array obtained by subtracting the first pH spectrum from each spectrum at each pH	[153]
HPLC-DAD data					
Tyrosine kinase inhibitors: vandetanib, pazopanib, afatinib and dasatinb	Human plasma	ATLD	Coelution of analytes and interferents	Elution time < 5.0 min	[210]
Benzodiazepines: alprazolam, clonazepam and diazepam	Human serum	ATLD	Matrix interferences and overlapped peaks	Correction of retention time shift; run time < 4.0 min; simple pretreatment and small amounts of solvents	[211]
Alkaloids: vincristine, vinblastine, vindoline, catharanthine and yohimbine	Traditional Chinese medicine and human serum	ATLD	Heavy overlaps and unknown interferences	Elution time < 7.5 min; multi-step purification was not required	[212]
Synthetic colorants: tartrazine (E102), sunset yellow (E110), carmine (E120), amaranth (E123), brilliant blue FCF (E133) and allura red AC (E129)	Beverage	ATLD	Varying interfering patterns from different chromatographic columns and sample matrices; coelution of analytes and interferents	Proving that chemometrics-assisted HPLC-DAD method can solve varying interfering patterns; little sample pretreatment; HPLC-UV method for confirmation	[213]

Table 4 (*continued*)

Analytes	Matrix	Algorithm	Challenge	Comment	Reference
Phytochemicals: gentiopicroside, loganic acid, swertiamarin and sweroside	Urine and feces	ATLD	Overlapping profiles between analytes and unknown interferences	Pharmacokinetic analysis; HPLC-MS method for confirmation	[214]
Polyphenols: GA, CGA, CA, p-HBA, VA, FA, RES, MY, MO, QCI, LU, KA and AP	Red wine	ATLD	Overlapped signals among solvent peaks, analytes and unknown interference; the presence of baseline drift	Simple sample pretreatment; elution time < 7.5 min; LC-MS/MS method for confirmation; PCA-LDA was used for the authentication of wines of different vintage years	[215]
Polyphenols: CA, CAT, CGA, EC, FA, GA, HYP, PB2, PCM, PLG, QCI and RUT	Apple peel and pulp	ATLD	Baseline drifts, coeluted peaks, unknown interferences	Elution time < 10 min; the content of polyphenols in the peel is usually higher than that in the pulp; HPLC-UV method for confirmation	[216]
Polyphenols: CGA, EC, CA, TF, PCM, HE, NA, CH, AP, KA, LU, QCI, MY, RUT, CAT, FA and iso-RH	Propolis	ATLD	Baseline drifts, coeluted peaks, unknown interferences	Elution time < 16.5 min; LC-MS/MS method for confirmation	[217]
Phytochemicals: andrographolide and dehydroandrographolide	Traditional Chinese medicine	ATLD	Matrix interferences and overlapped peaks	Traditional HPLC-UV method cannot be directly applied due to the presence of incomplete baseline separation; LC-MS method for confirmation	[218]
Non-steroidal anti-inflammatory drugs: NPX, KPF, MLX, FPF, DIF, PBZ, IPF, DCF, IDM, MFN, and CLC	Chinese patent drug and health product	ATLD	Baseline drifts, coeluted peaks, unknown interferences	They may be illegally added into Chinese patent drugs and health products; elution time < 14.5 min; HPLC-UV method for confirmation	[219]
Food Additives: AK, SAC, GLA, BA, SA, tartrazine (E102), amaranth (E123), carmine (E120) sunset yellow (E110), brilliant blue (E133), CAF	Beverage	ATLD	Coelution of analytes and interferents, baseline drifts	Elution time < 10 min; HPLC-UV method for confirmation	[220]
HPLC-FLD data					
Phenolic antioxidants: PG, BHA, BHT, TBHQ, OG, DG and NDGA	Vegetable oil	ATLD	Overlapping profiles between analytes and unknown interferences	Simple dilution step as pretreatment; elution time< 6 min	[221]
GPC-DAD data					
PAHs: CHR, NAP, ACN, FLU, PHE, ACE, ANT, PYR, BaA, GUA, BeP and BaP	Flue-dust and greasy-dirt	ATLD	Severely overlapped chromatograph peaks	Simple sample pretreatment; no specific PAHs separation column; very close peaks (only 3s difference in retention time) are resolved	[222]
LC-MS data					
Sulfonylurea-type oral antidiabetic agents: GLIP, TOLB, GLIC, GLIB, GLIM and GLIQ	Health tea and human plasma	ATLD	Co-eluted multi-analytes of interest in complex samples	Simple isocratic elution; elution time< 5 min; reducing the experimental time and cost	[223]
Mycotoxins: AFG2, AFG1, AFB2, AFB1, T2, ZOL, ZAN, ZON, OTA and STE	Maize and rice	ATLD	Co-eluted peaks, unknown interferences and baseline drifts	Elution time< 9 min; LC-MS/MS method for confirmation	[125]
B-group vitamins: VB1, VB2, VB3H, VB3N, VB5, VB6, VB7, VB9 and VB12	Energy drink	ATLD and APTLD	Overlapped peaks and uncalibrated interferents	Elution time<4.5 min; simple sample preparation; LC-MS/MS method for confirmation	[224]
Glucocorticoids: BC, BCDP, BD, BM, BMDP, BMV, COA, CP, DM, DMA, FLC, FLM, FP, TCA and TCAA	Face mask	ATLD	Co-eluted peaks, unknown interferences and baseline drifts; the presence of epimers	Elution time<11 min; LC-MS/MS method for confirmation	[225]
Estrogens: E1, α-E2, β-E2, E3, EE2, DES and BPA	Milk	ATLD	Overlapped peaks and uncalibrated interferents	Elution time<8 min; LC-MS/MS method for confirmation	[226]
Estrogens (system 1): BPA, β-E2,	Water (system 1) and urine (system 2)	ATLD	LC-MS data recorded at quadruple fragmentor	A novel data combination and partition strategy for	[280]

(*continued on next page*)

Table 4 (*continued*)

Analytes	Matrix	Algorithm	Challenge	Comment	Reference
DES and E1; Small biological molecules (system 2): xanthine, hypoxanthine, kynurenic acid, L-kynurenine, L-glutamic acid, L-tyrosine, L-tryptophan, L-phenylalanine			voltages in full scan mode in each chromatographic run; overlapped peaks and uncalibrated interferents	data preprocessing; data combination approach may provide higher sensitivity and improve significantly the prediction performances in most cases	
GC-MS data					
Plasticizers: 2,6-di-*tert*-butyl-4-methyl-phenol, diisobutyl phthalate, bis(2-ethylhexyl) adipate and diisononyl phthalate; UV stabilizer: benzophenone	Dummy made of natural rubber latex	PARAFAC and PARAFAC2	Matrix effects; finger-peak chromatographic signals; coelution of analytes and interferents	Standard addition method; PARAFAC can handle complex finger-peak signals caused by arrays of isomers	[227]
PAHs: CAN, FLU, PHE, ANT, PYR, BaA, CHR	PM10 (aerosol)	ATLD	Overlapped peaks and uncalibrated interferents	Run time<12 min	[228]
Electrochemical data					
N-acetylcysteine and acetaminophen	Serum and tablet	PARAFAC	Overlapped signals among analytes and interferents	Second-order data were generated using a change in pulse height of differential pulse voltammetry; BF3@MCM-41/DHB/CPE as a sensitive voltammetric sensor was designed for analytes; COW for correction of potential shift; HPLC method for confirmation	[229]
Temperature-dependent NIR spectra					
Terminal ethyl (C_2H_5) groups and mid-chain methylene (CH_2) groups	*n*-alkane mixtures	ATLD	Complex mixed signals	Quantitative estimation of the composition and the relative carbon atom numbers of *n*-alkane mixtures	[281]
Second-order LIBS data					
Base (Al and Cu) and noble (Au and Ag) elements	Printed circuit board (PCB)	PARAFAC	Spectral interferences	The depths were used as a third mode; after removal of interferents, it was possible to visualize where the element was more concentrated; PLS-DA models were built for noble elements to judge whether they existed in fragments	[170]

α-E2, 17α-estradiol; β-E2, 17-beta-estradiol; AA-I, aristolochic acid I; ACE, acenaphthene; ACN, acenaphthylene; AFB1, aflatoxin B1; AFB2, aflatoxin B2; AFG1, aflatoxin G1; AFG2, aflatoxin G2; AK, acesulfame potassium; AL-I, aristololactam I; ANT, anthracene; AP, apigenin; BA, benzoic acid; BaA, benzo[a]anthracene; BaP, benzo[a]pyrene; BbF, benzo[b]fluoranthene; BC, beclomethasone; BCDP, beclomethasone dipropionate; BD, budesonide; BkF, benzo[k]fluoranthene; BHA, 3-*tert*-butyl-4-hydroxyanisole; BHT, 3,5-di-*tert*-butyl-4-hydroxytoluene; BM, betamethasone; BMDP, betamethasone dipropionate; BMV, betamethasone 17-valerate; BeP, benzo[e]pyrene; BPA, bisphenol A; CA, caffeic acid; CAF, caffeine; CAT, (+)-catechin; CGA, chlorogenic acid; CH, chrysin; CHR, chrysene; CLC, celecoxib; COA, cortisone 21-acetate; CP, clobetasol 17-propionate; CPT-11, irinotecan; CV, crystal violet; DB[*a*,*l*]P, dibenzo[*a*,*l*]pyrene; DB[*a*,*h*]-P, dibenzo[*a*,*h*]pyrene; DB[*a*,*i*]P, dibenzo[*a*,*i*]pyrene; DB-[*a*,*e*]P, dibenzo[*a*,*e*]pyrene; DCF, diclofenac acid; DES, diethylstilbestrol; DG, dodecyl gallate; DM, dexamethasone; DMA, dexamethasone 21-acetate; DIF, diflunisal; E1, estrone; E3, estriol; EC, (−)-epicatechin; EE2, ethinylestradiol; FA, ferulic acid; FAD: flavin adenine dinucleotide; FLC, fluocinonide; FLM, fluorometholone; FLO, fluoranthene; FLU, fluorene; FP, fluticasone propionate; FPF, flurbiprofen; GA, gallic acid; GLA, glycyrrhizic acid; GLIB, glibenclamide; GLIC, gliclazide; GLIM, glimepiride; GLIP, glipizide; GLIQ, gliquidone; GUA, guaiazulene; HE, hesperetin; HYP, hyperin; IDM, indomethacin; IPF, ibuprofen; iso-RH, isorhamnetin; KA, kaempferol; KPF, ketoprofen; LCV, leucocrystal violet; LMG, leucomalachite green; LU, luteolin; MFN, mefenamic acid; MG, malachite green; MLX, meloxicam; MO, morin; MY, myricetin; N[2,3-*a*]P, naphtho[2,3-*a*]pyrene; NA, naringenin; NAP, naphthalene; NADH, nicotinamide adenine dinucleotide; NDGA, nordi-hydroguaiaretic acid; NPX, naproxen; OG, octyl gallate; OTA, ochratoxin A; PB2, procyanidin B2; PBZ, phenylbutazone; PCM, p-coumaric acid; PG, propyl gallate; p-HBA, p-Hydroxybenzoic acid; PHE, phenanthrene; PLG, phlorizin; PYR, pyrene; QCI, quercetin; RES, resveratrol; RUT, rutin; SA, sorbic acid; SAC, saccharin; STE, sterigmatocystin; T2, T-2 triol; TBHQ, tert-butylhydroquinone; TCA, triamcinolone acetonide; TCAA, triamcinolone acetonide acetate; TF, taxifolin; TOLB, tolbutamide; VA, vanillic acid; VB1, thiamine hydrochloride; VB2, riboflavin; VB3H, nicotinic acid; VB3N, nicotinamide; VB5, D-pantothenic acid hemicalcium salt; VB6, pyridoxine HCl; VB7, biotin; VB9, folic acid; VB12, cyanocobalamin; ZAN, zearalanone; ZOL, α-zearalenol; ZON, zearalenone.

transformed into an augmented bilinear matrix for processing, which cleverly manipulates the loss of trilinearity caused by time shifts. Recently, second-order calibration-assisted liquid chromatography with dual diode array-fluorescent detection method has been used for quantitative analysis of multiple analytes. A multivariate calibration-assisted method was proposed for the analysis of natural and synthetic sex hormones in environmental waters and sediments based on MCR-ALS modeling of three-way liquid chromatography with fluorescence and UV detection data [156]. The purpose of dual detection was to select the most

Table 5
Selected recent examples of second-order/three-way calibration based on other models or multiple models.

Analytes	Matrix	Algorithm	Challenge	Comment	Reference
EEM data					
Xenoestrogens: bisphenol A and nonylphenol	Plastic	U-PLS/RBL	Severe spectral overlapping among analytes and unknown interferences	Fluorescence enhanced by using methyl-β-cyclodextrin; analytes were quantified at parts per billion levels without the need of pre-concentration steps; HPLC-FLD method for confirmation	[230]
Pollutant: Tributyltin	Water and sediment	U-PLS/RBL	Overlapped signals among analytes and interferents	The use of nylon as a medium to extract, preconcentrate and enhance luminescence signals; Tributyltin-morin complex were directly measured in the solid surface.	[231]
Pollutants: carbamazepine, ofloxacin, piroxicam	Tap water, underground water and river water of different complexity	U-PLS/RBL	Severe spectral overlapping among analytes and unknown interferences	Analytes display photo-induced fluorescence upon UV irradiation; a simple solid-phase extraction with C18 membranes was used for the extraction/ preconcentration of analytes; a sample throughput of about 6 samples per hour.	[232]
Imidacloprid	Water spiked with additional foreign pesticides	PARAFAC and U-PLS/RBL	Overlapped signals among analytes and interferents	SPE-C18 for sample preparation; Analyte displays photo-induced fluorescence upon UV irradiation; LOD is at ng mL^{-1} level; HPLC-UV method for confirmation	[233]
Fluoroquinolones: moxifloxacin and ciprofloxacin	Urine	PARAFAC, SWATLD and U-PLS/RBL	Severe spectral overlapping between ciprofloxacin and urine background	Minimum sample preparation effort	[234]
Urea herbicides: isoproturon, linuron, monuron and rimsulfuron	Water and soil	U-PLS/RBL	Severe spectral overlapping among analytes and unknown interferences	Photoinduced fluorescence signals, obtained upon UV irradiation in micellar aqueous solutions; a simple, fast and eco-friendly method	[235]
Flavonoids: QCI and KA	Paprika	PARAFAC, U-PLS/RBL and N-PLS/RBL	Severe spectral overlapping among analytes and unknown interferences	The fluorescence properties of flavonoid compounds have been investigated and optimized	[236]
Polyphenols: CAT, EC, QCI, RES, CA, GA, PCM and VA	Red wine	PARAFAC and U-PLS/RBL	Severe spectral overlapping among analytes and unknown interferences	Front-face fluorescence spectroscopy method for data acquisition; no sample preparation; HPLC methods for confirmation	[237]
Vitamin: VB2	Urine with interferent drug	PARAFAC, U-PLS/RBL and N-PLS/RBL	Overlapped signals among analytes and interferents	Using second-order standard addition method; no previous clean up and separation steps; a sample throughput of about 4 samples per hour	[238]
Phytochemicals: α-asarone and β-asarone	Traditional Chinese medicine	PARAFAC, ATLD, APTLD, SWATLD, U-PLS/RBL and N-PLS/RBL	Severe spectral overlapping among analytes and unknown interferences	A simple, time-saving and low-cost method; HPLC-UV method for confirmation	[239]
Pesticides: CBZ, CAR, CHL and TSU	Environmental water	PARAFAC and U-PLS/RBL	Severe spectral overlapping among analytes and unknown interferences	LOD is at ng mL^{-1} level; simple sample pretreatment	[240]
Herbicide and its metabolite: glyphosate and (aminomethyl) phosphonic acid	Groundwater	MCR-ALS	Overlapped signals among analytes and interferent	Derivatization with 4-chloro-7-nitrobenzofurazan for fluorimetric detection; HPLC-UV method for confirmation	[241]

(*continued on next page*)

Table 5 (*continued*)

Analytes	Matrix	Algorithm	Challenge	Comment	Reference
Kinetic-spectroscopic data					
Co (II)	Various water, canned pineapple and vitamin B12 ampul	MCR-ALS	Extreme spectral overlapping among sample components	The determination of Co (II) based on its oxidation reaction with Fe (III) and 1, 10-phenantroline in micellar media; matrix augmentation in the spectral mode	[242]
Drug: acetaminophen	Novafen capsule	MCR-ALS	A linear dependency occurs; overlapped signals among analyte and interferents	The spectroelectrochemical data of acetaminophen oxidation were recorded; low cost and simple preparation	[243]
Amino acids: D,L-lys, leu and phe	Human plasma	MCR-ALS	Enantiomeric excess; overlapped signals among analytes and interferents	1-mercapto-2-propanol, o-phthaldialdehyde, as highly selective fluorogenic reagents, and amino acid (AA) enantiomers reacts with each other to yield two fluorescent diastereomers of D and L-AA; no separation approaches	[155]
Absorbance spectra–pH data					
Malachite green and crystal violet	Water	N-PLS/RBL	Lack of reproducibility of pH profiles and rank deficiency; spectral overlapping among analytes	A homemade apparatus was designed for data acquisition; high selectivity and low cost	[154]
HPLC-DAD data					
Antibiotics: Amoxicillin, metronidazole, sulfadiazine, sulfamerazine, ofloxacine and sulfamethoxazole	Wastewater	MCR-ALS and U-PLS/RBL	Co-elution of analytes and interferents	Run time < 4 min	[244]
Biogenic amines: ryptamine, 2-phenylethylamine, putrescine, cadaverine and histamine	Fish	MCR-ALS	Time misalignment and rank deficiency; co-elution of analytes and interferents with identical spectral profiles	Run time < 4 min in isocratic mode; low solvent consumption; time misalignment and rank deficiency were handled by icoshift and MCR-ALS	[245]
Pesticide residues: CBZ, TBZ, fuberidazole, CBF, CAR, NAP and FLT	Vegetables	MCR-ALS	Co-elution of analytes and interferents, peak shift, band shape changes	Chemometric cleanup alternatively to chemical cleanup	[246]
Nitroaromatic compounds: 1,2-DNB, 1,3-DNB, TNT, 2,4-DNT, 2-NT, 3-NT and 4-NT	Water	MCR-ALS	High structure-similarity of target analytes; co-elution of analytes and interferents	Run time < 10 min; a simple isocratic elution condition	[247]
Immunosuppressant drugs: everolimus, cyclosporine A and tacrolimus	Whole blood	MCR-ALS	Background drift, chromatographic shifts and co-elution of analytes and interferents	Elution time< 3 min; Simple sample treatment steps and low cost	[248]
Corticosteroids: prednisolone and methylprednisolone; mycophenolic acid	Human plasma	MCR-ALS	High structure-similarity of the selected corticosteroids; co-elution of analytes and interferents	Run time < 3 min through two simple isocratic elution methods	[249]
Antidiabetic drugs: gliclazide, glibenclamide and glimepiride; antihypertensive drugs: atenolol, enalapril and amlodipine	Serum	MCR-ALS and U-PLS/RBL	Co-elution of analytes and interferents	Run time < 3 min which was reduced by 50% considering previous reports	[250]
Preservatives: methylparaben, ethylparaben, propyl-paraben, butylparaben, phenoxyethanol, salicylic acid, methylisothiazolinone, 3-iodo-2-propynyl-n-butylcarbamate	Facial mask	ATLD and MCR-ALS	Severe signal overlapping among analytes and interferents; slight time shifts	ATLD method is competent for handling slight retention time shifts; traditional HPLC-UV method for confirmation	[122]
Small biological molecules: uric acid, creatinine,	Human urine	ATLD and MCR-ALS	Severe signal overlapping among analytes and	Run time < 6 min in isocratic mode;	[251]

Table 5 (*continued*)

Analytes	Matrix	Algorithm	Challenge	Comment	Reference
tyrosine, homovanillic acid, hippuric acid, indole-3-acetic acid, tryptophan and 2-methylhippuric acid			interferents; slight time shifts	traditional HPLC-UV method for confirmation	
Organic acids: malic, oxalic, formic, lactic, acetic, citric, pyruvic, succinic, tartaric, propionic and α-cetoglutaric	Fermented food	PARAFAC and U-PLS/RBL	Severe signal overlapping among analytes and interferents; distortions in the time sensors among chromatograms	Run time < 12 min in isocratic mode; ion-exchange HPLC method for confirmation	[252]
Pesticide residues: CBZ, TBZ, fuberidazole, CBF, CAR, FLT and NAP	Vegetables	MCR-ALS	Signal overlapping among analytes and interferents	Comparison for univariate and multi-way calibration	[253]
Tea polyphenols: GA, EGC, EGCG, EC and ECG	Chinese tea	ATLD, MCR-ALS and ATLD-MCR	Retention time shifts; signal overlapping among analytes and interferents	MCR-ALS and ATLD-MCR performed better than ATLD in the case of larger time shifts	[282]
LC-MS data					
Immunosuppressants: cyclosporine-A and tacrolimus	Human blood and water	MCR-ALS	Background drift, chromatographic shifts and co-elution of analytes and interferents	Matrix effect was handled by constructing the matrix matched calibration set; very low LOD	[254]
Polyphenols: GA, CAT, CA, EC, CGA, PCM, FA, TF, LU, MY and QCI	Propolis	ATLD and MCR-ALS	Chromatographic shifts, serious co-eluted peaks and diverse unknown interferences	Elution time < 7 min; traditional LC-MS/MS method for confirmation	[283]
GC-MS data					
PAHs: ACN, FLU, PHE, ANT, PYR, BaA, BbF, BkF, BaP, IP, DBahA, BghiP, CHR	Tap and hookah waters	MCR-ALS	Signal overlapping among analytes and interferents	Ultrasound-assisted emulsification microextraction before GC analysis; MS in full scan mode	[255]
Organic acid metabolites: propanedioic acid, fumaric acid, succinic acid, malic acid, citric acid, myristic acid, palmitic acid, linoleic acid, linolenic acid, oleic acid, stearic acid	Tobacco	MCR-ALS	Signal overlapping among analytes and interferents	Classification of tobacco samples from various growth zones based on quantitative results; MS in full scan mode	[256]
HPLC-FLD or RTEFM data					
PAHs: FLU, CHR, PHE, ANT, PYR, BaA, BaP, BbF, CHR,	Smoked paprika	MCR-ALS	Co-elution of analytes and interferents	A simple isocratic elution	[257]
PAHs: 1-, 2-, 3-, 4- and 9-hydroxyphenanthrene	Milk	U-PLS/RBL, N-PLS/RBL and MCR-ALS	Co-elution of analytes and interferents	Run time < 5.5 min in isocratic mode	[258]
PAHs: DBahA, IP, BghiP, CHR, BaA, BbF, BaP, BkF	Tea infusion	U-PLS/RBL and MCR-ALS	Signal overlapping among analytes and interferents	Quantifying PAHs at the ng L^{-1} (sub-ppb) level; run time < 6 min in isocratic mode; EEMF method for comparison and traditional HPLC-FLD method for confirmation	[259]
HPLC-DAD-FLD or fusion data					
Sex hormones: AE, DES, β-E2, EE2, E3, E1, HEX, LEV, MEST, NOR, and PROG	Water and sediment	MCR-ALS	Co-elution of analytes and interferents	A single chromatographic run in isocratic mode; quantification of analytes based primarily on the most suitable detector	[156]
Veterinary drugs: CFT, CLB, ENR, IMID, DIFL, CTC, FLUM, DCF, PGN, DZP, TMP, BMV, IBF, MBT, PSL, CAP, FXN, DNC, PYRA, FBZ and ABZ	Poultry litter	MCR-ALS	Severe signal overlapping among analytes and interferents	Isocratic elution; quantification of analytes based primarily on the most suitable detector	[157]
Endocrine disruptors: DBP, FLT, PYR, BaA, NPb, BbF, BaP, DBA, BghiP, DMP, NOR, CAR, BPA and NAP	Water	MCR-ALS	Some analytes cannot be quantitatively estimated from individual detectors and in cases of low selectivity; signal overlapping among analytes and interferents	A strategy to obtain the LC-DAD-FLD fused data; results obtained by LC-DAD data, LC-FLD data and LC-DAD-FLD fused data were compared	[158]

(*continued on next page*)

Table 5 (*continued*)

Analytes	Matrix	Algorithm	Challenge	Comment	Reference
Electrochemical data					
Norepinephrine, paracetamol and uric acid	Human serum and synthetic sample	U-PLS/RBL, ANN/RBL, N-PLS/RBL, MCR-ALS and PARAFAC2	strong voltammetric overlapped signals among analytes and interferents; baseline- and potential shifts;	Recording second-order DPV data at different pulse heights; oxidized glassy carbon electrode (OGCE) was used; shift and baseline corrected by COW and AsLSSR, respectively; U-PLS/RBL showed better performance in this case	[260]
Ethiofencarb	Tap water with added interference	MCR-ALS and U-PLS/RBL	Overlapped signals among analyte and interferents; baseline shifts	Ethiofencarb is hydrolysed in alkaline media; voltammograms were generated at different hydrolysis times; AsLS for background correction	[159]
Sulfamethoxazole and sulfamethizole	Human serum and urine	MCR-ALS	Overlapped signals among analyte and interferents; potential shifts	Modified carbon paste electrode with Fe doped ZnO nanorods as an electrochemical sensor; recording second-order DPV data at different pulse heights; COW for potential shift correction	[261]
Ascorbic and uric acids and dopamine	Human serum	U-PLS/RBL	Overlapped signals among analyte and interferents; baseline- and potential shifts	The second-order data used were a result of the cross product obtained from the forward and reverse currents (through a single square wave voltammetric experiment); the data processing with AsLS and COW	[160]
Antiparkinson agents: LDP, CDP, MDP, BA, TOL and ENT	Human serum	MCR-ALS and PARAFAC2	strong voltammetric overlapped signals among analytes and interferents; Baseline- and potential shifts	Recording second-order DPV data at different pulse heights; shift and baseline corrected by COW and AsLSSR, respectively; HPLC-UV method for confirmation	[262]
Temperature-dependent NIR spectra					
Volume fraction of ethanol (%)	binary water-ethanol mixture	PARAFAC, ATLD and U-PCA	Quantitative and structural information hidden in the complex NIR spectra	PARAFAC and ATLD can directly capture related quantitative and structural information; MLR combined with the scores of algorithms was used for final quantitative analysis	[168]

β-E2, 17-beta-estradiol; 1,2-DNB, 1,2-dinitrobenzene; 1,3-DNB, 1,3-dinitrobenzene; 2,4-DNT, 2,4-dinitrotoluene; 2-NT, 2-nitrotoluene; 3-NT, 3-nitrotoluene; 4-NT, 4-nitrotoluene; ABZ, albendazole; ACN, acenaphthylene; AE, androstenedione; ANT, anthracene; BA, benserazide; BaA, benzo[a]anthracene; BaP, benzo[a]pyrene; BbF, benzo[b]fluoranthene; BghiP, benzo[g,h,i]perylene; BkF, benzo[k]fluoranthene; BMV, betamethasone; BPA, bisphenol A; CA, caffeic acid; CAF, caffeine; CAP, chloramphenicol; CAR, carbaryl; CAT, (+)-catechin; CBF, carbofuran; CBZ, carbendazim; CDP, carbidopa; CFT, ceftiofur; CGA, chlorogenic acid; CHL, chlorothalonil; CHR, chrysene; CLB, clenbuterol; CTC, chlortetracycline; DBahA, dibenz[ah]anthracene; DBP, dibutyl phthalate; DCF, diclofenac; DES, diethylstilbestrol; DIFL, difloxacin; DMP, dimethyl phthalate; DNC, nicarbazin; DZP, diazepam; E1, estrone; E3, estriol; EE2, ethinylestradiol; EC, (−)-epicatechin; ECG, epicatechin gallate; EGC, epigallocatechin; EGCG, epigallocatechin gallate; ENR, enrofloxacin; ENT, entacapone; FBZ, fenbendazole; FA, ferulic acid; FLT, flutriafol; FLU, fluorene; FLUM, flumequine; FLT, fluoranthene FXN, flunixin; GA, gallic acid; HEX, hexestrol; IBF, ibuprofen; IMID, imidacloprid; IP, indeno[1,2,3-c,d]-pyrene; LDP, levodopa; leu, leucine; LEV, levonorgestrel; LU, luteolin; lys, lysine; MBT, menbutone; MDP, methyldopa; phe, phenylalanine; MEST, mestranol; MY, myricetin; NAP, 1-naphthol; NOR, norethisterone; NORF, norflurazon; NP, 4-Nonylphenol; PCM, p-coumaric acid; PGN, progesterone; PHE, phenanthrene; PROG, progesterone; PSL, prednisolone; PYR, pyrene; PYRA, pyrantel; QCI, quercetin; RTEFM, retention time-emission spectra matrices; TBZ, thiabendazole; TF, taxifolin; TMP, trimethoprim; TNT, 2,4,6-trinitrotoluene; TOL, tolcapone; TSU, tsumacide.

suitable signal for each analyte. The similar strategy was also used for simultaneous determination of twenty-one veterinary active ingredients in poultry litter [157]. LC-DAD and LC-FLD second-order data, collected in a single chromatographic run, were firstly fused and treated using chemometric algorithms for the quantitation of co-eluted fluorescent and non-fluorescent analytes. LC-DAD, LC-FLD and fused LC-DAD-FLD data were processed by MCR-ALS, respectively, and their results were compared. The benefit of fusion was highlighted when analytes cannot be quantitatively estimated from individual detectors and in cases of low selectivity [158]. In a word, when second-order calibration method is applied in chromatographic data, overlapping chromatographic signals and unknown interferences will no longer affect the accurate quantitative analysis of target

analytes, which means that analysis time and the use of organic solvents will be greatly reduced, and some pretreatment steps can be avoided.

In addition, some electrochemical techniques can also generate second-order data, which combined with three-way calibration method has been successfully used for the direct quantitative analysis of multiple analytes of interest in complex systems. Jalalvand et al. has reviewed applications and challenges of multi-way calibration in electrochemical analysis [17]. Differential pulse voltammetry (DPV) is the most frequently used technique for the generation of second-order electrochemical data by recording second-order DPV data at different pulse heights. A few second-order electrochemical data were generated by recording voltammograms at different reaction time [159] or based on square wave voltammetry (SWV) [160]. Generally, they are nonlinear second-order data reflected in the strong signal shifts, peak broadening or nonproportional increase in the peak height. Therefore, shift correction and baseline correction were recommended. According to Jalalvand, some chemometric methods such as COW [117], icoshift [119], Gaussian peak adjustment (GPA) [161], GPA with transversal constraints (GPA2D) [162], asymmetric logistic peak adjustment (ALPA) [163], *shiftfit* [164,165] and *pHfit* [166] can be used for correcting the shifts, and asymmetric least squares spline regression (AsLSSR) can be used for baseline elimination [167]. Recent related examples based on different second-order calibration models are collected in Tables 4 and 5. Strong voltammetric overlapped signals among analytes and interferents can be solved by second-order calibration method, which means that second-order electrochemical methods can be used as a cheap and convenient alternative for the quantification of target analytes in complex systems.

Temperature-dependent NIR spectra combined with second-order calibration can obtain the structural and quantitative information of the mixed solutions [79]. Recently, Cui et al. used U-PCA, PARAFAC and ATLD to analyze temperature-dependent NIR spectra data of binary water-ethanol mixtures (data set 1). Three modes in data set 1 were temperature, wavenumber and sample (samples with different ethanol volume fractions), respectively. Compared with U-PCA, PARAFAC and ATLD can directly capture the relevant sources of information about the physical and chemical changes in a system. Then the quantification of different ethanol volume fractions in the predicted samples was achieved by using multivariate linear regression (MLR) for the scores of these algorithms. Furthermore, they used U-PCA, four-way PARAFAC and AQLD to study a four-way data array (data set 2), whose four modes were wavenumber, temperature, samples with different isopropanol volume fractions and samples with different water volume fractions, respectively. These algorithms can still extract the quantitative information of temperature, isopropanol, ethanol and water. Similarly, the final quantitative analysis should be achieved by combining MLR and the scores of algorithms [168]. In addition, the same research group also used ATLD-based method for standardization of NIR spectra measured on multi-instrument, which may be an efficient way when a simultaneous transfer of the spectra measured on more than two instruments is needed [169].

Very recently, Castro et al. used PARAFAC to model three-way laser-induced breakdown spectroscopy (LIBS) data, characterizing base (Al and Cu) and noble (Au and Ag) elements on a printed circuit board (PCB) from hard disk [170]. PARAFAC was used for this type of data for the first time. Firstly, a PCB was cut in 77 fragments, and a 4×4 matrix with 10 laser pulses in each point of the matrix was obtained in each fragment by LIBS. The data was arranged in an $I \times J \times K$ three-way array, where I refers to 1210 sample points, J refers to emission lines (wavelengths) and K is the pulses (depth, from 1 to 10), and then decomposed by PARAFAC. Through PARAFAC decomposition, the emission lines and relative concentrations of the elements of interest were extracted, and the contribution of the concomitants was removed. Finally, the relative concentrations of target base elements were used to create a map of the PCB colored by concentration, and it was possible visualize the main position of the element on the PCB; in order to verify the presence or absence of the noble elements in the fragments, PLS-DA models were built after using PARAFAC to remove interferences.

5.2. Examples of four-way calibration

There is no doubt on the fact that third-order/four-way calibration has outstanding analytical qualities. As mentioned in Section 3.4.3, in addition to the second-order advantage, third-order/four-way calibration allows the development of methods with higher sensitivity and selectivity. Sensitivity increases since the measurement of redundant data reduces the relative impact of the noise in the signal, and selectivity is improved because the overall selectivity is positively contributed by each additional instrumental mode [11,171]. Moreover, third-order/four-way calibration can be used for the data with severe collinearity which limits the use of second-order/three-way calibration. These important features have been summarized as part of the third-order advantage.

With the advancement of instruments, the acquisition of third-order data is becoming faster and easier. Table 6 summarizes the recent examples of third-order/four-way calibration attached with the related comments based on different data types. These third-order data are mainly obtained through EEM-based and chromatography-based methods. EEM-based third-order data are generated by recording EEMs data as a function of reaction time, pH, fluorescence lifetime or other chemical treatments. EEM-kinetics data is one of the most common third-order data. The kinetic evolution involves analytes degradation, oxidation/reduction or new spectrally active products produced as a new mode. It is worth noting that this type of four-way data array has a strict quadrilinear structure only when the reaction conforms to a first-order kinetic model. The related first application was published in 2003 for quantifying adrenaline and noradrenaline concentrations from mixtures of catecholamines [172]. Adrenaline and noradrenaline were derived to the corresponding fluorescing lutines (3,5,6-trihydroxyindole derivatives). The lutine reaction was run in a flow system and EEMs were obtained during the kinetic evolution. N-PLS and four-way PARAFAC used for solving the data array gave similar results.

In most cases, the four-way data array obtained by EEMs coupled with pH mode satisfies the quadrilinearity. Therefore, it can be regarded as a relatively simple way to acquire quadrilinear data and often used for new algorithms evaluation. Taking a recent work as an example, Kang et al. proposed four-way EEM-pH-sample data array coupled with CAQLD algorithm for the simultaneous quantitative analysis of metabolic coenzymes flavin adenine dinucleotide (FAD) and flavin mononucleotide (FMN) in the cell [173]. The spectra of FAD and FMN overlapped seriously due to their high similarity and unknown interference, which prevented the second-order calibration from obtaining correct results. However, through introducing the pH mode to construct the EEM-pH-sample four-way data array and combining it with four-way calibration method, highly collinearity with serious interference was solved. A LC-MS/MS one-way calibration method confirmed the accuracy of the results. “Third-order advantage” was reflected in this work.

As early as in 1988, there have been some reports about three-way EEM-lifetime array for multidimensional analysis [174–176]. In 2005, four-way EEM-lifetime-sample data combined with four-way calibration began to be used for quantitative intent [177]. The work used four-way data based on laser-excited time-resolved

Table 6
Selected recent examples of third-order/four-way calibration.

Analytes	Matrix	Algorithm	Data generation and characteristic	Comment	Reference
EEM-kinetics data					
Tyrosine and levodopa	Human plasma	AQLD	EEMs obtained during the kinetic evolution of polyphenol oxidase oxidation	Serious collinearity leaded second-order calibration methods to fail in quantitative analysis, but it was solved by third-order calibration method; comparison with LC-MS/MS method	[263]
Vitamin B1	Multivitamin complexes	Four-way PARAFAC	EEMs during the kinetic evolution of oxidation catalyzed by Hg^{2+} in alkaline medium	Analyte was converted into a fluorescent derivative; standard addition method	[264]
Nicotinamide adenine dinucleotide and flavin adenine dinucleotide	Human plasma	RSWAQLD	EEMs obtained during the kinetic evolution	Quantitative kinetic analysis of the degradation reaction of NADH and the formation reaction of FAD; real-time and nondestructive analysis	[191]
PAHs: BaP, DBA, BbF, BkF, BaA	Water	Four-way PARAFAC	EEMs obtained during the kinetic evolution of the Fenton degradation	Water samples was subjected to a solid-phase extraction; methyl-β-cyclodextrin for fluorescence enhancement; 4 min per sample	[25]
Azinphos-methyl	Apple, pear and peach juice samples	Four-way PARAFAC and U-PLS/RTL	EEMs recorded at different times after UV-light irradiation	Analyte was converted into a highly fluorescent product; standard addition method to overcome the matrix effect	[265]
Bisphenol A and nonylphenol	Food-contact plastics	Four-way PARAFAC, U-PLS/RTL and MCR-ALS	Measuring the EEMs as a function of reaction time during their Fenton degradation	Data collinearity was overcome by third-order advantage; methyl-β-cyclodextrin for fluorescence enhancement; 4.5 min per sample; HPLC-FLD method (30 min) for confirmation	[266]
Fluoroquinolones: ciprofloxacin, norfloxacin and flumequine	Fish farming water	U-PLS/RTL	EEMs recorded at different times after UV-light irradiation	Second-order calibration algorithm was unsatisfactory due to high spectral overlap	[267]
EEM-pH data					
Metabolic coenzymes: flavin adenine dinucleotide and flavin mononucleotide	Cancer cell	CAQLD	Relatively discrete pH levels (2.2, 2.6, 3.0, 3.4, 3.8, 4.2 and 4.6) as the third mode	This dataset is highly collinear with serious interference; four-way calibration method provided higher sensitivity and more resolving power than three-way calibration method; LC-MS/MS method for confirmation	[173]
Xanthopterin and isoxanthopterin	Human urine and serum	FACM, AQLD and four-way PARAFAC	Relatively discrete pH levels (6.5, 7.0, 7.5 and 8.0) as the third mode	Data array was designed for algorithm performance comparison and evaluation	[88]
Fluoroquinolones: iprofloxacin, ofloxacin and norfloxacin	Urine	Four-way PARAFAC	A well-designed flow-injection method for generating the pH-gradient; EEMs were recorded while pH was continuously changing.	Four-way data array obtained in a flow system might not be strictly quadrilinear, however, the breaking of the quadrilinearity of the data can be avoided in the selected experimental conditions.	[26]
EEM-time resolved fluorescence data					
PAHs: Metabolites of BaP	Urine	U-PLS/RTL	EEMs are recording during the delay time after excitation pulse at 77 K	The fiber optic probe for measuring EEMs from the surface of SPE membranes; the entire experimental procedure took <10 min per sample	[178]
EEM-other chemical treatment data					
Pesticides: carbaryl, carbendazim and 1-naphthol	Iceberg lettuce	Four-way PARAFAC	Three dilution levels of extract as the third instrumental mode	Standard addition method for solving matrix effects	[268]
PAHs: PHE, PYR, ANT and FLU	Water with humic acid	Four-way PARAFAC	EEMs recorded at different levels of fluorescent quencher concentration	The quantitative results of four-way calibration were higher than those of three-way calibration	[269]

Table 6 (*continued*)

Analytes	Matrix	Algorithm	Data generation and characteristic	Comment	Reference
Phytochemicals: schizandrol A and schizandrol B	Dulbecco's modified eagle medium	FSWANRF and four-way PARAFAC	EEMs recorded at different solvents	Serious collinearity and high background interference hindered three-way calibration	[270]
Aflatoxins B1 and B2	Peanut	BLLS/RBL and PARAFAC	EEMs recorded at different solvents; this four-way data was converted to the three-way data by augmentation	Severe collinearity in both excitation and emission modes	[271]
PAHs: acenaphthene and naphthalene	Solvent: ultrapure water, methanol and ethanol	AWRCQLD, four-way PARAFAC, APQLD and APTLD	EEMs recorded at different solvents	AWRCQLD algorithm is the best in this case; three-way calibration method based on APTLD for comparison	[272]
PAHs: PHE, naphthalene and acenaphthene	Tea	Four-way PARAFAC	EEMs recorded at different temperatures	The quantitative results obtained by four-way PARAFAC were better than those obtained by three-way PARAFAC	[273]
Cochineal	Strawberry jam	Four-way PARAFAC	EEMs recorded at different levels of fluorescent quencher concentration	Carmoisine acted as a quencher; HPLC-DAD method as a comparison	[27]
LC-EEM data					
Chlorophylls a and b, Pheophytins a and b	Olive oil	APARAFAC and MCR-ALS	Multiple injections were implemented at different excitation wavelengths and collecting multiple time-emission matrixes	APARAFAC was proposed for handling non-quadrilinear four-way data	[89]
Fluoroquinolones: ofloxacin, ciprofloxacin and danofloxacin	Water with other fluoroquinolones as uncalibrated interferences	APARAFAC and MCR-ALS	Each chromatographic fraction was collected and then used for EEM acquisition	These models were more flexible regarding changes in elution profiles from sample to sample; APARAFAC performed better than MCR-ALS in this case	[180]
Pesticides: carbendazim, fuberidazole, thiabendazole, carbofuran, carbaryl and naphthol	Fruit juice	Four-way PARAFAC, U-PLS/RTL and MCR-ALS	Multiple injections were implemented at different excitation wavelengths and collecting multiple time-emission matrixes	U-PLS/RTL performed better than other algorithms in this case due to high collinearity among spectra	[181]
PAHs: FLO, PYR, BaA, CHR, BbF, BkF, BaP and DBA	Underground and stream water	Four-way PARAFAC	On-line chromatographic-EEM analysis; using a fast-scanning spectrofluorimeter; the reduction of the linear flow rate	Third-order data recorded on-line, saving a large total analysis time	[274]
Agrochemicals: rimsulfuron, fuberidazole, carbaryl, naproxen, albendazole, tamoxifen	Environmental water	MCR-ALS	On-line chromatographic-EEM analysis; using a fast-scanning spectrofluorimeter with a postcolumn UV reactor; the reduction of the linear flow rate	Rimsulfuron and tamoxifen exhibit virtually no native fluorescence; run time < 11 min	[275]
PAHs: BaA, CHR, BbF, BaP	Tea	MCR-ALS	On-line chromatographic-EEM analysis; using a fast-scanning spectrofluorimeter	The mutual dependence between excitation and time profiles; a new strategy based on MCR-ALS for data processing; 9 min per sample	[276]
Dyes: fluorescein, eosin Y and resorufin	Water	APARAFAC	On-line chromatographic-EEM analysis; using a spectrometer system based on a charged coupled device	Fast data acquisition and run time < 4.5 min; inexpensive direct imaging of EEM	[277]
LC^2-DAD data					
Furanocoumarins: psoralen, angelicin and 8-methoxypsoralen	Synthetic samples	MCR-ALS	2D assisted liquid chromatography was presented; LC × LC equipped with dual DADs (a diode array detector placed at the end of each column)	First using MCR-ALS to process the second dimensional DAD data and then using the resolved spectra to initiate MCR-ALS analysis of the first dimensional DAD data	[278]
GC^2-MS data					
PAH: 3,6-dimethylphenantrane	Heavy fuel oil	MCR-ALS and PARAFAC	Comprehensive two-dimensional gas	Super augmented matrix for MCR-ALS analysis;	[279]

(*continued on next page*)

Table 6 (*continued*)

Analytes	Matrix	Algorithm	Data generation and characteristic	Comment	Reference
			chromatography system with a mass spectrometer	augmented three-way data array for PARAFAC analysis	
Third-order DPV data					
Levodopa, carbidopa, methyldopa, acetaminophen, tramadol, lidocaine, tolperisone, ofloxacin, levofloxacin and norfloxacin	Synthetic samples	U-PLS/RTL and N-PLS/RTL	Third-order DPV data were recorded by changes in pulse height and pulse duration of DPV signals	Potential shift correction using COW algorithm; multi-walled carbon nanotubes modified glassy carbon electrode was used	[183]
Third-order temperature-dependent NIR spectra data					
Volume fraction of isopropanol and volume fraction of water (%)	Ternary water-ethanol-isopropanol mixture	Four-way PARAFAC, AQLD and U-PCA	Four modes were wavenumber, temperature, samples with different isopropanol volume fractions and samples with different water volume fractions	Water-ethanol of different volume ratio was used as the solvent and isopropanol of different volume fraction was regarded as the solute; MLR combined with the scores of algorithms was used for final quantitative analysis	[168]

ANT, anthracene; BaA, benz[a]anthracene; BaP, benzo[a]pyrene; BbF, benzo[b]fluoranthene; BkF, benzo[k]fluoranthene; CHR, chrysene; DBA, dibenz[a,h]anthracene; FLO, fluoranthene; FLU, fluorene; PHE, phenanthrene; PYR, pyrene.

Shpol'skii spectroscopy coupled to four-way PARAFAC to determine 2,3,7,8-tetrachloro-dibenzo-paradioxin (2,3,7,8-TCDD) in complex environmental samples. Five excitation wavelengths (317.2, 317.3, 317.4, 317.5 and 317.6 nm) were selected to preferentially enhance the phosphorescence of 2,3,7,8-TCDD in the complex matrixes. The third-order data of each sample was obtained by collecting emission wavelength-time matrixes at five excitation wavelengths. Calibration was implemented in combination with a standard addition method. The complete sample analysis time is less than 15 min with only 100 μL of n-heptane. Recently, Alfarhani et al. proposed a method for the direct analysis of three benzo[a]pyrene metabolites in urine samples by using time-resolved excitation emission cube (TREEC) data arrays and four-way calibration algorithms [178]. TREEC refers to the superposition of time-resolved excitation-emission matrixes (TREEMs) recorded at different time windows from the laser excitation pulse. Five selected time windows were used for the generation of TREEC of each sample. Better prediction results were obtained by U-PLS/RTL even in the presence of strong spectral and lifetime overlapping.

Moreover, some chemical treatments can produce a new instrumental mode for data, which coupled with EEMs also generates the third-order data. Common chemical treatments include using different levels of fluorescence quencher, different solvents, different levels of dilution and different temperatures. Recent examples are summarized in Table 6. In addition, a recent review has also covered the most examples of four- and five-way EEM luminescence-based data with multi-way calibration over the years [22].

Currently, chromatography-based third-order data are produced by two ways. One way is measuring EEMs as a function of the elution time (obtaining LC-EEM data), and the other way is using comprehensive two-dimensional liquid or gas chromatography (LC^2 or GC^2) with spectral detection. There are three methodologies that can be used to generate third-order LC-EEM data: (1) Fraction collection. This methodology is based on the collection of discrete fractions at the end of the chromatographic procedure, and then the EEM of each collected fraction being recorded. It was firstly proposed by Bro and a multilinear analysis was employed for a qualitative purpose [179]. In 2015, Alcaráz et al. also use this methodology to obtain LC-EEM data for quantitative analysis and model evaluation [180]. At the end of the chromatographic procedure, each fraction was collected every 2 s in a 96-wells plate, which is often used for enzyme-linked immunosorbent assays, and allowing the automatic collection of 60 μL in every well. The collection started after 37 s from the initial time of run and ended in 87 s, therefore 25 fractions were collected for each run. Finally, all EEMs of fractions were obtained by a luminescence spectrometer. After analyzing a series of samples, a four-way LC-EEM-sample data array was generated. (2) Multiple injections. The LC-EEM data of each sample is obtained by multiple chromatographic runs at different excitation wavelengths. Based on this methodology, the obtained LC-EEM data arrays coupled with four-way calibration method have been used for the simultaneous determination of chlorophylls *a* and *b*, pheophytins a and b in olive oil [89] and six pesticides in fruit juice [181]. The four-way data array is non-quadrilinear due to inevitable chromatographic retention time shifts in multiple runs. Therefore, some algorithms that do not rely on the strict quadrilinear structure, such as MCR-ALS, APARAFAC and U-PLS/RTL, may work better when handling this type of data. (3) On-line EEMs data acquisition. This methodology is achieved by a fast-scanning spectrofluorimeter with a flow cell connected at the end of the LC instrument, which saves time and cost compared to the previous two methodologies and is in line with the green analytical method. The related examples applied for the determination of multiple analytes are summarized in Table 6. Although it seems the most attractive one, a weakness is that the analyte concentration at the beginning of each EEM may be different than at the end, because fluorescence matrices are recorded in a finite time. Therefore, excitation mode is dependent on the retention time mode, resulting in a non-quadrilinear data array (Olivieri et al. classified it into non-quadrilinear type 4 [182]). According to the reported applications, the more flexible algorithms described above are still applicable to such data.

Two-dimensional gas chromatography with mass spectrometric detection (GC^2-MS) or two-dimensional liquid chromatography with diode array detection (LC^2-DAD) can also obtain third-order chromatographic data. The related four-way data array includes two retention time modes, a MS mode or DAD mode, and a sample mode. Although four-way data can be generated directly from this type of instrument, there are fewer related applications in four-way calibration as these instruments are not common. Moreover, the use of two dimensions significantly enhances the separation power compared to traditional one-dimensional chromatography and greatly increases the amount of data, therefore, third-order

calibration is usually applied to a small part of the entire data array. Several examples in multi-way chromatographic calibration were also introduced in a review [23].

In terms of electrochemistry, the combination of third-order DPV data and four-way calibration algorithms was firstly proposed by Jalalvand et al. [183]. The DPV response of each sample was recorded 36 times. 6 current-potential matrices were recorded at 6 different pulse durations. Each matrix consists of six vectors which were recorded at six different pulse heights. Therefore, four modes of the four-way data array were potential, pulse height, pulse duration and sample, respectively. COW was used for potential shift correction. The performances of U-PLS/RTL and N-PLS/RBL were compared. Finally, U-PLS/RTL was chosen for the analysis of the electrochemical responses of a multi-walled carbon nanotubes modified glassy carbon electrode (MWCNTs/GCE) sensor for the simultaneous determination of ten selected analytes in human serum samples.

5.3. Examples of five-way calibration

In theory, five-way calibration has higher analytical qualities than the four-way calibration. However, the acquisition of a five-way data array requires extensive experiments to obtain more instrument modes, or relies on complex higher-order instruments. What's more, quinquelinearity breaking modes or interdependent modes may become common as instrumental modes increase. Therefore, analysts need to be more cautious when dealing with this type of data. Until now, only four examples have involved the quantitative application of five-way data, which have been collected in Table 7. The first example of fourth-order/five-way calibration was accomplished by Maggio et al. [28]. In this work, a five-way fluorescence excitation-emission-kinetic-pH-sample data array was obtained by recording the EEMs of the samples as a function of the reaction time and at different pH values. It coupled with U-PLS/RQL, five-way PARAFAC and four-way PARAFAC was used for determining carbaryl in the presence of fuberidazole and thiabendazole as uncalibrated interferents, respectively. Because the pH and time profiles are mutually dependent, the best PARAFAC model is the four-way case, which deals with the augmented four-way data array obtained by concatenating the pH and time modes of the original five-way data. By contrast, the novel U-PLS/RQL achieved a superior performance for quantitative analysis due to its inherent latent-structured flexibility.

Qing et al. proposed a novel AQQLD algorithm for processing five-way HPLC-DAD-kinetic-pH-sample data array [30]. The kinetics of naptalam hydrolysis in two systems with uncalibrated interferents were quantitatively investigated. Five-way data was obtained by recording the kinetic evolution of HPLC—DAD signals of samples at different pH values. The serious chromatographic retention time shifts were corrected by a peak alignment method ASSD. Compared to five-way PARAFAC, AQQLD has the advantages of fast convergence and being insensitive to the number of components.

Two recent examples of five-way calibration are from the same research group. Nie et al. constructed a five-way emission-excitation-UV irradiation time-volume-sample data array by recording the EEMs of samples with different river water addition volumes at different UV irradiation times [87]. It coupled with AFWRQQLD algorithm for the determination of non-fluorescent imidacloprid in spiked river samples. Introducing the volume mode can extract the relationship between the target analyte and the volume of environmental water, therefore the purpose of overcoming the matrix

Table 7
Examples of four-order/five-way calibration.

Analytes	Matrix	Algorithm	Data generation and characteristic	Comment	Reference
Carbaryl	Water with interfering agrochemicals	U-PLS/RQL, five-way PARAFAC and four-way PARAFAC	Excitation-emission-kinetic-pH-sample data array; recording the EEMs of the samples as a function of the reaction time and at different pH values; the four-way data obtained by combining the time and pH modes for the decomposition of four-way PARAFAC	1-naphthol as the hydrolysis product of carbaryl; pH and time profiles are mutually dependent; time profiles may introduce an additional source of quadrilinearity loss	[28]
Naptalam	Synthetic samples	Five-way PARAFAC and AQQLD	HPLC-DAD-kinetic-pH-sample data array; recording the kinetic evolution of HPLC-DAD signals of samples at different pH values	AQQLD was proposed; serious chromatographic peak shifts were corrected	[30]
Imidacloprid	Environmental water	AFWRQQLD	Emission-excitation-UV irradiation time-volume of river water-sample data array	Five-way calibration was designed for overcome the matrix effect from environmental water; imidacloprid with no native fluorescence; three-, four- and five-way calibrations were used and compared	[87]
Diclofenac sodium	Environmental water	AFWRQQLD, five-way PARAFAC and AQQLD	Emission-excitation-irradiation time -pH-sample data array	AFWRQQLD and Five-way PARAFAC obtained slightly better results; diclofenac sodium with unstable fluorescence properties	[29]

effect from environmental water was achieved. Li et al. proposed a method that combines five-way EEM-irradiation time-pH-sample data array with five-way calibration for quantification of a non-steroidal anti-inflammatory drug (NSAID) diclofenac sodium in river water [29]. With the increase of irradiation time, the fluorescence intensity of diclofenac sodium gradually increased. Therefore, it could be an instrument mode that provided high sensitivity. Three algorithms including AFWRQQLD, five-PARAFAC and AQQLD were used for data processing, and the first two showed slightly better results in this case.

6. Conclusions and outlook

In order to achieve accurate quantitative analysis, traditional analytical strategies usually require tedious sample pretreatments, such as separation, enrichment, purification, extraction, and long-time gradient elution. These processes often need to consume a lot of toxic organic solvents and manpower, which obviously violates the purpose of protecting the environment and controlling pollution. Chemical multi-way calibration has outstanding "second-order or higher-order advantages." It can be regard as replacing or enhancing traditional "physical/chemical separation" with the help of green and smart "mathematical separation", which avoids or greatly simplifies the sample pretreatment process and reduces analysis time. Moreover, the influence of background matrix and interference signal can be eliminated, so as to achieve the simultaneous, fast and accurate quantitative analysis of multiple components of interest even in the presence of unknown interferences. In this sense, the combination of multi-way calibration and modern high-order instruments can not only take full advantage of the high sensitivity of these instruments, but also minimize the impact of the entire analysis process on the environment. The innovative analytical strategy is fully consistent with the requirements of green analytical chemistry.

Because of the above-mentioned advantages, multi-way calibration has become a research hotspot in the field of analytical chemistry, and numerous related theories and applications have been developed. This review systematically introduces the multilinear models, algorithms with second-order or higher-order advantages, general considerations and recent representative applications for multi-way calibration. It is both a guide for beginners and a work summary in recent years. There is no doubt that in the future, multi-way calibration will be combined with more emerging high-order instruments, which may show more potentials and advantages for qualitative and quantitative analysis of multiple components in complex systems.

Acknowledgments

The authors gratefully acknowledge the National Natural Science Foundation of China (Grant No. 21575039, 21775039 and 21521063) for financial support.

Appendix A. Supplementary data

Supplementary data to this article can be found online at https://doi.org/10.1016/j.trac.2020.115954.

References

[1] C.N. Ho, G.D. Christian, E.R. Davidson, Application of the method of rank annihilation to quantitative analyses of multicomponent fluorescence data from the video fluorometer, Anal. Chem. 50 (1978) 1108–1113.
[2] R. Bro, Review on multiway analysis in chemistry—2000–2005, Crit. Rev. Anal. Chem. 36 (2006) 279–293.
[3] M. Ortiz, L. Sarabia, Quantitative determination in chromatographic analysis based on n-way calibration strategies, J. Chromatogr. A 1158 (2007) 94–110.
[4] G.M. Escandar, A.C. Olivieri, N.K.M. Faber, H.C. Goicoechea, A.M. de la Peña, R.J. Poppi, Second-and third-order multivariate calibration: data, algorithms and applications, Trends Anal. Chem. 26 (2007) 752–765.
[5] H.-L. Wu, J.-F. Nie, Y.-J. Yu, R.-Q. Yu, Multi-way chemometric methodologies and applications: a central summary of our research work, Anal. Chim. Acta 650 (2009) 131–142.
[6] H.C. Goicoechea, M.J. Culzoni, M.G. García, M.M. Galera, Chemometric strategies for enhancing the chromatographic methodologies with second-order data analysis of compounds when peaks are overlapped, Talanta 83 (2011) 1098–1107.
[7] A. Olivieri, G. Escandar, A.M. De La Peña, Second-order and higher-order multivariate calibration methods applied to non-multilinear data using different algorithms, Trends Anal. Chem. 30 (2011) 607–617.
[8] A.C. Olivieri, Recent advances in analytical calibration with multi-way data, Anal. Methods 4 (2012) 1876–1886.
[9] K.R. Murphy, C.A. Stedmon, D. Graeber, R. Bro, Fluorescence spectroscopy and multi-way techniques. PARAFAC, Anal. Methods 5 (2013) 6557–6566.
[10] C. Ruckebusch, L. Blanchet, Multivariate curve resolution: a review of advanced and tailored applications and challenges, Anal. Chim. Acta 765 (2013) 28–36.
[11] G.M. Escandar, H.C. Goicoechea, A.M. de la Peña, A.C. Olivieri, Second-and higher-order data generation and calibration: a tutorial, Anal. Chim. Acta 806 (2014) 8–26.
[12] H.L. Wu, Y. Li, R.Q. Yu, Recent developments of chemical multiway calibration methodologies with second-order or higher-order advantages, J. Chemometr. 28 (2014) 476–489.
[13] A.C. Olivieri, Analytical figures of merit: from univariate to multiway calibration, Chem. Rev. 114 (2014) 5358–5378.
[14] A.C. Olivieri, Practical guidelines for reporting results in single-and multi-component analytical calibration: a tutorial, Anal. Chim. Acta 868 (2015) 10–22.
[15] M. Montemurro, G.G. Siano, M.R. Alcaráz, H.C. Goicoechea, Third order chromatographic-excitation–emission fluorescence data: advances, challenges and prospects in analytical applications, Trends Anal. Chem. 93 (2017) 119–133.
[16] G.M. Escandar, A.C. Olivieri, A road map for multi-way calibration models, Analyst 142 (2017) 2862–2873.
[17] A.R. Jalalvand, H.C. Goicoechea, D.N. Rutledge, Applications and challenges of multi-way calibration in electrochemical analysis, Trends Anal. Chem. 87 (2017) 32–48.
[18] M. Vosough, Current challenges in second-order calibration of hyphenated chromatographic data for analysis of highly complex samples, J. Chemometr. 32 (2018) e2976.
[19] M. Navarro-Reig, C. Bedia, R. Tauler, J. Jaumot, Chemometric strategies for peak detection and profiling from multidimensional chromatography, Proteomics 18 (2018) 1700327.
[20] S.M. Azcarate, A. de Araújo Gomes, A.M. de la Peña, H.C. Goicoechea, Modeling second-order data for classification issues: data characteristics, algorithms, processing procedures and applications, Trends Anal. Chem. 107 (2018) 151–168.
[21] A.C. Olivieri, G.M. Escandar, Analytical chemistry assisted by multi-way calibration: a contribution to green chemistry, Talanta 204 (2019) 700–712.
[22] M.R. Alcaraz, O. Monago-Maraña, H.C. Goicoechea, A.M. de la Peña, Four-and five-way excitation-emission luminescence-based data acquisition and modeling for analytical applications. A review, Anal. Chim. Acta 1083 (2019) 41–57.
[23] G.M. Escandar, A.C. Olivieri, Multi-way chromatographic calibration—a review, J. Chromatogr. A 1587 (2019) 2–13.
[24] K.S. Booksh, B.R. Kowalski, Theory of analytical chemistry, Anal. Chem. 66 (1994) 782A–791A.
[25] M.D. Carabajal, J.A. Arancibia, G.M. Escandar, Excitation-emission fluorescence-kinetic data obtained by Fenton degradation. Determination of heavy-polycyclic aromatic hydrocarbons by four-way parallel factor analysis, Talanta 165 (2017) 52–63.
[26] A.P. Pagani, G.A. Ibañez, Four-way calibration applied to the processing of pH-modulated fluorescence excitation-emission matrices. Analysis of fluoroquinolones in the presence of significant spectral overlapping, Microchem. J. 132 (2017) 211–218.
[27] L. Rubio, S. Sanllorente, L.A. Sarabia, M.C. Ortiz, Fluorescence determination of cochineal in strawberry jam in the presence of carmoisine as a quencher by means of four-way PARAFAC decomposition, Food Chem. 290 (2019) 178–186.
[28] R.M. Maggio, A. Muñoz de la Peña, A.C. Olivieri, Unfolded partial least-squares with residual quadrilinearization: a new multivariate algorithm for processing five-way data achieving the second-order advantage. Application to fourth-order excitation-emission-kinetic-pH fluorescence analytical data, Chemometr. Intell. Lab. Syst. 109 (2011) 178–185.
[29] J. Li, J. Xu, W. Jin, Z. Yi, C. Cai, X. Huang, J. Nie, Y. Zhang, Fluorescent kinetics combined with fourth-order calibration for the determination of diclofenac sodium in environmental water, Anal. Bioanal. Chem. 411 (2019) 2019–2029.
[30] X.-D. Qing, H.-L. Wu, X.-H. Zhang, Y. Li, H.-W. Gu, R.-Q. Yu, A novel fourth-order calibration method based on alternating quinquelinear

decomposition algorithm for processing high performance liquid chromatography–diode array detection– kinetic-pH data of naptalam hydrolysis, Anal. Chim, Acta 861 (2015) 12–24.
[31] L.R. Tucker, Some mathematical notes on three-mode factor analysis, Psychometrika 31 (1966) 279–311.
[32] R.A. Harshman, Foundations of the PARAFAC Procedure: Models and Conditions for an "Explanatory" Multimodal Factor Analysis, 1970.
[33] J.D. Carroll, J.-J. Chang, Analysis of individual differences in multidimensional scaling via an N-way generalization of "Eckart-Young" decomposition, Psychometrika 35 (1970) 283–319.
[34] R. Bro, PARAFAC. Tutorial and applications, Chemometr. Intell. Lab. Syst. 38 (1997) 149–171.
[35] H.-L. Wu, M. Shibukawa, K. Oguma, An alternating trilinear decomposition algorithm with application to calibration of HPLC–DAD for simultaneous determination of overlapped chlorinated aromatic hydrocarbons, J. Chemometr. 12 (1998) 1–26.
[36] Z.P. Chen, H.L. Wu, R.Q. Yu, On the self-weighted alternating trilinear decomposition algorithm—the property of being insensitive to excess factors used in calculation, Chemometr. Intell. Lab. Syst. 15 (2001) 439–453.
[37] R.A. Harshman, S. Hong, 'Stretch'vs 'slice'methods for representing three-way structure via matrix notation, J. Chemometr. 16 (2002) 198–205.
[38] H.Y. Fu, H.L. Wu, Y.J. Yu, L.L. Yu, S.R. Zhang, J.F. Nie, S.F. Li, R.Q. Yu, A new third-order calibration method with application for analysis of four-way data arrays, J. Chemometr. 25 (2011) 408–429.
[39] X.D. Qing, H.L. Wu, X.F. Yan, Y. Li, L.Q. Ouyang, C.C. Nie, R.Q. Yu, Development of a novel alternating quadrilinear decomposition algorithm for the kinetic analysis of four-way room-temperature phosphorescence data, Chemometr. Intell. Lab. Syst. 132 (2014) 8–17.
[40] L.-X. Xie, H.-L. Wu, X.-H. Zhang, T. Wang, L. Zhu, S.-X. Xiang, Z. Liu, R.-Q. Yu, "Slicing" data array in quadrilinear component model: an alternative quadrilinear decomposition algorithm for third-order calibration method, Chemometr. Intell. Lab. Syst. 167 (2017) 12–22.
[41] R. Tauler, Multivariate curve resolution applied to second order data, Chemometr. Intell. Lab. Syst. 30 (1995) 133–146.
[42] S. Wold, P. Geladi, K. Esbensen, J. Öhman, Multi-way principal components-and PLS-analysis, J. Chemometr. 1 (1987) 41–56.
[43] R. Bro, Multiway calibration. multilinear pls, J. Chemometr. 10 (1996) 47–61.
[44] J. Öhman, P. Geladi, S. Wold, Residual bilinearization. Part 1: theory and algorithms, J. Chemometr. 4 (1990) 79–90.
[45] A.C. Olivieri, On a versatile second-order multivariate calibration method based on partial least-squares and residual bilinearization: second-order advantage and precision properties, J. Chemometr. 19 (2005) 253–265.
[46] A.C. Olivieri, G.M. Escandar, H.C. Goicoechea, A.M. de la Peña, Unfolded and Multiway Partial Least-Squares with Residual Multilinearization: Fundamentals, Elsevier, 2015, pp. 347–363.
[47] R. Tauler, M. Maeder, A. de Juan, Multiset data analysis: extended multivariate curve resolution, in: S. Brown, R. Tauler, R. Walczak (Editors), Comprehensive Chemometrics vol. 2, Elsevier, Amsterdam, 2009, pp. 473–505.
[48] J. Jaumot, A. de Juan, R. Tauler, MCR-ALS GUI 2.0: new features and applications, Chemometr. Intell. Lab. Syst. 140 (2015) 1–12.
[49] J.B. Kruskal, Rank, decomposition, and uniqueness for 3-way and N-way arrays, Multiway Data Analysis (1989) 7–18.
[50] J.B. Kruskal, Three-way arrays: rank and uniqueness of trilinear decompositions, with application to arithmetic complexity and statistics, Linear. Algebra. Appl. 18 (1977) 95–138.
[51] N.D. Sidiropoulos, R. Bro, On the uniqueness of multilinear decomposition of N-way arrays, J. Chemometr. 14 (2000) 229–239.
[52] C.-N. Ho, G.D. Christian, E.R. Davidson, Simultaneous multicomponent rank annihilation and applications to multicomponent fluorescent data acquired by the video fluorometer, Anal. Chem. 53 (1981) 92–98.
[53] E. Sanchez, B.R. Kowalski, Generalized rank annihilation factor analysis, Anal. Chem. 58 (1986) 496–499.
[54] K.S. Booksh, Z. Lin, Z. Wang, B.R. Kowalski, Extension of trilinear decomposition method with an application to the flow probe sensor, Anal. Chem. 66 (1994) 2561–2569.
[55] A.-L. Xia, H.-L. Wu, D.-M. Fang, Y.-J. Ding, L.-Q. Hu, R.-Q. Yu, Alternating penalty trilinear decomposition algorithm for second-order calibration with application to interference-free analysis of excitation–emission matrix fluorescence data, J. Chemometr. 19 (2005) 65–76.
[56] Y.-J. Yu, H.-L. Wu, J.-F. Nie, S.-R. Zhang, S.-F. Li, Y.-N. Li, S.-H. Zhu, R.-Q. Yu, A comparison of several trilinear second-order calibration algorithms, Chemometr. Intell. Lab. Syst. 106 (2011) 93–107.
[57] Y.J. Yu, H.L. Wu, C. Kang, Y. Wang, J. Zhao, Y.N. Li, Y.J. Liu, R.Q. Yu, Algorithm combination strategy to obtain the second-order advantage: simultaneous determination of target analytes in plasma using three-dimensional fluorescence spectroscopy, J. Chemometr. 26 (2012) 197–208.
[58] J.-H. Jiang, H.-L. Wu, Z.-P. Chen, R.-Q. Yu, Coupled vectors resolution method for chemometric calibration with three-way data, Anal. Chem. 71 (1999) 4254–4262.
[59] J.H. Jiang, H.L. Wu, Y. Li, R.Q. Yu, Alternating coupled vectors resolution (ACOVER) method for trilinear analysis of three-way data, J. Chemometr. 13 (1999) 557–578.
[60] Y. Li, J.-H. Jiang, H.-L. Wu, Z.-P. Chen, R.-Q. Yu, Alternating coupled matrices resolution method for three-way arrays analysis, Chemometr. Intell. Lab. Syst. 52 (2000) 33–43.
[61] J.H. Jiang, H.L. Wu, Y. Li, R.Q. Yu, Three-way data resolution by alternating slice-wise diagonalization (ASD) method, J. Chemometr. 14 (2000) 15–36.
[62] Z.-P. Chen, H.-L. Wu, Y. Li, R.-Q. Yu, Novel constrained PARAFAC algorithm for second-order linear calibration, Anal. Chim. Acta 423 (2000) 187–196.
[63] Z.P. Chen, Y. Li, R.Q. Yu, Pseudo alternating least squares algorithm for trilinear decomposition, J. Chemometr. 15 (2001) 149–167.
[64] Y.Z. Cao, Z.P. Chen, C.Y. Mo, H.L. Wu, R.Q. Yu, A PARAFAC algorithm using penalty diagonalization error (PDE) for three-way data array resolution, Analyst 125 (2000) 2303–2310.
[65] A.-L. Xia, H.-L. Wu, D.-M. Fang, Y.-J. Ding, L.-Q. Hu, R.-Q. Yu, Determination of daunomycin in human plasma and urine by using an interference-free analysis of excitation-emission matrix fluorescence data with second-order calibration, Anal. Sci. 22 (2006) 1189–1195.
[66] A.-L. Xia, H.-L. Wu, S.-H. Zhu, Q.-J. Han, Y. Zhang, R.-Q. Yu, Determination of psoralen in human plasma using excitation-emission matrix fluorescence coupled to second-order calibration, Anal. Sci. 24 (2008) 1171–1176.
[67] L.-Q. Hu, H.-L. Wu, Y.-J. Ding, D.-M. Fang, A.l. Xia, R.-Q. Yu, Alternating asymmetric trilinear decomposition for three-way data arrays analysis, Chemometr. Intell. Lab. Syst. 82 (2006) 145–153.
[68] J.-F. Nie, H.-L. Wu, S.-R. Zhang, Y.-J. Yu, R.-Q. Yu, Self-weighted alternating normalized residue fitting algorithm with application to quantitative analysis of excitation-emission matrix fluorescence data, Anal. Methods 2 (2010) 1918–1926.
[69] Y. Li, H.-L. Wu, C.-C. Nie, H.-W. Gu, X.-D. Qing, Q. Zuo, R.-Q. Yu, An alternating coupled two-unequal residual functions algorithm for second-order calibration, Anal. Methods 6 (2014) 6322–6331.
[70] C. Kang, H.-L. Wu, J.-J. Song, H. Xu, Y.-J. Liu, Y.-J. Yu, X.-H. Zhang, R.-Q. Yu, A flexible trilinear decomposition algorithm for three-way calibration based on the trilinear component model and a theoretical extension of the algorithm to the multilinear component model, Anal. Chim. Acta 878 (2015) 63–77.
[71] L. Tan, Y. Zhang, Q. Yang, N. Chen, W. Du, L.-J. Tang, J.-H. Jiang, R.-Q. Yu, A novel algorithm for second-order calibration of three-way data in fluorescence assays of multiple breast cancer-related DNAs, Talanta 195 (2019) 433–440.
[72] J. Jaumot, R. Gargallo, A. de Juan, R. Tauler, A graphical user-friendly interface for MCR-ALS: a new tool for multivariate curve resolution in MATLAB, Chemometr. Intell. Lab. Syst. 76 (2005) 101–110.
[73] T. Wang, H.-L. Wu, Y.-J. Yu, W.-J. Long, L. Cheng, A.-Q. Chen, R.-Q. Yu, A simple method for direct modeling of second-order liquid chromatographic data with retention time shifts and holding the second-order advantage, J. Chromatogr. A 1605 (2019) 360360.
[74] H.A. Kiers, J.M. Ten Berge, R. Bro, PARAFAC2—Part I. A direct fitting algorithm for the PARAFAC2 model,, J. Chemometr. 13 (1999) 275–294.
[75] R. Bro, C.A. Andersson, H.A. Kiers, PARAFAC2—Part II. Modeling chromatographic data with retention time shifts, J. Chemometr. 13 (1999) 295–309.
[76] M.B. Anzardi, J.A. Arancibia, A.C. Olivieri, Interpretation of matrix chromatographic-spectral data modeling with parallel factor analysis 2 and multivariate curve resolution, J. Chromatogr. A 1604 (2019) 460502.
[77] M. Linder, R. Sundberg, Second-order calibration: bilinear least squares regression and a simple alternative, Chemometr. Intell. Lab. Syst. 42 (1998) 159–178.
[78] A.C. Olivieri, A combined artificial neural network/residual bilinearization approach for obtaining the second-order advantage from three-way nonlinear data, J. Chemometr. 19 (2005) 615–624.
[79] A.C. Peinado, F. van den Berg, M. Blanco, R. Bro, Temperature-induced variation for NIR tensor-based calibration, Chemometr. Intell. Lab. Syst. 83 (2006) 75–82.
[80] R. Shan, Y. Zhao, M. Fan, X. Liu, W. Cai, X. Shao, Multilevel analysis of temperature dependent near-infrared spectra, Talanta 131 (2015) 170–174.
[81] X. Cui, X. Liu, X. Yu, W. Cai, X. Shao, Water can be a probe for sensing glucose in aqueous solutions by temperature dependent near infrared spectra, Anal. Chim. Acta 957 (2017) 47–54.
[82] L. Han, X. Cui, W. Cai, X. Shao, Three–level simultaneous component analysis for analyzing the near–infrared spectra of aqueous solutions under multiple perturbations, Talanta 217 (2020) 121036.
[83] X. Shao, X. Cui, X. Yu, W. Cai, Mutual factor analysis for quantitative analysis by temperature dependent near infrared spectra, Talanta 183 (2018) 142–148.
[84] A.-L. Xia, H.-L. Wu, S.-F. Li, S.-H. Zhu, L.-Q. Hu, R.-Q. Yu, Alternating penalty quadrilinear decomposition algorithm for an analysis of four-way data arrays, J. Chemometr. 21 (2007) 133–144.
[85] Y.-J. Liu, H.-L. Wu, C. Kang, H.-W. Gu, J.-F. Nie, S.-S. Li, Z.-Y. Su, R.-Q. Yu, Four-way self-weighted alternating normalized residue fitting algorithm with application for the analysis of serotonin in human plasma, Anal. Sci. 28 (2012) 1097–1104.
[86] C. Kang, H.-L. Wu, Y.-J. Yu, Y.-J. Liu, S.-R. Zhang, X.-H. Zhang, R.-Q. Yu, An alternative quadrilinear decomposition algorithm for four-way calibration with application to analysis of four-way fluorescence excitation–emission–pH data array, Anal. Chim. Acta 758 (2013) 45–57.
[87] J.-F. Nie, B. Li, Y. Zhang, J.-L. Fan, Z.-S. Yi, Z.-R. Cai, High-order calibration for the spectrofluorimetric determination of pesticides based on photochemical derivatization. A solution of the problems of inner-filter effects and matrix interferences in complex environmental water, Chemometr. Intell. Lab. Syst. 156 (2016) 36–53.

[88] T. Wang, H.-L. Wu, L.-X. Xie, W.-J. Long, L. Cheng, R.-Q. Yu, A novel quadrilinear decomposition method for four-way data arrays analysis based on algorithms combination strategy: comparison and application, Chemometr. Intell. Lab. Syst. 185 (2019) 92–104.
[89] S.A. Bortolato, V.A. Lozano, A.M. de la Peña, A.C. Olivieri, Novel augmented parallel factor model for four-way calibration of high-performance liquid chromatography–fluorescence excitation–emission data, Chemometr. Intell. Lab. Syst. 141 (2015) 1–11.
[90] J.A. Arancibia, A.C. Olivieri, D.B. Gil, A.E. Mansilla, I. Durán-Merás, A.M. de la Peña, Trilinear least-squares and unfolded-PLS coupled to residual trilinearization: new chemometric tools for the analysis of four-way instrumental data, Chemometr. Intell. Lab. Syst. 80 (2006) 77–86.
[91] P.C. Damiani, I. Durán-Merás, A. García-Reiriz, A. Jiménez-Girón, A. Muñoz de la Peña, A.C. Olivieri, Multiway partial least-squares coupled to residual trilinearization: a genuine multidimensional tool for the study of third-order data. Simultaneous analysis of procaine and its metabolite p-aminobenzoic acid in equine serum, Anal. Chem. 79 (2007) 6949–6958.
[92] A. García-Reiriz, P.C. Damiani, A.C. Olivieri, F. Cañada-Cañada, A. Muñoz de la Peña, Nonlinear four-way kinetic-excitation– emission fluorescence data processed by a variant of parallel factor Analysis and by a neural network model achieving the second-order advantage: malonaldehyde determination in olive oil samples, Anal. Chem. 80 (2008) 7248–7256.
[93] X.D. Qing, H.L. Wu, X.H. Zhang, Y. Li, H.W. Gu, J. Wen, X.Z. Shen, R.Q. Yu, A new alternating weighted quadrilinear decomposition algorithm with application for analysis of non-quinquelinear five-way data arrays, Sci. China Chem. 46 (2016) 401–410.
[94] C.A. Andersson, R. Bro, The N-way toolbox for MATLAB, Chemometr. Intell. Lab. Syst. 52 (2000) 1–4.
[95] M. Jalali-Heravi, H. Parastar, M. Kamalzadeh, R. Tauler, J. Jaumot, MCRC software: a tool for chemometric analysis of two-way chromatographic data, Chemometr. Intell. Lab. Syst. 104 (2010) 155–171.
[96] P.J. Gemperline, E. Cash, Advantages of soft versus hard constraints in self-modeling curve resolution problems. Alternating least squares with penalty functions, Anal. Chem. 75 (2003) 4236–4243.
[97] A.C. Olivieri, H.-L. Wu, R.-Q. Yu, MVC2: a MATLAB graphical interface toolbox for second-order multivariate calibration, Chemometr. Intell. Lab. Syst. 96 (2009) 246–251.
[98] A.C. Olivieri, H.-L. Wu, R.-Q. Yu, MVC3: a MATLAB graphical interface toolbox for third-order multivariate calibration, Chemometr. Intell. Lab. Syst. 116 (2012) 9–16.
[99] S.J. Mazivila, S.A. Bortolato, A.C. Olivieri, MVC3_GUI: a MATLAB graphical user interface for third-order multivariate calibration. An upgrade including new multi-way models, Chemometr. Intell. Lab. Syst. 173 (2018) 21–29.
[100] L.G. Thygesen, Å. Rinnan, S. Barsberg, J.K.S. Møller, Stabilizing the PARAFAC decomposition of fluorescence spectra by insertion of zeros outside the data area, Chemometr. Intell. Lab. Syst. 71 (2004) 97–106.
[101] G. Tomasi, R. Bro, PARAFAC and missing values, Chemometr. Intell. Lab. Syst. 75 (2005) 163–180.
[102] R. Bro, S. De Jong, A fast non-negativity-constrained least squares algorithm, J. Chemometr. 11 (1997) 393–401.
[103] R. Bro, N.D. Sidiropoulos, Least squares algorithms under unimodality and non-negativity constraints, J. Chemometr. 12 (1998) 223–247.
[104] R. Bro, N.D. Sidiropoulos, A.K. Smilde, Maximum likelihood fitting using ordinary least squares algorithms, J. Chemometr. 16 (2002) 387–400.
[105] R.D. JiJi, K.S. Booksh, Mitigation of Rayleigh and Raman spectral interferences in multiway calibration of excitation– emission matrix fluorescence spectra, Anal. Chem. 72 (2000) 718–725.
[106] R.D. JiJi, G.G. Andersson, K.S. Booksh, Application of PARAFAC for calibration with excitation–emission matrix fluorescence spectra of three classes of environmental pollutants, J. Chemometr. 14 (2000) 171–185.
[107] R.G. Zepp, W.M. Sheldon, M.A. Moran, Dissolved organic fluorophores in southeastern US coastal waters: correction method for eliminating Rayleigh and Raman scattering peaks in excitation–emission matrices, Mar. Chem. 89 (2004) 15–36.
[108] M. Bahram, R. Bro, C. Stedmon, A. Afkhami, Handling of Rayleigh and Raman scatter for PARAFAC modeling of fluorescence data using interpolation, J. Chemometr. 20 (2006) 99–105.
[109] Å. Rinnan, K.S. Booksh, R. Bro, First order Rayleigh scatter as a separate component in the decomposition of fluorescence landscapes, Anal. Chim. Acta 537 (2005) 349–358.
[110] Y. Li, H.-L. Wu, Y.-J. Yu, S.-R. Zhang, Y. Chen, D.-Z. Tu, C.-C. Nie, H. Xu, R.-Q. Yu, A novel method to handle Rayleigh scattering in three-way excitation-emission fluorescence data, Anal. Methods 4 (2012) 3987–3996.
[111] F.A. Chiappini, M.R. Alcaraz, H.C. Goicoechea, A.C. Olivieri, A graphical user interface as a new tool for scattering correction in fluorescence data, Chemometr. Intell. Lab. Syst. 193 (2019) 103810.
[112] E. Comas, R.A. Gimeno, J. Ferré, R.M. Marcé, F. Borrull, F.X. Rius, Time shift correction in second-order liquid chromatographic data with iterative target transformation factor analysis, Anal. Chim. Acta 470 (2002) 163–173.
[113] B.J. Prazen, R.E. Synovec, B.R. Kowalski, Standardization of second-order chromatographic/spectroscopic data for optimum chemical analysis, Anal. Chem. 70 (1998) 218–225.
[114] C.G. Fraga, B.J. Prazen, R.E. Synovec, Comprehensive two-dimensional gas chromatography and chemometrics for the high-speed quantitative analysis of aromatic isomers in a jet fuel using the standard addition method and an objective retention time alignment algorithm, Anal. Chem. 72 (2000) 4154–4162.
[115] C.G. Fraga, B.J. Prazen, R.E. Synovec, Objective data alignment and chemometric analysis of comprehensive two-dimensional separations with run-to-run peak shifting on both dimensions, Anal. Chem. 73 (2001) 5833–5840.
[116] Y.-J. Yu, H.-L. Wu, J.-F. Niu, J. Zhao, Y.-N. Li, C. Kang, R.-Q. Yu, A novel chromatographic peak alignment method coupled with trilinear decomposition for three dimensional chromatographic data analysis to obtain the second-order advantage, Analyst 138 (2013) 627–634.
[117] N.-P.V. Nielsen, J.M. Carstensen, J. Smedsgaard, Aligning of single and multiple wavelength chromatographic profiles for chemometric data analysis using correlation optimised warping, J. Chromatogr. A 805 (1998) 17–35.
[118] T. Skov, F. van den Berg, G. Tomasi, R. Bro, Automated alignment of chromatographic data, J. Chemometr. 20 (2006) 484–497.
[119] F. Savorani, G. Tomasi, S.B. Engelsen, icoshift: a versatile tool for the rapid alignment of 1D NMR spectra, J. Magn. Reson. 202 (2010) 190–202.
[120] G. Tomasi, F. Savorani, S.B. Engelsen, icoshift: an effective tool for the alignment of chromatographic data, J. Chromatogr. A 1218 (2011) 7832–7840.
[121] R.G. Sadygov, F. Martin Maroto, A.F. Hühmer, ChromAlign: a two-step algorithmic procedure for time alignment of three-dimensional LC–MS chromatographic surfaces, Anal. Chem. 78 (2006) 8207–8217.
[122] X.-L. Yin, H.-W. Gu, A.R. Jalalvand, Y.-J. Liu, Y. Chen, T.-Q. Peng, Dealing with overlapped and unaligned chromatographic peaks by second-order multivariate calibration for complex sample analysis: fast and green quantification of eight selected preservatives in facial masks, J. Chromatogr. A 1573 (2018) 18–27.
[123] J.M. Amigo, T. Skov, R. Bro, ChroMATHography: solving chromatographic issues with mathematical models and intuitive graphics, Chem. Rev. 110 (2010) 4582–4605.
[124] Y. Zhang, H.-L. Wu, A.L. Xia, L.-H. Hu, H.-F. Zou, R.-Q. Yu, Trilinear decomposition method applied to removal of three-dimensional background drift in comprehensive two-dimensional separation data, J. Chromatogr. A 1167 (2007) 178–183.
[125] Z. Liu, H.-L. Wu, L.-X. Xie, Y. Hu, H. Fang, X.-D. Sun, T. Wang, R. Xiao, R.-Q. Yu, Chemometrics-enhanced liquid chromatography-full scan-mass spectrometry for interference-free analysis of multi-class mycotoxins in complex cereal samples, Chemometr. Intell. Lab. Syst. 160 (2017) 125–138.
[126] X.-D. Qing, H.-L. Wu, H.-W. Gu, X.-L. Yin, J. Wen, X.-Z. Shen, R.-Q. Yu, Removal of background drift nonlinear interference in 3-D spectral arrays for multi-way calibration using trilinear decomposition methods, Acta Chim. Sinica 74 (2016) 277–284.
[127] Y.-J. Yu, H.-L. Wu, H.-Y. Fu, J. Zhao, Y.-N. Li, S.-F. Li, C. Kang, R.-Q. Yu, Chromatographic background drift correction coupled with parallel factor analysis to resolve coelution problems in three-dimensional chromatographic data: quantification of eleven antibiotics in tap water samples by high-performance liquid chromatography coupled with a diode array detector, J. Chromatogr. A 1302 (2013) 72–80.
[128] K. István, R. Rajkó, G. Keresztury, Towards the solution of the eluent elimination problem in high-performance liquid chromatography–infrared spectroscopy measurements by chemometric methods, J. Chromatogr. A 1104 (2006) 154–163.
[129] J. Kuligowski, G. Quintás, R. Tauler, B. Lendl, M. de la Guardia, Background correction and multivariate curve resolution of online liquid chromatography with infrared spectrometric detection, Anal. Chem. 83 (2011) 4855–4862.
[130] B.C. Mitchell, D.S. Burdick, Slowly converging PARAFAC sequences: swamps and two-factor degeneracies, J. Chemometr. 8 (1994) 155–168.
[131] Z.-P. Chen, Z. Liu, Y.-Z. Cao, R.-Q. Yu, Efficient way to estimate the optimum number of factors for trilinear decomposition, Anal. Chim. Acta 444 (2001) 295–307.
[132] R. Bro, H.A. Kiers, A new efficient method for determining the number of components in PARAFAC models, J. Chemometr. 17 (2003) 274–286.
[133] Y. Li, H.-L. Wu, X.-D. Qing, Q. Zuo, Y. Chen, R.-Q. Yu, A novel method to estimate the chemical rank of three-way data for second-order calibration, Chemometr. Intell. Lab. Syst. 127 (2013) 177–184.
[134] Y.-J. Liu, G. Postma, H.-L. Wu, H.-W. Gu, C. Kang, J. Jansen, L. Duponchel, Angle Distribution of Loading Subspace (ADLS) for estimating chemical rank in multivariate analysis: applications in spectroscopy and chromatography, Talanta 194 (2019) 90–97.
[135] X.-D. Qing, Y. Li, J. Wen, X.-Z. Shen, C.-Y. Li, X.-L. Liu, J. Xie, A new method to determine the number of chemical components of four-way data from mixtures, Microchem. J. 135 (2017) 114–121.
[136] M. Meloun, J. Čapek, P. Mikšık, R.G. Brereton, Critical comparison of methods predicting the number of components in spectroscopic data, Anal. Chim. Acta 423 (2000) 51–68.
[137] E.R. Malinowski, Determination of the number of factors and the experimental error in a data matrix, Anal. Chem. 49 (1977) 612–617.
[138] F.C. Sanchez, J. Toft, B. Van den Bogaert, D. Massart, Orthogonal projection approach applied to peak purity assessment, Anal. Chem. 68 (1996) 79–85.
[139] D. Louwerse, A.K. Smilde, H.A. Kiers, Cross-validation of multiway component models, J. Chemometr. 13 (1999) 491–510.
[140] Z.-P. Chen, Y.-Z. Liang, J.-H. Jiang, Y. Li, J.-Y. Qian, R.-Q. Yu, Determination of the number of components in mixtures using a new approach incorporating chemical information, J. Chemometr. 13 (1999) 15–30.

[141] H.-P. Xie, J.-H. Jiang, G.-L. Shen, R.-Q. Yu, Estimation of the chemical rank for the three-way data: a principal norm vector orthogonal projection approach, Comput. Chem. 26 (2002) 183–190.
[142] M. Wasim, R.G. Brereton, Determination of the number of significant components in liquid chromatography nuclear magnetic resonance spectroscopy, Chemometr. Intell. Lab. Syst. 72 (2004) 133–151.
[143] H.-P. Xie, J.-H. Jiang, N. Long, G.-L. Shen, H.-L. Wu, R.-Q. Yu, Estimation of chemical rank of a three-way array using a two-mode subspace comparison approach, Chemometr. Intell. Lab. Syst. 66 (2003) 101–115.
[144] L. Hu, H. Wu, J. Jiang, Y. Ding, A. Xia, R. Yu, Use of pseudo-sample extraction and the projection technique to estimate the chemical rank of three-way data arrays, Anal. Bioanal. Chem. 384 (2006) 1493–1500.
[145] L.-Q. Hu, H.-L. Wu, J.-H. Jiang, Q.-J. Han, A.-L. Xia, R.-Q. Yu, Estimating the chemical rank of three-way data arrays by a simple linear transform incorporating Monte Carlo simulation, Talanta 71 (2007) 373–380.
[146] A.-L. Xia, H.-L. Wu, Y. Zhang, S.-H. Zhu, Q.-J. Han, R.-Q. Yu, A novel efficient way to estimate the chemical rank of high-way data arrays, Anal. Chim. Acta 598 (2007) 1–11.
[147] J.-F. Nie, H.-L. Wu, J.-Y. Wang, Y.-J. Liu, R.-Q. Yu, The chemical rank estimation for excitation-emission matrix fluorescence data by region-based moving window subspace projection technique and Monte Carlo simulation, Chemometr. Intell. Lab. Syst. 104 (2010) 271–280.
[148] Y. Li, H.-L. Wu, X.-H. Zhang, Y. Chen, H.-W. Gu, Q. Zuo, Y. Zhang, S.-S. Guo, X.-Y. Liu, R.-Q. Yu, Estimating the chemical rank of three-way fluorescence data by vector subspace projection with Monte Carlo simulation, Chemometr. Intell. Lab. Syst. 136 (2014) 15–23.
[149] Y.-J. Yu, H.-Y. Fu, H.-W. Gu, Y. Li, C. Kang, Y.-P. Wang, H.-L. Wu, Chemical rank estimation for second-order calibration by discrete Fourier transform coupled with robust statistical analysis, Chemometr. Intell. Lab. Syst. 141 (2015) 47–57.
[150] K. Fang, Uniform Design and Uniform Design Table vol. 1, Science Press, Beijing, 1994, pp. 1–18.
[151] K.-T. Fang, D.K. Lin, P. Winker, Y. Zhang, Uniform design: theory and application, Technometrics 42 (2000) 237–248.
[152] D.B. Gil, A.M. de la Peña, J.A. Arancibia, G.M. Escandar, A.C. Olivieri, Second-order advantage achieved by unfolded-partial least-squares/residual bilinearization modeling of Excitation–Emission fluorescence data presenting inner filter effects, Anal. Chem. 78 (2006) 8051–8058.
[153] S. Masoum, A. Gholami, M. Hemmesi, S. Abbasi, Quality assessment of the saffron samples using second-order spectrophotometric data assisted by three-way chemometric methods via quantitative analysis of synthetic colorants in adulterated saffron, Spectrochim. Acta A 148 (2015) 389–395.
[154] S. Yu, X. Yuan, J. Yang, J. Yuan, J. Shi, Y. Wang, Y. Chen, S. Gao, A chemometric-assisted method for the simultaneous determination of malachite green and crystal violet in water based on absorbance–pH data generated by a homemade pH gradient apparatus, Spectrochim. Acta A 150 (2015) 403–408.
[155] A. Naghashian-Haghighi, B. Hemmateenejad, M. Shamsipur, Determination of enantiomeric excess of some amino acids by second-order calibration of kinetic-fluorescence data, Anal. Biochem. 550 (2018) 15–26.
[156] R.L. Pérez, G.M. Escandar, Multivariate calibration-assisted high-performance liquid chromatography with dual UV and fluorimetric detection for the analysis of natural and synthetic sex hormones in environmental waters and sediments, Environ. Pollut. 209 (2016) 114–122.
[157] C.M. Teglia, P.M. Peltzer, S.N. Seib, R.C. Lajmanovich, M.J. Culzoni, H.C. Goicoechea, Simultaneous multi-residue determination of twenty one veterinary drugs in poultry litter by modeling three-way liquid chromatography with fluorescence and absorption detection data, Talanta 167 (2017) 442–452.
[158] R.B. Pellegrino Vidal, G.A. Ibañez, G.M. Escandar, Advantages of data fusion: first multivariate curve resolution analysis of fused liquid chromatographic second-order data with dual diode array-fluorescent detection, Anal. Chem. 89 (2017) 3029–3035.
[159] N.M. Diez, A.G. Cabanillas, A. Silva Rodríguez, H.C. Goicoechea, Second-order advantage maintenance with voltammetric data modeling for quantitation of ethiofencarb in the presence of interferences, Talanta 132 (2015) 851–856.
[160] A.M. Granero, G.D. Pierini, S.N. Robledo, M.S. Di Nezio, H. Fernández, M.A. Zon, Simultaneous determination of ascorbic and uric acids and dopamine in human serum samples using three-way calibration with data from square wave voltammetry, Microchem. J. 129 (2016) 205–212.
[161] S. Cavanillas, J.M. Díaz-Cruz, C. Ariño, M. Esteban, Parametric signal fitting by Gaussian peak adjustment: a new multivariate curve resolution method for non-bilinear voltammetric measurements, Anal. Chim. Acta 689 (2011) 198–205.
[162] S. Cavanillas, N. Serrano, J.M. Díaz-Cruz, C. Arino, M. Esteban, Parametric Signal Fitting by Gaussian Peak Adjustment: implementation of 2D transversal constraints and its application for the determination of p K a and complexation constants by differential pulse voltammetry, Analyst 138 (2013) 2171–2180.
[163] M. Kooshki, J.M. Díaz-Cruz, H. Abdollahi, C. Ariño, M. Esteban, Asymmetric logistic peak as a suitable function for the resolution of highly asymmetric voltammograms in non-bilinear systems, Analyst 136 (2011) 4696–4703.
[164] A. Alberich, J.M. Díaz-Cruz, C. Ariño, M. Esteban, Potential shift correction in multivariate curve resolution of voltammetric data. General formulation and application to some experimental systems, Analyst 133 (2008) 112–125.
[165] A. Alberich, J.M. Díaz-Cruz, C. Ariño, M. Esteban, Combined use of the potential shift correction and the simultaneous treatment of spectroscopic and electrochemical data by multivariate curve resolution: analysis of a Pb (II)–phytochelatin system, Analyst 133 (2008) 470–477.
[166] J.M.D. Cruz, J. Sanchís, E. Chekmeneva, C. Ariño, M. Esteban, Non-linear multivariate curve resolution analysis of voltammetric pH titrations, Analyst 135 (2010) 1653–1662.
[167] P.H. Eilers, I.D. Currie, M. Durbán, Fast and compact smoothing on large multidimensional grids, Comput. Stat. Data Anal. 50 (2006) 61–76.
[168] X. Cui, J. Zhang, W. Cai, X. Shao, Chemometric algorithms for analyzing high dimensional temperature dependent near infrared spectra, Chemometr. Intell. Lab. Syst. 170 (2017) 109–117.
[169] Y. Liu, W. Cai, X. Shao, Standardization of near infrared spectra measured on multi-instrument, Anal. Chim. Acta 836 (2014) 18–23.
[170] J.P. Castro, E.R. Pereira-Filho, R. Bro, Laser-induced breakdown spectroscopy (LIBS) spectra interpretation and characterization using parallel factor analysis (PARAFAC): a new procedure for data and spectral interferences processing fostering waste electrical and electronic equipment (WEEE) recycling process, J. Anal. Atom. Spectrom 35 (2020) 1115–1124.
[171] F. Allegrini, A.C. Olivieri, Analytical figures of merit for partial least-squares coupled to residual multilinearization, Anal. Chem. 84 (2012) 10823–10830.
[172] R.P.H. Nikolajsen, K.S. Booksh, Å.M. Hansen, R. Bro, Quantifying catecholamines using multi-way kinetic modelling, Anal. Chim. Acta 475 (2003) 137–150.
[173] C. Kang, H.-L. Wu, M.-L. Xu, X.-F. Yan, Y.-J. Liu, R.-Q. Yu, Simultaneously quantifying intracellular FAD and FMN using a novel strategy of intrinsic fluorescence four-way calibration, Talanta 197 (2019) 105–112.
[174] M.D. Russell, M. Gouterman, Excitation-emission-lifetime analysis of multicomponent systems—I. Principal component factor analysis, Spectrochim. Acta A 44 (1988) 857–861.
[175] M.D. Russell, M. Gouterman, Excitation-emission-lifetime analysis of multicomponent systems—II. Synthetic model data, Spectrochim. Acta A 44 (1988) 863–872.
[176] M.D. Russell, M. Gouterman, J.A. van Zee, Excitation-emission-lifetime analysis of multicomponent systems—III. Platinum, palladium and rhodium porphyrins, Spectrochim. Acta A 44 (1988) 873–882.
[177] H.C. Goicoechea, S. Yu, A.C. Olivieri, A.D. Campiglia, Four-way data coupled to parallel factor model applied to environmental Analysis: determination of 2,3,7,8-Tetrachloro-dibenzo-para-dioxin in highly contaminated waters by Solid–Liquid extraction laser-excited time-resolved Shpol'skii spectroscopy, Anal. Chem. 77 (2005) 2608–2616.
[178] B. Alfarhani, M. Al-Tameemi, H.C. Goicoechea, F. Barbosa, A.D. Campiglia, Direct analysis of benzo[a]pyrene metabolites with strong overlapping in both the spectral and lifetime domains, Microchem. J. 137 (2018) 51–61.
[179] R. Bro, Multi-way analysis in the food industry, models, algorithms, and applications, Ph. D. Thesis, University of Amsterdam, Amsterdam, 1998.
[180] M.R. Alcaráz, S.A. Bortolato, H.C. Goicoechea, A.C. Olivieri, A new modeling strategy for third-order fast high-performance liquid chromatographic data with fluorescence detection. Quantitation of fluoroquinolones in water samples, Anal. Bioanal. Chem. 407 (2015) 1999–2011.
[181] M. Montemurro, L. Pinto, G. Véras, A. de Araújo Gomes, M.J. Culzoni, M.C. Ugulino de Araújo, H.C. Goicoechea, Highly sensitive quantitation of pesticides in fruit juice samples by modeling four-way data gathered with high-performance liquid chromatography with fluorescence excitation-emission detection, Talanta 154 (2016) 208–218.
[182] A.C. Olivieri, G.M. Escandar, Practical Three-Way Calibration, Elsevier, Waltham, MA, USA, 2014.
[183] A.R. Jalalvand, M.-B. Gholivand, H.C. Goicoechea, Multidimensional voltammetry: four-way multivariate calibration with third-order differential pulse voltammetric data for multi-analyte quantification in the presence of uncalibrated interferences, Chemometr. Intell. Lab. Syst. 148 (2015) 60–71.
[184] Y. Hu, H.-L. Wu, X.-L. Yin, H.-W. Gu, C. Kang, S.-X. Xiang, H. Xia, R.-Q. Yu, Chemometrics-assisted determination of amiloride and triamterene in biological fluids with overlapped peaks and unknown interferences, Bioanalysis 7 (2015) 1685–1697.
[185] L. Hu, C. Yin, Multi-way calibration coupling with fluorescence spectroscopy to determine magnolol and honokiol in herb and plasma samples, Anal. Methods 7 (2015) 5913–5923.
[186] H.-Y. Fu, H.-D. Li, C. Ni, T.-M. Yang, Y. Fan, H. Zhang, J. Yang, L. Chen, Y.-B. She, Micellar enhanced three-dimensional excitation-emission matrix fluorescence for rapid determination of antihypertensives in human plasma with aid of second-order calibration methods, J. Spectrosc. 2015 (2015) 11.
[187] X.-L. Yin, H.-L. Wu, H.-W. Gu, Y. Hu, H. Xia, L. Wang, R.-Q. Yu, Second-order calibration method applied to process three-way excitation–emission-kinetic fluorescence data: a novel tool for real-time quantitative analysis of the lactone hydrolysis of irinotecan in human plasma, Chemometr. Intell. Lab. Syst. 146 (2015) 447–456.
[188] H. Xia, H.-L. Wu, H.-W. Gu, X.-L. Yin, H. Fang, R.-Q. Yu, Simultaneous determination of naphazoline and pyridoxine in eye drops using excitation–emission matrix fluorescence coupled with second-order calibration method based on alternating trilinear decomposition algorithm, Chin. Chem. Lett. 26 (2015) 1446–1449.
[189] H.Y. Fu, H.D. Li, M. Shao, T.M. Yang, X. Zhang, R.J. Xu, Y.J. Wei, S.H. Chen, C. Ni, H.L. Wu, Simultaneous determination of Repaglinide and Irbesartan in

biological plasmas using micellar enhanced excitation-emission matrix fluorescence coupled with ATLD method, Sci. China Chem. 59 (2016) 816–823.
[190] Y. Hu, H.-L. Wu, X.-L. Yin, H.-W. Gu, R. Xiao, L. Wang, H. Fang, R.-Q. Yu, Interference-free spectrofluorometric quantification of aristolochic acid I and aristololactam I in five Chinese herbal medicines using chemical derivatization enhancement and second-order calibration methods, Spectrochim. Acta A 175 (2017) 229–238.
[191] C. Kang, H.-L. Wu, C. Zhou, S.-X. Xiang, X.-H. Zhang, Y.-J. Yu, R.-Q. Yu, Quantitative fluorescence kinetic analysis of NADH and FAD in human plasma using three-and four-way calibration methods capable of providing the second-order advantage, Anal. Chim. Acta 910 (2016) 36–44.
[192] Z. Liu, H.-L. Wu, H.-W. Gu, X.-L. Yin, L.-X. Xie, Y. Hu, H. Xia, S.-X. Xiang, R.-Q. Yu, Interference-free analysis of aflatoxin B 1 and G 1 in various foodstuffs using trilinear component modeling of excitation–emission matrix fluorescence data enhanced through photochemical derivatization, RSC Adv. 6 (2016) 25850–25863.
[193] A.F.T. Moore, H.C. Goicoechea, F. Barbosa, A.D. Campiglia, Parallel factor Analysis of 4.2 K excitation–emission matrices for the direct determination of Dibenzopyrene isomers in coal-tar samples with a cryogenic fiber-optic probe coupled to a commercial spectrofluorimeter, Anal. Chem. 87 (2015) 5232–5239.
[194] S. Ju, J. Deng, J. Cheng, N. Xiao, K. Huang, C. Hu, H. Zhao, J. Xie, X. Zhan, Determination of leucomalachite green, leucocrystal violet and their chromic forms using excitation–emission matrix fluorescence coupled with second-order calibration after dispersive liquid–liquid microextraction, Food Chem. 185 (2015) 479–487.
[195] A. Gholami, S. Masoum, A. Mohsenikia, S. Abbasi, Chemometrics-assisted excitation–emission fluorescence analytical data for rapid and selective determination of optical brighteners in the presence of uncalibrated interferences, Spectrochim. Acta A 153 (2016) 108–117.
[196] L. Wang, H.-L. Wu, X.-L. Yin, Y. Hu, H.-W. Gu, R.-Q. Yu, Simultaneous determination of umbelliferone and scopoletin in Tibetan medicine Saussurea laniceps and traditional Chinese medicine Radix angelicae pubescentis using excitation-emission matrix fluorescence coupled with second-order calibration method, Spectrochim. Acta A 170 (2017) 104–110.
[197] L. Zhu, H.-L. Wu, L.-X. Xie, H. Fang, S.-X. Xiang, Y. Hu, Z. Liu, T. Wang, R.-Q. Yu, A chemometrics-assisted excitation–emission matrix fluorescence method for simultaneous determination of arbutin and hydroquinone in cosmetic products, Anal. Methods 8 (2016) 4941–4948.
[198] M. Mora-Granados, D. González-Gómez, A. Gallego-Picó, Feasibility of the determination of three flavan-3-ols metabolites in urine samples via parallel factor analysis of fluorescence emission matrices, J. Funct. Foods 37 (2017) 303–309.
[199] M. Spagnuolo, F. Marini, L. Sarabia, M. Ortiz, Migration test of Bisphenol A from polycarbonate cups using excitation-emission fluorescence data with parallel factor analysis, Talanta 167 (2017) 367–378.
[200] R. Xiao, H.-L. Wu, Y. Hu, X.-L. Yin, H.-W. Gu, Z. Liu, T. Wang, X.-D. Sun, R.-Q. Yu, Simultaneous determination of warfarin and aspirin contents in biological fluids using excitation-emission matrix fluorescence coupled with a second-order calibration method, Anal. Sci. 33 (2017) 29–34.
[201] H.-W. Gu, S.-H. Zhang, B.-C. Wu, W. Chen, J.-B. Wang, Y. Liu, A green chemometrics-assisted fluorimetric detection method for the direct and simultaneous determination of six polycyclic aromatic hydrocarbons in oilfield wastewaters, Spectrochim. Acta A 200 (2018) 93–101.
[202] Y.-Y. Chang, H.-L. Wu, H. Fang, T. Wang, Z. Liu, Y.-Z. Ouyang, Y.-J. Ding, R.-Q. Yu, Rapid, simultaneous and interference-free determination of three rhodamine dyes illegally added into chilli samples using excitation-emission matrix fluorescence coupled with second-order calibration method, Spectrochim. Acta A 204 (2018) 141–149.
[203] L. Rubio, S. Sanllorente, L.A. Sarabia, M.C. Ortiz, Determination of cochineal and erythrosine in cherries in syrup in the presence of quenching effect by means of excitation-emission fluorescence data and three-way PARAFAC decomposition, Talanta 196 (2019) 153–162.
[204] Y.-Y. Yuan, S.-T. Wang, Q. Cheng, D.-M. Kong, X.-G. Che, Simultaneous determination of carbendazim and chlorothalonil pesticide residues in peanut oil using excitation-emission matrix fluorescence coupled with three-way calibration method, Spectrochim. Acta A 220 (2019) 117088.
[205] X.-D. Sun, H.-L. Wu, Y. Chen, J.-C. Chen, R.-Q. Yu, Chemometrics-assisted calibration transfer strategy for determination of three agrochemicals in environmental samples: solving signal variation and maintaining second-order advantage, Chemometr. Intell. Lab. Syst. 194 (2019) 103869.
[206] T. Liu, X.-G. Li, J.-Y. Wang, D.-L. Liu, Y.-J. Wei, Time-resolved fluorescence and chemometrics-assisted excitation–emission fluorescence for qualitative and quantitative analysis of scopoletin and scopolin in Erycibe obtusifolia Benth, Spectrochim. Acta A 219 (2019) 96–103.
[207] Y. Chen, H.-L. Wu, X.-D. Sun, T. Wang, H. Fang, Y.-Y. Chang, L. Cheng, Y.-J. Ding, R.-Q. Yu, Simultaneous and fast determination of bisphenol A and diphenyl carbonate in polycarbonate plastics by using excitation-emission matrix fluorescence couples with second-order calibration method, Spectrochim. Acta A 216 (2019) 283–289.
[208] M. Montemurro, R. Brasca, M.J. Culzoni, H.C. Goicoechea, High-performance organized media-enhanced spectrofluorimetric determination of pirimiphos-methyl in maize, Food Chem. 278 (2019) 711–719.
[209] Y.-Z. Ouyang, H.-L. Wu, H. Fang, T. Wang, X.-D. Sun, Y.-Y. Chang, Y.-J. Ding, R.-Q. Yu, Rapid and simultaneous determination of three fluoroquinolones in animal-derived foods using excitation-emission matrix fluorescence coupled with second-order calibration method, Spectrochim. Acta A 224 (2020) 117458.
[210] S.X. Xiang, H.L. Wu, C. Kang, L.X. Xie, X.L. Yin, H.W. Gu, R.Q. Yu, Fast quantitative analysis of four tyrosine kinase inhibitors in different human plasma samples using three-way calibration-assisted liquid chromatography with diode array detection, J. Sep. Sci. 38 (2015) 2781–2788.
[211] M. Vosough, N.J. Iravani, Matrix-free analysis of selected benzodiazepines in human serum samples using alternating trilinear decomposition modeling of fast liquid chromatography diode array detection data, Talanta 148 (2016) 454–462.
[212] Z. Liu, H.-L. Wu, Y. Li, H.-W. Gu, X.-L. Yin, L.-X. Xie, R.-Q. Yu, Rapid and simultaneous determination of five vinca alkaloids in Catharanthus roseus and human serum using trilinear component modeling of liquid chromatography–diode array detection data, J. Chromatogr. B 1026 (2016) 114–123.
[213] X.-L. Yin, H.-L. Wu, H.-W. Gu, Y. Hu, L. Wang, H. Xia, S.-X. Xiang, R.-Q. Yu, Chemometrics-assisted high performance liquid chromatography-diode array detection strategy to solve varying interfering patterns from different chromatographic columns and sample matrices for beverage analysis, J. Chromatogr. A 1435 (2016) 75–84.
[214] T.-M. Yang, Y.-X. Liu, H.-Y. Fu, W. Lan, H.-B. Su, H.-B. Tang, Q.-B. Yin, H.-D. Li, L.-P. Wang, H.-L. Wu, Pharmacokinetic analysis of four bioactive iridoid and secoiridoid glycoside components of radix gentianae Macrophyllae and their synergistic excretion by HPLC-DAD combined with second-order calibration, Nat. Prod. Bioprospect. 7 (2017) 445–459.
[215] Z. Liu, H.L. Wu, L.X. Xie, Y. Hu, H. Fang, X.D. Sun, T. Wang, R. Xiao, R. Yu, Direct and interference-free determination of thirteen phenolic compounds in red wines using chemometrics-assisted HPLC-DAD strategy for the authentication of vintage year, Anal. Methods 9 (2017).
[216] T. Wang, H.L. Wu, L.X. Xie, L. Zhu, Z. Liu, X.D. Sun, R. Xiao, R.Q. Yu, Fast and simultaneous determination of 12 polyphenols in apple peel and pulp by using chemometrics-assisted high-performance liquid chromatography with diode array detection, J. Sep. Sci. 40 (2017) 1651–1659.
[217] Q. Liu, H.-L. Wu, Z. Liu, R. Xiao, T. Wang, Y. Hu, Y.-J. Ding, R.-Q. Yu, Chemometrics-assisted HPLC-DAD as a rapid and interference-free strategy for simultaneous determination of 17 polyphenols in raw propolis, Anal. Methods 10 (2018) 5577–5588.
[218] X.L. Yin, H.W. Gu, Q. Wu, T.Q. Peng, S.H. Zhang, Y. Liu, Second-order calibration serves as a remedial measure for the simultaneous determination of andrographolide and dehydroandrographolide in Andrographis paniculata and its preparations by HPLC without complete baseline separation, J. Sep. Sci. 41 (2018) 3232–3240.
[219] T. Wang, H.-L. Wu, L.-X. Xie, Z. Liu, W.-J. Long, L. Cheng, Y.-J. Ding, R.-Q. Yu, Simultaneous and interference-free determination of eleven non-steroidal anti-inflammatory drugs illegally added into Chinese patent drugs using chemometrics-assisted HPLC-DAD strategy, Sci. China Chem. 61 (2018) 739–749.
[220] X.-D. Sun, H.-L. Wu, Z. Liu, Y. Chen, Q. Liu, Y.-J. Ding, R.-Q. Yu, Rapid and sensitive detection of multi-class food additives in beverages for quality control by using HPLC-DAD and chemometrics methods, Food Anal. Methods 12 (2019) 381–393.
[221] J.-Y. Wang, H.-L. Wu, Y.-M. Sun, H.-W. Gu, Z. Liu, Y.-J. Liu, R.-Q. Yu, Simultaneous determination of phenolic antioxidants in edible vegetable oils by HPLC–FLD assisted with second-order calibration based on ATLD algorithm, J. Chromatogr. B 947–948 (2014) 32–40.
[222] X.-D. Qing, H.-B. Zhou, X.-H. Zhang, H.-L. Wu, C.-Y. Chen, S.-W. Xu, S.-S. Li, Alternating trilinear decomposition of highly overlapped chromatograms for simultaneously targeted quantification of 15 PAHs in samples of pollution source, Microchem. J. 146 (2019) 742–752.
[223] H.-W. Gu, H.-L. Wu, S.-S. Li, X.-L. Yin, Y. Hu, H. Xia, H. Fang, R.-Q. Yu, P.-Y. Yang, H.-J. Lu, Chemometrics-enhanced full scan mode of liquid chromatography–mass spectrometry for the simultaneous determination of six co-eluted sulfonylurea-type oral antidiabetic agents in complex samples, Chemometr. Intell. Lab. Syst. 155 (2016) 62–72.
[224] Y. Hu, H.-L. Wu, X.-L. Yin, H.-W. Gu, R. Xiao, L.-X. Xie, Z. Liu, H. Fang, L. Wang, R.-Q. Yu, Rapid and interference-free analysis of nine B-group vitamins in energy drinks using trilinear component modeling of liquid chromatography-mass spectrometry data, Talanta 180 (2018) 108–119.
[225] W.J. Long, H.L. Wu, T. Wang, L.X. Xie, Y. Hu, H. Fang, L. Cheng, Y.J. Ding, R.Q. Yu, Chemometrics-assisted liquid chromatography with full scan mass spectrometry for the interference-free determination of glucocorticoids illegally added to face masks, J. Sep. Sci. 41 (2018) 3527–3537.
[226] X.-D. Sun, H.-L. Wu, Z. Liu, L.-X. Xie, Y. Hu, H. Fang, T. Wang, R. Xiao, Y.-J. Ding, R.-Q. Yu, Chemometrics-assisted liquid chromatography-full scan mass spectrometry for simultaneous determination of multi-class estrogens in infant milk powder, Anal. Methods 10 (2018) 1459–1471.
[227] M.L. Oca, L. Rubio, L.A. Sarabia, M.C. Ortiz, Dealing with the ubiquity of phthalates in the laboratory when determining plasticizers by gas chromatography/mass spectrometry and PARAFAC, J. Chromatogr. A 1464 (2016) 124–140.
[228] X. Luo, X.-D. Qing, X.-C. Miao, S. Xiang, H.-J. Chen, X.-H. Zhang, M. He, Chemometric-assisted fast quantification and source apportionment of PAHs in

PM10 using gas chromatography-mass spectrometry, Int. J. Environ. Anal. Chem. (2019) 1–13.
[229] K.Z. Farahani, A. Benvidi, M. Rezaeinasab, S. Abbasi, M. Abdollahi-Alibeik, A. Rezaeipoor-Anari, M.A.K. Zarchi, S.S.A.D.M. Abadi, Potentiality of PARAFAC approaches for simultaneous determination of N-acetylcysteine and acetaminophen based on the second-order data obtained from differential pulse voltammetry, Talanta 192 (2019) 439–447.
[230] R.B.P. Vidal, G.A. Ibañez, G.M. Escandar, Chemometrics-assisted cyclodextrin-enhanced excitation–emission fluorescence spectroscopy for the simultaneous green determination of bisphenol A and nonylphenol in plastics, Talanta 143 (2015) 162–168.
[231] M.A. Bravo, G.M. Escandar, A.C. Olivieri, E. Bardin, L.F. Aguilar, W. Quiroz, A novel application of nylon membranes for tributyltin determination in complex environmental samples by fluorescence spectroscopy and multivariate calibration, Chemometr. Intell. Lab. Syst 148 (2015) 77–84.
[232] M.d.C. Hurtado-Sánchez, V.A. Lozano, M.I. Rodríguez-Cáceres, I. Durán-Merás, G.M. Escandar, Green analytical determination of emerging pollutants in environmental waters using excitation–emission photoinduced fluorescence data and multivariate calibration, Talanta 134 (2015) 215–223.
[233] E. Fuentes, C. Cid, M.E. Báez, Determination of imidacloprid in water samples via photochemically induced fluorescence and second-order multivariate calibration, Talanta 134 (2015) 8–15.
[234] M. Vosough, S.N. Eshlaghi, R. Zadmard, On the performance of multiway methods for simultaneous quantification of two fluoroquinolones in urine samples by fluorescence spectroscopy and second-order calibration strategies, Spectrochim. Acta A 136 (2015) 618–624.
[235] V.A. Lozano, G.M. Escandar, Simultaneous determination of urea herbicides in water and soil samples based on second-order photoinduced fluorescence data, Anal. Methods 8 (2016) 7396–7404.
[236] O. Monago-Maraña, I. Durán-Merás, T. Galeano-Díaz, A.M. de la Peña, Fluorescence properties of flavonoid compounds. Quantification in paprika samples using spectrofluorimetry coupled to second order chemometric tools, Food Chem. 196 (2016) 1058–1065.
[237] M. Cabrera-Bañegil, M.d.C. Hurtado-Sánchez, T. Galeano-Díaz, I. Durán-Merás, Front-face fluorescence spectroscopy combined with second-order multivariate algorithms for the quantification of polyphenols in red wine samples, Food Chem. 220 (2017) 168–176.
[238] M.L. Privitera, V.A. Lozano, Development of a second-order standard addition fluorescence method for the direct determination of riboflavin in human urine samples without previous clean up and separation steps, Microchem. J. 133 (2017) 60–66.
[239] X.-M. Bai, T. Liu, D.-L. Liu, Y.-J. Wei, Simultaneous determination of α-asarone and β-asarone in Acorus tatarinowii using excitation-emission matrix fluorescence coupled with chemometrics methods, Spectrochim. Acta A 191 (2018) 195–202.
[240] Y.-Y. Yuan, S.-T. Wang, S.-Y. Liu, Q. Cheng, Z.-F. Wang, D.-M. Kong, Green approach for simultaneous determination of multi-pesticide residue in environmental water samples using excitation-emission matrix fluorescence and multivariate calibration, Spectrochim. Acta A (2019) 117801.
[241] A.L. Pérez, G. Tibaldo, G.H. Sánchez, G.G. Siano, N.R. Marsili, A.V. Schenone, A novel fluorimetric method for glyphosate and AMPA determination with NBD-Cl and MCR-ALS, Spectrochim. Acta A 214 (2019) 119–128.
[242] A. Naseri, B. Ghasemzadeh, K. Asadpour-Zeynali, Second-order advantage in determining Co (II) in real samples using kinetic-spectrophotometric data matrices and multivariate curve resolution-alternating least square approach, J. Iran. Chem. Soc. 13 (2016) 679–687.
[243] K. Asadpour-Zeynali, S. Maryam Sajjadi, F. Taherzadeh, Second order advantage obtained by spectroelectrochemistry along with novel carbon nanotube modified mesh electrode: application for determination of acetaminophen in Novafen samples, Spectrochim. Acta A 153 (2016) 674–680.
[244] M. Vosough, M. Rashvand, H.M. Esfahani, K. Kargosha, A. Salemi, Direct analysis of six antibiotics in wastewater samples using rapid high-performance liquid chromatography coupled with diode array detector: a chemometric study towards green analytical chemistry, Talanta 135 (2015) 7–17.
[245] L. Pinto, C.H. Díaz Nieto, M.A. Zón, H. Fernández, M.C.U. de Araujo, Handling time misalignment and rank deficiency in liquid chromatography by multivariate curve resolution: quantitation of five biogenic amines in fish, Anal. Chim. Acta 902 (2016) 59–69.
[246] E.S. Sousa, L. Pinto, M.C.U. de Araujo, A chemometric cleanup using multivariate curve resolution in liquid chromatography: quantification of pesticide residues in vegetables, Microchem. J. 134 (2017) 131–139.
[247] Y. Zhao, Y. Yuan, J. Chen, M. Li, X. Pu, Chemometrics-enhanced high performance liquid chromatography strategy for simultaneous determination on seven nitroaromatic compounds in environmental water, Chemometr. Intell. Lab. Syst. 174 (2018) 149–155.
[248] M. Vosough, S.M. Tehrani, Development of a fast HPLC-DAD method for simultaneous quantitation of three immunosuppressant drugs in whole blood samples using intelligent chemometrics resolving of coeluting peaks in the presence of blood interferences, J. Chromatogr. B 1073 (2018) 69–79.
[249] F. Rezaei, M. Sheikholeslami, M. Vosough, M. Maeder, Handling of highly coeluted chromatographic peaks by multivariate curve resolution for a complex bioanalytical problem: quantitation of selected corticosteroids and mycophenolic acid in human plasma, Talanta 187 (2018) 1–12.
[250] C.M. Monzón, C.M. Teglia, M.R. Delfino, H.C. Goicoechea, Multiway calibration strategy with chromatographic data exploiting the second-order advantage for quantitation of three antidiabetic and three antihypertensive drugs in serum samples, Microchem. J. 136 (2018) 185–192.
[251] X.-D. Sun, H.-L. Wu, Z. Liu, Y. Chen, J.-C. Chen, L. Cheng, Y.-J. Ding, R.-Q. Yu, Target-based metabolomics for fast and sensitive quantification of eight small molecules in human urine using HPLC-DAD and chemometrics tools resolving of highly overlapping peaks, Talanta 201 (2019) 174–184.
[252] P. Mortera, F.A. Zuljan, C. Magni, S.A. Bortolato, S.H. Alarcón, Multivariate analysis of organic acids in fermented food from reversed-phase high-performance liquid chromatography data, Talanta 178 (2018) 15–23.
[253] E.S. Sousa, M.P. Schneider, L. Pinto, M.C.U. de Araujo, A. de Araújo Gomes, Chromatographic quantification of seven pesticide residues in vegetable: univariate and multiway calibration comparison, Microchem. J. 152 (2020) 104301.
[254] M.N. Sheikholeslami, M. Vosough, H.M. Esfahani, On the performance of multivariate curve resolution to resolve highly complex liquid chromatography–full scan mass spectrometry data for quantification of selected immunosuppressants in blood and water samples, Microchem. J. 152 (2020) 104298.
[255] M. Ahmadvand, H. Sereshti, H. Parastar, Chemometric-based determination of polycyclic aromatic hydrocarbons in aqueous samples using ultrasound-assisted emulsification microextraction combined to gas chromatography–mass spectrometry, J. Chromatogr. A 1413 (2015) 117–126.
[256] H.-Y. Fu, H.-D. Li, B. Wang, J.-L. Cai, J.-W. Guo, H.-P. Cui, X.-B. Zhang, Y.-J. Yu, Quantification of acid metabolites in complex plant samples by using second-order calibration coupled with GC-mass spectrometry detection to resolve the influence of seriously overlapped chromatographic peaks, Anal. Methods 8 (2016) 747–755.
[257] O. Monago-Maraña, R.L. Pérez, G.M. Escandar, A. Muñoz De La Peña, T. Galeano-Díaz, Combination of liquid chromatography with multivariate curve resolution-alternating least-squares (MCR-ALS) in the quantitation of polycyclic aromatic hydrocarbons present in paprika samples, J. Agric. Food Chem. 64 (2016) 8254–8262.
[258] E. Martín Tornero, A. Espinosa-Mansilla, A. Muñoz de la Peña, I. Durán Merás, Phenanthrene metabolites determination in human breast and cow milk by combining elution time-emission fluorescence data with multiway calibration, Talanta 188 (2018) 299–307.
[259] M.A. Bravo, A. Gonzalez, B. Valverde, W. Quiroz, C. Toledo-Neira, Evaluation of three-way fluorescence data-based for simultaneous determination of polycyclic aromatic hydrocarbons in tea infusion samples at sub-ppb levels by second-order multivariate calibration, Microchem. J. 151 (2019) 104208.
[260] A.R. Jalalvand, M.-B. Gholivand, H.C. Goicoechea, T. Skov, Generation of non-multilinear three-way voltammetric arrays by an electrochemically oxidized glassy carbon electrode as an efficient electronic device to achieving second-order advantage: challenges, and tailored applications, Talanta 134 (2015) 607–618.
[261] M. Meshki, M. Behpour, S. Masoum, Application of Fe doped ZnO nanorods-based modified sensor for determination of sulfamethoxazole and sulfamethizole using chemometric methods in voltammetric studies, J. Electroanal. Chem. 740 (2015) 1–7.
[262] G. Mohammadi, K. Rashidi, M. Mahmoudi, H.C. Goicoechea, A.R. Jalalvand, Exploiting second-order advantage from mathematically modeled voltammetric data for simultaneous determination of multiple antiparkinson agents in the presence of uncalibrated interference, J. Taiwan Inst. Chem. E 88 (2018) 49–61.
[263] L.-X. Xie, H.-L. Wu, Y. Fang, C. Kang, S.-X. Xiang, L. Zhu, X.-L. Yin, H.-W. Gu, Z. Liu, R.-Q. Yu, Simultaneous determination of tyrosine and levodopa in human plasma using enzyme-induced excitation-emission-kinetic third-order calibration method, Chemometr. Intell. Lab. Syst. 148 (2015) 9–19.
[264] W.D. Fragoso, A.C. Olivieri, Chemometric modeling of kinetic-fluorescent third-order data for thiamine determination in multivitamin complexes, Microchem. J. 128 (2016) 42–46.
[265] M. Montemurro, G.G. Siano, M.J. Culzoni, H.C. Goicoechea, Automatic generation of photochemically induced excitation-emission-kinetic four-way data for the highly selective determination of azinphos-methyl in fruit juices, Sensor. Actuator. B Chem. 239 (2017) 397–404.
[266] M.D. Carabajal, J.A. Arancibia, G.M. Escandar, Excitation-emission fluorescence-kinetic third-order/four-way data: determination of bisphenol A and nonylphenol in food-contact plastics, Talanta 197 (2019) 348–355.
[267] A. Osorio, C. Toledo-Neira, M.A. Bravo, Critical evaluation of third-order advantage with highly overlapped spectral signals. Determination of fluoroquinolones in fish-farming waters by fluorescence spectroscopy coupled to multivariate calibration, Talanta 204 (2019) 438–445.
[268] L. Rubio, L.A. Sarabia, M.C. Ortiz, Standard addition method based on four-way PARAFAC decomposition to solve the matrix interferences in the determination of carbamate pesticides in lettuce using excitation–emission fluorescence data, Talanta 138 (2015) 86–99.
[269] R. Yang, N. Zhao, X. Xiao, S. Yu, J. Liu, W. Liu, Determination of polycyclic aromatic hydrocarbons by four-way parallel factor analysis in presence of humic acid, Spectrochim. Acta A 152 (2016) 384–390.
[270] X.-H. Zhang, H.-L. Wu, X.-L. Yin, Y. Li, X.-D. Qing, H.-W. Gu, C. Kang, R.-Q. Yu, Exploiting third-order advantage using four-way calibration method for direct quantitative analysis of active ingredients of Schisandra chinensis in

DMEM by processing four-way excitation–emission-solvent fluorescence data, Chemometr. Intell. Lab. Syst. 155 (2016) 46–53.
[271] S.M. Sajjadi, H. Abdollahi, R. Rahmanian, L. Bagheri, Quantifying aflatoxins in peanuts using fluorescence spectroscopy coupled with multiway methods: resurrecting second-order advantage in excitation–emission matrices with rank overlap problem, Spectrochim. Acta A 156 (2016) 63–69.
[272] T. Liu, L. Zhang, S. Wang, Y. Cui, Y. Wang, L. Liu, Z. Yang, Four-dimensional data coupled to alternating weighted residue constraint quadrilinear decomposition model applied to environmental analysis: determination of polycyclic aromatic hydrocarbons, Spectrochim. Acta A 193 (2018) 507–517.
[273] F. Shang, Y. Wang, J. Wang, L. Zhang, P. Cheng, S. Wang, Determination of three polycyclic aromatic hydrocarbons in tea using four-way fluorescence data coupled with third-order calibration method, Microchem. J. 146 (2019) 957–964.
[274] M.D. Carabajal, J.A. Arancibia, G.M. Escandar, On-line generation of third-order liquid chromatography–excitation-emission fluorescence matrix data. Quantitation of heavy-polycyclic aromatic hydrocarbons, J. Chromatogr. A 1527 (2017) 61–69.
[275] R.B. Pellegrino Vidal, A.C. Olivieri, G.A. Ibañez, G.M. Escandar, Online third-order liquid chromatographic data with native and photoinduced fluorescence detection for the quantitation of organic pollutants in environmental water, ACS Omega 3 (2018) 15771–15779.
[276] M.D. Carabajal, J.A. Arancibia, G.M. Escandar, Multivariate curve resolution strategy for non-quadrilinear type 4 third-order/four way liquid chromatography–excitation-emission fluorescence matrix data, Talanta 189 (2018) 509–516.
[277] M.R. Alcaraz, E. Morzán, C. Sorbello, H.C. Goicoechea, R. Etchenique, Multiway analysis through direct excitation-emission matrix imaging, Anal. Chim. Acta 1032 (2018) 32–39.
[278] D.W. Cook, S.C. Rutan, D.R. Stoll, P.W. Carr, Two dimensional assisted liquid chromatography – a chemometric approach to improve accuracy and precision of quantitation in liquid chromatography using 2D separation, dual detectors, and multivariate curve resolution, Anal. Chim. Acta 859 (2015) 87–95.
[279] A. Eftekhari, H. Parastar, Multivariate analytical figures of merit as a metric for evaluation of quantitative measurements using comprehensive two-dimensional gas chromatography–mass spectrometry, J. Chromatogr. A 1466 (2016) 155–165.
[280] X.-D. Sun, H.-L. Wu, J.-C. Chen, A.-Q. Chen, Y. Chen, Y.-Z. Ouyang, Y.-J. Ding, R.-Q. Yu, Exploration advantages of data combination and partition: first chemometric analysis of liquid chromatography–mass spectrometry data in full scan mode with quadruple fragmentor voltages, Anal. Chim. Acta 1110 (2020) 158–168.
[281] L.H. Qi, W.S. Cai, X.G. Shao, Effect of temperature on mear-infrared spectra of n-alkanes, Acta Chim. Sinica 74 (2016) 172–178.
[282] X.-H. Zhang, Q. Zhou, Z. Liu, X.-D. Qing, J.-J. Zheng, S.-T. Mu, P.-H. Liu, Comparison of three second-order multivariate calibration methods for the rapid identification and quantitative analysis of tea polyphenols in Chinese teas using high-performance liquid chromatography, J. Chromatogr. A (2020) 460905.
[283] W.-J. Long, H.-L. Wu, T. Wang, M.-Y. Dong, R.-Q. Yu, Exploiting second-order advantage from mathematically modeled liquid chromatography-mass spectrometry data for simultaneous determination of polyphenols in Chinese propolis, Microchem. J. (2020) 105003.